Aalto University
School of Engineering

Jani Mäkelä

Energy efficiency of a digital hydraulic multi-pressure actuator for use in load-lifting applications

Thesis submitted as partial fulfilment of the requirements for degree of Master in Science (Technology).

Espoo 31.07.2020

Supervisor: Professor Matti Pietola
Advisor: Jyrki Kajaste, D.Sc. (Tech.)

Aalto University
School of Engineering

Aalto University, P.O. BOX 11000, 00076
AALTO
www.aalto.fi

Abstract of master's thesis

Author	Jani Mäkelä
Title of thesis	Energy efficiency of a digital hydraulic multi-pressure actuator for use in load-lifting applications
Master programme	Mechanical Engineering
Code	ENG25
Thesis supervisor	Professor Matti Pietola
Thesis advisor(s)	Jyrki Kajaste, D.Sc. (Tech.)
Date	31.07.2020
Number of pages	80
Language	English

Abstract

The purpose of this thesis is to determine the energy efficiency of the digital hydraulic multi-pressure actuator (DHMPA) for use in load-lifting applications. In order to accomplish this, three different characteristic efficiencies are defined; traditional, total, and regeneration efficiency. The traditional efficiency represents a comparable figure to that in traditional hydraulic systems. However, it does not consider energy regeneration, and thus, does not reflect the true efficiency of the DHMPA. Therefore, the total efficiency considering the regeneration, is defined. Furthermore, the regeneration efficiency describes how efficiently load-mass potential energy can be restored to the system. In addition, novel digital hydraulic technologies are reviewed and the operation of the DHMPA unit is studied.

The efficiency figures are determined based on experimental measurement results. The test setup consists of pump unit, load-lifting test rig and the DHMPA. Measurements are done with a separate data acquisition system and the data acquired is analysed in MATLAB. Measured quantities are pressures, flow rates, positions, and temperatures of the system during the 500-cycle lifting-lowering test of the 1180 kg load-mass. The collected data is used for calculating the energy balance of the system, which can then be used for determining the three characteristic efficiencies of the system. In addition, the system performance is evaluated based on this data.

The results show that the DHMPA is feasible for use in load-lifting applications. However, some unexpected errors occurred in the positioning of the load-mass. Nevertheless, the performance can be improved by careful tuning and dimensioning of the DHMPA components. Although the system performance requires further investigation, the energy-efficiency is highly competitive to that of conventional hydraulic systems. The traditional efficiency was 128%, yielding approximately 3-4 times lower energy consumption than the traditional systems. The total efficiency exceeded 63%, which is remarkably higher than that of traditional systems. Furthermore, the potential energy from the load-mass could be regenerated with efficiency of 80%. Therefore, this study showed that the DHMPA has a significant energy-saving potential in load-lifting applications. However, in order to optimize the system performance and efficiency, a further study will be needed.

Keywords digital hydraulics, multi-pressure actuator, energy-efficiency

Aalto-yliopisto
Insinööritieteiden
korkeakoulu

Aalto-yliopisto, PL 11000, 00076 AALTO
www.aalto.fi
Diplomityön tiivistelmä

Tekijä Jani Mäkelä

Työn nimi Digitaalihydraulisen monipainejärjestelmän hyötysuhteen määrittäminen kuormaa nostaviin sovelluksiin

Maisteriohjelma Mechanical Engineering **Koodi** ENG25

Työn valvoja Professori Matti Pietola

Työn ohjaaja(t) Tekniikan tohtori Jyrki Kajaste

Päivämäärä 31.07.2020 **Sivumäärä** 80 **Kieli** Englanti

Tiivistelmä

Tämän diplomityön tarkoituksena on määrittää digitaalihydraulisen monipainejärjestelmän (DHMPA) hyötysuhde kuormaa nostavia sovelluksia varten. Tämän tavoitteen saavuttamiseksi, kolme ominaista hyötysuhdelukua määritetään: perinteinen, kokonais- ja talteenottohyötysuhde. Perinteinen hyötysuhde antaa vertailukelpoisen luvun perinteisten hydraulijärjestelmien kanssa. Se ei kuitenkaan ota huomioon talteenotettua energiaa, eikä siten kuvasta järjestelmän todellista hyötysuhdetta. Tämän vuoksi määritetään kokonaishyötysuhde, joka huomioi energian talteenoton. Talteenottohyötysuhde puolestaan kuvaa, kuinka tehokkaasti massan nostoon sidottu potentiaalienergia voidaan ottaa takaisin järjestelmään. Lisäksi esitellään muita uusia digitaalihydrauliikan sovelluksia sekä perehdytään tarkemmin DHMPA:n toimintaan.

Hyötysuhdeluvut määritetään kokeellisten mittaustulosten avulla. Testijärjestelmä koostuu hydraulikoneikosta, massaa nostavasta testipenkistä sekä DHMPA-yksiköstä. Mittausdata kerätään erillisellä tiedonkeruujärjestelmällä ja se analysoidaan MATLAB-ohjelmistolla. Mitattavia suureita ovat järjestelmän paineet, tilavuusvirrat, asemat sekä lämpötilat 500-askelisen, 1180 kg:n massaa nostavan ja laskevan testiohjelman aikana. Näiden tietojen avulla määritetään järjestelmän energiatase, josta puolestaan voidaan johtaa halutut hyötysuhdeluvut. Lisäksi näiden tietojen avulla voidaan arvioida järjestelmän toimintaa ja suorituskykyä.

Tulokset näyttävät, että DHMPA-yksikköä voidaan soveltaa kuormaa nostavissa sovelluksissa. Testiajon aikana esiintyi kuitenkin odottamattomia asemavirheitä. Näitä virheitä voidaan minimoida virittämällä ja mitoittamalla järjestelmä huolellisesti. Vaikka tämä vaatiikin lisätutkimusta, voidaan todeta, että DHMPA:n hyötysuhde on hyvin kilpailukykyinen perinteisiin järjestelmiin verrattuna. Perinteinen hyötysuhde oli 128%, mikä tarkoittaa noin 3-4 kertaa pienempää energian kulutusta tavanomaisiin järjestelmiin verrattuna. Kokonaishyötysuhteeksi saatiin yli 63%, joka on merkittävästi parempi kuin perinteisten järjestelmien. Massan potentiaalienergia kyettiin ottamaan talteen 80% hyötysuhteella. Tutkimuksen avulla osoitettiin, että DHMPA voi tarjota huomattavan energiansäästöpotentiaalin massaa nostaviin järjestelmiin. Lisätutkimusta kuitenkin tarvitaan suorituskyvyn ja hyötysuhteen optimoimiseksi.

Avainsanat digitaalihydrauliikka, monipainejärjestelmä, hyötysuhde

Preface

I want to thank Vesa Siitari for providing such an interesting thesis topic and giving an opportunity to conduct an independent work during the project. I would like to thank Jyrki Kajaste for acting as the advisor for this thesis. Thank you for sharing your expertise in hydraulic research and teaching me during my studies. I would also like to thank Antti Sinkkonen for being always ready to help me with the test setup or any other problem. In addition, I would like to thank the research group and laboratory staff for all the help during my thesis work.

The thesis extends the previous research of the Digital Hydraulic Multi-Pressure Actuator. The topic was selected in order to obtain further information of the efficiency of the DHMPA unit in a load-lifting test rig. The research was conducted as a part of EZE project in Aalto University and it was funded by Fiellberg Fluid Oy.

Espoo 31.7.2020

Jani Mäkelä

Table of Contents

Symbols .....
Abbreviations .....
1 Introduction 1
1.1 Background 1
1.2 Motivation 2
1.3 Thesis Aim and Scope 2
2 Energy Efficiency and Hydraulic Technologies 3
2.1 Hydraulic Energy Efficiency 3
2.2 Conventional Hydraulic Technologies 5
2.3 Digital Hydraulic Technologies 8
2.3.1 Overview 8
2.3.2 Hydraulic Switching Control 10
2.3.3 Digital Flow Control Unit 10
2.3.4 Digital Valve System 11
2.3.5 Multi-Chamber Cylinder 12
2.3.6 Digital Hydraulic Transformer 13
2.3.7 Independent Metering 14
2.3.8 Digital Hydraulic Pump-Motor 15
2.3.9 Digital Hydraulic Power Management System 16
2.3.10 Displacement controlled system 17
2.3.11 Direct Driven Hydraulic Drive 18
2.3.12 Hydraulic Energy Recovery System 19
2.3.13 Digital Hydraulic Multi-Pressure Actuator 20
3 Setup Description 25
3.1 Digital Hydraulic Multi-Pressure Actuator 25
3.2 Components and Test Rig 30
3.3 Test Case Parameters 36
4 Results 39
4.1 Performance Analysis 39
4.1.1 Positioning 39
4.1.2 Pressure Levels 40
4.1.3 Flow Rates 42
4.1.4 Temperature 47
4.1.5 Cylinder Force 48
4.2 Energy Efficiency Analysis 49
4.2.1 Power Consumption 49
4.2.2 Energy Balance 53
4.2.3 Energy Efficiency 57
5 Discussion 61
5.1 The Effect of Operating Pressure Range 61
5.2 Performance and Efficiency Evaluation 69
5.3 Result Validation 71
5.4 Future work 72
6 Conclusion 75
References 77

Symbols

SYMBOL	DESCRIPTION	UNIT
A_{A}	Effective area in cylinder chamber A	m^2
A_{B}	Effective area in cylinder chamber B	m^2
A_{accu}	Effective accumulator piston area	m^2
A_{chamber}	Effective chamber area	m^2
E_{HP}	HP line cumulative energy	J
$E_{\mathrm{accu,pos}}$	Positive cumulative accumulator input energy	J
E_{in}	Energy input	J
E_{out}	Energy output	J
E_{pot}	Potential energy	J
E_{reg}	Regenerated energy	J
$E_{\mathrm{reg,ave}}$	Average regenerated energy per one cycle	J
$E_{\mathrm{reg,est}}$	Estimated total regenerated energy	J
E_{tot}	Total energy	J
$F(\mathrm{i})$	i^{th} control force candidate	N
F_{out}	Output force	N
F_{ref}	Force reference	N
$K_{\mathrm{I_{pos}}}$	Position controller integral gain	$1/\mathrm{s}^2$
$K_{\mathrm{I_{vel}}}$	Velocity controller integral gain	$\mathrm{N/m}$
$K_{\mathrm{P_{pos}}}$	Position controller proportional gain	$1/\mathrm{s}$
$K_{\mathrm{P_{vel}}}$	Velocity controller proportional gain	$\mathrm{Ns/m}$
N_{chambers}	Number of chambers	-
N_{supply}	Number of supply lines	-
P	Power	W

P_{h}	Hydraulic power	W
P_{in}	Power input	W
P_{out}	Power output	W
V_{accu}	Accumulator hydraulic fluid volume	m^3
W_{sw}	Switching cost weight	-
W_{V}	Volume cost weight	-
W_{cf}	Crossflow cost weight	-
g	Gravitational acceleration	$\mathrm{m/s}^2$
h	Lifting height	M
m	Mass	kg
n	Number of cycles	-
n_{lift}	Number of lifting cycles	-
n_{low}	Number of lowering cycles	-
p	Pressure	Pa
p_{A}	A chamber pressure	Pa
p_{B}	B chamber pressure	Pa
$p_{\mathrm{A_{cand}}}(\mathrm{i})$	i^{th} pressure candidate for chamber A	Pa
$p_{\mathrm{B_{cand}}}(\mathrm{i})$	i^{th} pressure candidate for chamber B	Pa
p_{in}	Pressure input	Pa
$p_{\mathrm{LP,PRV}}$	LP PRV opening pressure	Pa
p_{max}	Maximum working pressure	Pa
p_{min}	Minimum working pressure	Pa
p_{out}	Pressure output	Pa
$p_{\mathrm{pre,HP}}$	HP gas pre-charge pressure	Pa
$p_{\mathrm{pre,LP}}$	LP gas pre-charge pressure	Pa
q_{v}	Volumetric flow rate	m^3/s

$q_{\mathrm{v,accu}}$	Volumetric accumulator flow rate	m^3/s
$q_{\mathrm{v,chamber}}$	Volumetric chamber flow rate	m^3/s
$q_{\mathrm{v,in}}$	Volumetric flow rate input	m^3/s
$q_{\mathrm{v,out}}$	Volumetric flow rate output	m^3/s
t_0	Start time	s
t_1	End time	s
v	Velocity	m/s
v_{accu}	Accumulator piston velocity	m/s
v_{cyl}	Cylinder piston velocity	m/s
v_{ref}	Velocity reference	m/s
x	Measured position	m
x_{accu}	Accumulator piston position	m
x_{ref}	Position reference	m
$x_{\mathrm{tol,1}}$	Stop positioning tolerance	m
$x_{\mathrm{tol,2}}$	Start positioning tolerance	m
x_0	Start position	m
Δx	Step size	m
Δt	Step hold time	s
η_{h}	Hydraulic efficiency	-
η_{reg}	Regeneration efficiency	-
η_{tot}	Total system efficiency	-
η_{trad}	Traditional efficiency	-

Abbreviations

ABBREVIATION	MEANING
DC	Displacement Controlled
DC S-P	Displacement Controlled Serial-Parallel
DDH	Direct Driven Hydraulic
DFCU	Digital Flow Control Unit
DHMPA	Digital Hydraulic Multi-Pressure Actuator
DHPMS	Digital Hydraulic Power Management System
DHRS	Direct Hydraulic Recovery System
DHT	Digital Hydraulic Transformer
DVS	Digital Valve System
FDD	Fault Detection and Diagnosis
HMI	Human-Machine Interface
HP	High-Pressure
IM	Independent Metering
IMV	Independent Metering Valve
IHRS	Indirect Hydraulic Recovery System
LP	Low-Pressure
LS	Load Sensing
NRMM	Non-Road Mobile Machines
PCM	Pulse Code Modulation
PCV	Proportional Control Valve
PLC	Programmable Logic Controller
PRV	Pressure Relief Valve
PWM	Pulse Width Modulation
SMISMO	Separate Meter-In, Separate Meter-Out

1 Introduction

1.1 *Background*

Over the past decades, the energy efficiency of hydraulic systems has become increasingly important for reducing fuel consumption, minimizing emissions, and improving profitability. In 2008, fluid power covered 2.3 – 3.0% of the total transmitted energy in the United States [1]. Therefore, as hydraulic systems are widely in use across different fields and are essential in various applications, the level of energy efficiency can have a significant effect on overall energy consumption. Typically, hydraulic systems are vital in many mobile and industrial applications because they provide good energy density and easy power transmission [2] [3]. However, commonly used hydraulic systems can have poor energy efficiency, thus wasting a significant amount of the energy produced instead of utilizing it as output work [4]. In the past decades, much research has focused on developing more energy-efficient hydraulics to address this issue. The advent of digital technologies has brought new opportunities for control, allowing the development of novel concepts for energy saving digital hydraulics [5].

Although traditional hydraulics can offer robust, cost-effective solutions, the efficiency is typically low because actuator output power is controlled by throttling-based valves. In order to output the power required for working actuators, various types of valves, including proportional control valves (PCV), have been used to throttle the flow from the high-pressure source. This throttling leads to significant power losses in control edges as the energy is transformed into heat [6]. The worst-case scenario is that the system operates with low loads, and while idling, the hydraulic oil is guided through the pressure relief valve (PRV) back to the tank. This leads to wasting a vast amount of hydraulic energy. For instance, a typical load-lifting application with even a modern, load sensing (LS) system can perform only up to 36% efficiency [7]. Therefore, improving hydraulic technologies has a great potential in offering energy savings. Nevertheless, valve-controlled systems can provide accurate control for hydraulic systems and have a simple, cost-effective structure [6]. In addition, they can be easily used to control multiple actuators with variating loads simultaneously. For these reasons, the majority of today's hydraulic systems in heavy vehicles and machinery are valve-controlled systems.

Research in digital hydraulics aims to overcome the disadvantages of traditional hydraulics. However, digital hydraulics have different characteristics from those of conventional hydraulics, as digital control is achieved by replacing analogue components with digital discrete-state components [4]. Consequently, utilization of these components yields a discrete power output for the hydraulic machine. The output resolution is determined by the number of the parallel digital components and their flow characteristics. Furthermore, modern digital hydraulics based on multiple pressure levels can minimize throttling losses in control edges as the output force can be balanced from the available pressures by digitally controlled valves that are either fully open or fully closed. For example, in [8], as high as 77% reduction in energy consumption was achieved compared to a traditional LS system. In addition to improved energy efficiency, digital hydraulics can also offer further improvements compared to traditional hydraulics. For example, parallel digital valves together with programmable controller can increase fault tolerance of the system, as the fault can be automatically detected and isolated [9].

1.2 *Motivation*

Although conventional hydraulic systems waste a notable amount of energy, the efficiency of individual components is typically good, ranging between 70-95 percent. The main reason for poor overall efficiency lies in the utilization of the produced energy. This motivates research to concentrate on improving system design. If the system is not carefully designed, the overall efficiency can decrease to a fraction of that for the individual components. For instance, consider the log-lifting case presented in [10]: "If the lifting height is assumed to be 2 m, duration of the loading cycle 5 s and mass of logs 1020 kg per cycle, the theoretical power needed is 4 kW when loading and -4 kW when unloading. The traditional log loader uses easily more than 40 kW in both cases and the efficiency is below 10 percent." As demonstrated in the example, the total efficiency can be significantly lower than the efficiency of the typical system components. Moreover, since a traditional hydraulic system does not recover energy, energy is consumed both in the lowering and lifting phases.

For improving the efficiency of a hydraulic work machine, a proof-of-concept device of a digital hydraulic multi-pressure actuator (DHMPA) has been built and the concept has been studied in several research articles. These studies have shown promising results, thus motivating further development of the DHMPA. For example, the first experimental results implied energy savings of up to 77% compared to a traditional LS system [8]. However, as the DHMPA has been tested only in a few applications, it still requires further investigation. For instance, no study has concentrated on a vertical load-lifting application. Therefore, this thesis will determine the efficiency of the DHMPA in a cyclic lifting-lowering duty cycle. This is an interesting application, as the DHMPA does not only minimize throttling losses, but also recovers energy from the working actuator in the lowering phase.

1.3 *Thesis Aim and Scope*

The aim of this thesis is to determine the energy efficiency of the DHMPA for use in load-lifting applications. This is achieved by conducting an experiment with a DHMPA unit applied to a vertical load-lifting test rig. The experiment consists of a 500-cycle test case that uses a pre-defined duty cycle to control the reference position of the DHMPA. During the test, the hydraulic energy input and output values are measured by an independent data acquisition system. The data is then analysed for determining the overall efficiency.

Since this thesis concentrates on only the hydraulic efficiency of the DHMPA unit, it excludes efficiency analysis of the prime energy source and hence, the efficiency of a hydraulic pump or an electric motor are not considered in this study. Moreover, the electric energy consumed by control electronics is excluded. Nevertheless, the thesis will consider hydraulic energy consumed in the working cylinder. Consequently, the DHMPA is observed as a single unit that has one pressure input, one tank output and two working actuator connections. Observing these input/output energies allows the total efficiency to be determined for the DHMPA.

The rest of this thesis is divided into five chapters. Chapter 2 presents the theoretical background for determining hydraulic energy efficiency and reviews the literature on digital hydraulics. Chapter 3 describes the test setup and test cases analysed in this study. Chapter 4 presents and analyses the experimental data. Chapter 5 discusses and validates the results and suggests further improvements for the DHMPA. Chapter 6 concludes the thesis by summarizing the research and evaluating results of the DHMPA for use in load-lifting applications.

2 Energy Efficiency and Hydraulic Technologies

2.1 *Hydraulic Energy Efficiency*

As the aim of this thesis is to determine the hydraulic efficiency of the DHMPA unit, it is critical to understand how energy efficiency is defined and energy consumption measured in hydraulic systems. Therefore, this section describes the factors establishing energy efficiency in hydraulic systems and shows calculations for overall efficiency.

A typical method for expressing system efficiency is to calculate the ratio of input and output powers, defined as follows:

$$\eta_{\mathrm{tot}} = \frac{P_{\mathrm{out}}}{P_{\mathrm{in}}}, \tag{1}$$

where η_{tot} is the total efficiency of the system [-],
P_{out} is the output power of the system [W], and
P_{in} is the input power to the system [W]. [2]

Therefore, the total efficiency corresponds to a dimensionless value between 0 and 1. An ideal system with no power losses would perform with an efficiency of 1. However, real-life applications can only approach this efficiency, since power losses are always present. Moreover, Equation (1) can be applied only to cases with constant power. Nevertheless, if system input and output powers change over time, the energy efficiency can be calculated from cumulative energies as shown in Equation (2):

$$\eta_{\mathrm{tot}} = \frac{\sum E_{\mathrm{out}}}{\sum E_{\mathrm{in}}}, \tag{2}$$

where η_{tot} is the total efficiency of the system [-],
E_{out} is the output energy of the system [J], and
E_{in} is the input energy to the system [J].

This is a more convenient definition, since many practical experiments include cases, where input and output power vary over time. Cumulative input and output energies can be calculated by integrating power:

$$E_{\mathrm{tot}} = \int_{t_0}^{t_1} P \, \mathrm{d}t, \tag{3}$$

where E_{tot} is the total energy [J],
t_0 is the time in the interval beginning [s],
t_1 is the time in the interval end [s], and
P is the power curve during time interval [W].

As a consequence, only definition of hydraulic power is needed for solving the efficiency of a hydraulic system. The hydraulic power is defined as

$$P_{\mathrm{h}} = q_{\mathrm{v}} \cdot p, \tag{4}$$

where P_{h} is the hydraulic power [W],
q_{v} is the volumetric flow rate [m^3/s], and
p is dominant pressure [Pa]. [2]

Therefore, based on Equations (1), (2), (3) and (4), the hydraulic efficiency can be expressed as in Equation (5).

$$\eta_{\mathrm{h}} = \frac{\sum E_{\mathrm{out}}}{\sum E_{\mathrm{in}}} = \frac{\int_{t_0}^{t_1} q_{\mathrm{v,out}} \cdot p_{\mathrm{out}}\, \mathrm{d}t}{\int_{t_0}^{t_1} q_{\mathrm{v,in}} \cdot p_{\mathrm{in}}\, \mathrm{d}t}, \tag{5}$$

where η_{h} is the hydraulic efficiency of the system [-],
$q_{\mathrm{v,out}}$ is the volumetric flow rate output [m^3/s],
$q_{\mathrm{v,in}}$ is the volumetric flow rate input [m^3/s],
p_{out} is the output pressure [Pa], and
p_{in} is the input pressure [Pa].

However, for the purpose of this thesis, the corresponding efficiency is calculated by replacing the hydraulic output energy with cumulative lifted potential energy. The input energy is calculated similarly as in Equation (5). The amount of potential energy can be determined more straightforward and reliably, as it is only dependent on the mass and position, while pressure and flow rate spikes can cause significant errors in the hydraulic energy calculation. Here, this efficiency will be referred to as “traditional efficiency”, as it does not consider energy regeneration in the system but only pumped input energy and lifted potential energy. The traditional energy of the DHMPA can be defined as follows:

$$\eta_{\mathrm{trad}} = \frac{\sum E_{\mathrm{out}}}{\sum E_{\mathrm{in}}} = \frac{n \cdot m \cdot g \cdot h}{\int_{t_0}^{t_1} q_{\mathrm{v,in}} \cdot p_{\mathrm{in}}\, \mathrm{d}t}, \tag{6}$$

where η_{trad} is the traditional efficiency of the system [-],
n is the number of lift cycles [-],
m is the mass of the load [kg],
g is the gravitational acceleration [m/s^2],
h is the lifting height [m],
$q_{\mathrm{v,in}}$ is the volumetric flow rate input [m^3/s], and
p_{in} is the input pressure [Pa].

As this study concentrates on the efficiency of the DHMPA, it is important to understand the application-specific characteristics affecting the overall efficiency. In this thesis, the lifting-lowering cycle with a constant mass is a so-called zero-energy process. In addition, the DHMPA unit is capable of regenerating energy. Therefore, the traditional energy efficiency (Equation 5) cannot be directly defined for this type of process. Nevertheless, a corresponding figure can be determined from cumulative energies by using the cumulative lifting energy as the output energy and the sum of pumped and regenerated energy as input energy. The total efficiency of the DHMPA can then be defined as follows:

$$\eta_{\text{tot}} = \frac{\sum E_{\text{out}}}{\sum E_{\text{in}} + \sum E_{\text{reg}}}, \tag{7}$$

where η_{tot} is the total hydraulic efficiency of the system [-],
E_{out} is the output energy [J],
E_{in} is input energy [J], and
E_{reg} is input energy [J].

Furthermore, as the DHMPA can regenerate energy during the lifting-lowering cycle, this thesis defines the regeneration efficiency. It corresponds to the ratio of regenerated and recoverable energy in the system. The amount of the regenerated energy corresponds to the amount of energy restored to the system, while recoverable energy would be equivalent to the load-mass potential energy. An ideal regenerator could restore all the potential energy of the load-mass. The regeneration efficiency is defined as follows:

$$\eta_{\text{reg}} = \frac{\sum E_{\text{reg}}}{\sum E_{\text{pot}}}, \tag{8}$$

where η_{reg} is the total hydraulic efficiency of the system [-],
E_{out} is the output energy [J],
E_{in} is input energy [J], and
E_{reg} is input energy [J].

Equations (6), (7) and (8) will be utilized in this thesis for determining the hydraulic efficiency of the DHMPA unit. In order to avoid errors caused by the energy stored in the system, the energies involved are calculated over the test cycle instead of one lifting-lowering cycle. This ensures that the error caused by the energy stored between the beginning and the end of the test will be negligible.

2.2 *Conventional Hydraulic Technologies*

Hydraulic systems have been in use since the end of nineteenth century and have been utilized in various applications, including mills, war machines and power transmission systems [6]. The advantage of hydraulic systems has always been their high torque-to-inertia ratio and fewer constraints in system design, since the power is transmitted through pipes and hoses [2] [6]. In addition, since the power density is excellent, hydraulic devices require less space than other technologies [2]. Furthermore, hydraulic systems combined with digital technology offer a competitive potential in today's industrial applications, where good controllability and high power are crucial. For making the best use of digital hydraulics, it is essential to understand the theory underlying in conventional hydraulics. Therefore, this section reviews non-digital hydraulic systems and their working principle.

Generally, in hydraulic systems, actuator velocity can be either positive or negative. At the same time, the input power can be either of the two signs. This yields a so-called four-quadrant operation, shown in Figure 1. In Quadrants I and III, the input power is positive, while that in II and IV is negative. Typically, hydraulic systems operate in all four quadrants. [11]

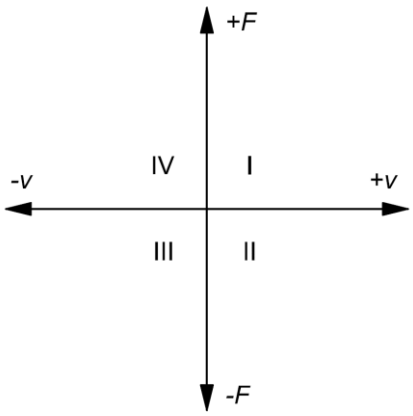

Figure 1. Four-quadrant operation space [11]

Hydraulic systems can be divided into hydrostatic and hydrodynamic systems. The difference between these two is that hydrostatic systems utilize potential energy for energy transfer, while hydrodynamic systems use kinetic energy [2]. All hydraulic systems discussed in this thesis are hydrostatic systems, since their performance is based on a high pressure (potential energy) supply, which is then transformed into mechanical movement of an actuator.

Hydrostatic systems can be either open or closed systems. In open systems, a tank is utilized, and the system first takes and then returns the required fluid to the tank. Valve-controlled actuators are commonly used with these systems. Closed systems do not usually include separate tank, though the use of pressure accumulators is possible. Closed systems are commonly used for driving hydraulic motors. The hydraulic systems used in industrial applications are typically open, hydrostatic systems. An example of an open hydrostatic system is presented in Figure 2. [2]

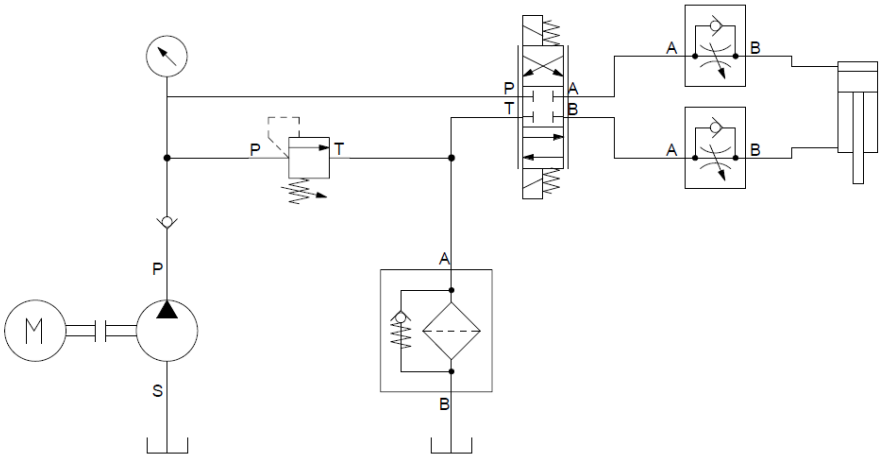

Figure 2. Hydraulic diagram of a simple hydrostatic, open circuit system [2]

As shown in Figure 2, this type of valve-controlled system can be very simple, thus providing a low-cost solution. However, it is obvious that the system energy efficiency is poor due to substantial energy losses. Major losses occur because the actuator velocity is controlled by throttling valves, and a fixed displacement pump produces a constant flow rate at high pressure, even when the used actuator is stationary.

For achieving better efficiency, pump-controlled systems have been considered as a competitor to valve-controlled systems [6]. Pump-controlled systems can be based on a speed-variable motor or a variable displacement pump. Either way, the concept has been proven to be more efficient, though it faces some issues with flow compensation when using a differential cylinder [12]. Some alternatives for this compensation are discussed for example in [12]. Speed-controlled pumps can also cause some additional costs if frequency converters or/and digital controllers are utilized in order to control the speed [13]. In addition, pump-controlled systems lack a robust and a simple control method. Thus, they need to be further studied in order to utilize their full potential [12].

The two concepts presented above – throttling and volumetric control – have their own advantages and disadvantages. So-called LS systems combine and utilize the best aspects of these two, and are designed to provide an independent actuator velocity with any load. In addition, they can save energy by producing only the required flow rate at demanded pressure levels [14]. Because the concept has been proven to be efficient, modern hydraulic systems most commonly are LS systems [4]. However, their efficiency is still limited, especially with multiple-actuator systems, since the pressure demand can be set only by one actuator. Therefore, all the other actuators working with lower pressure levels need to be throttled, thus yielding significant pressure losses [4]. The operating principle of a LS system for two valve-controlled actuators is shown in Figure 3.

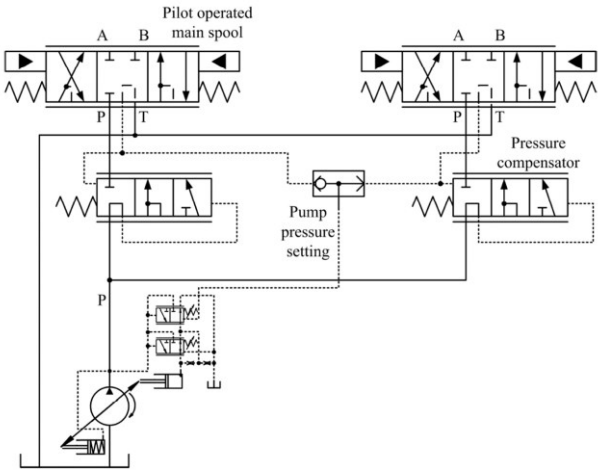

Figure 3. Load sensing system for two closed-center valves [15]

As shown in Figure 3, the highest load pressure is transmitted to the pump control through a shuttle valve. With this reference pressure and suitable pressure margin, the controller adjusts the pump pressure accordingly, which will then generate corresponding flow rate matching the actuator demand. The throttling losses are highest when the pressure difference between working actuators is large. Thus, LS system efficiency at its best when a single actuator is used. However, a good overall efficiency can be maintained by installing multiple LS units in the system, one for each actuator, though this increases costs as well. [15]

As traditional hydraulic systems are commonly throttling, volumetric or LS-controlled, it is obvious that the total efficiency of the most traditional systems is usually poor. LS systems can offer the best potential for energy saving, but even with these the total efficiency has been reported to be only as high as 36% [7]. In addition, these are the most complex systems of these three alternatives and do not perform efficiently in all applications. The two others,

constant and variable flow pumps, are fairly simple solutions but their efficiency is poor. The comparison of the three alternatives is presented in Figure 4.

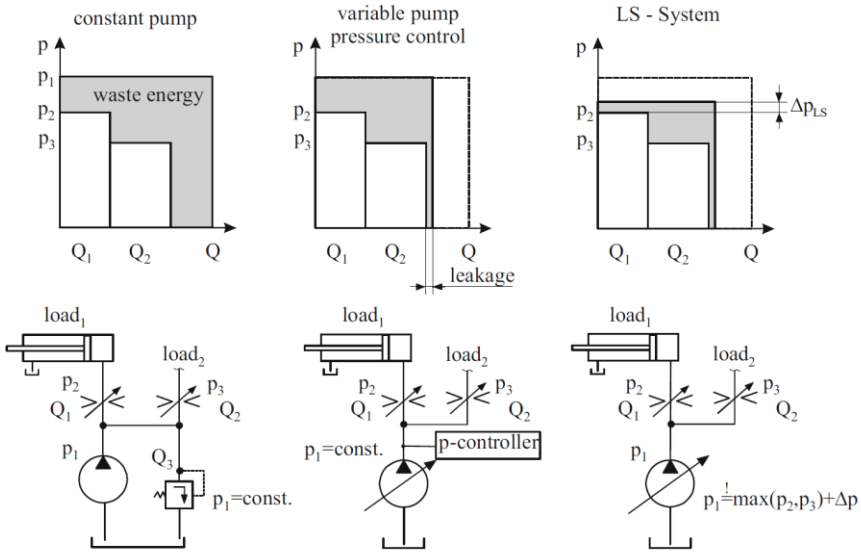

Figure 4. Comparison of wasted power in throttling, volumetric and LS-control [13]

As shown in Figure 4, the throttling-controlled systems will always have poor performance, since the amount of produced energy remains the same, even when output power is zero. Pressure controlled systems have potential for energy saving, though their controllability is difficult, and they require flow compensation for differential actuators. Although they are not as efficient as LS systems, they are better than PRV systems. LS controlled systems can compensate both flow rate and pressure, thus offering the best potential for energy saving compared to the other two alternatives. However, LS systems are complex, and their efficiency is not usually very good on multi-actuator machines due to differential pressure demands. As a consequence, other solutions are needed in order to improve the energy efficiency of hydraulic systems. Therefore, the next section discusses the digital alternatives and novel energy saving hydraulic technologies.

2.3 *Digital Hydraulic Technologies*

2.3.1 Overview

During the last decade, digital hydraulics have gained much attention, and they have been widely studied, as the energy consumption and efficiency have become more important in the system design [11]. In addition, new hydraulic applications, for example in the field of robotics, require good energy efficiency, low costs and good controllability, which cannot be offered by traditional hydraulics [16]. Digital hydraulics can provide solutions to tackle these challenges by offering more robust and relatively simple control with discrete states of the components. The fault tolerance can also be significantly improved by using parallel components in the system. In addition, control systems are not limited to one application due to their programmability. Although the individual components are simpler, the overall control system can become more complex. Also, the number of components will increase, and the resolution of the system is limited as discrete-state components are utilized. Therefore, designing the system becomes more challenging and multidisciplinary skills by engineers are needed in fields of hydraulics, mechanics, electronics and programming [11].

Nevertheless, digital hydraulics can be applied to almost any hydraulic system. Karvonen has reviewed different possibilities in [11], and as an example, Figure 5 presents traditional and digital versions of a control edge, a variable-displacement pump, a power management system, a variable-pressure accumulator and a variable displacement cylinder.

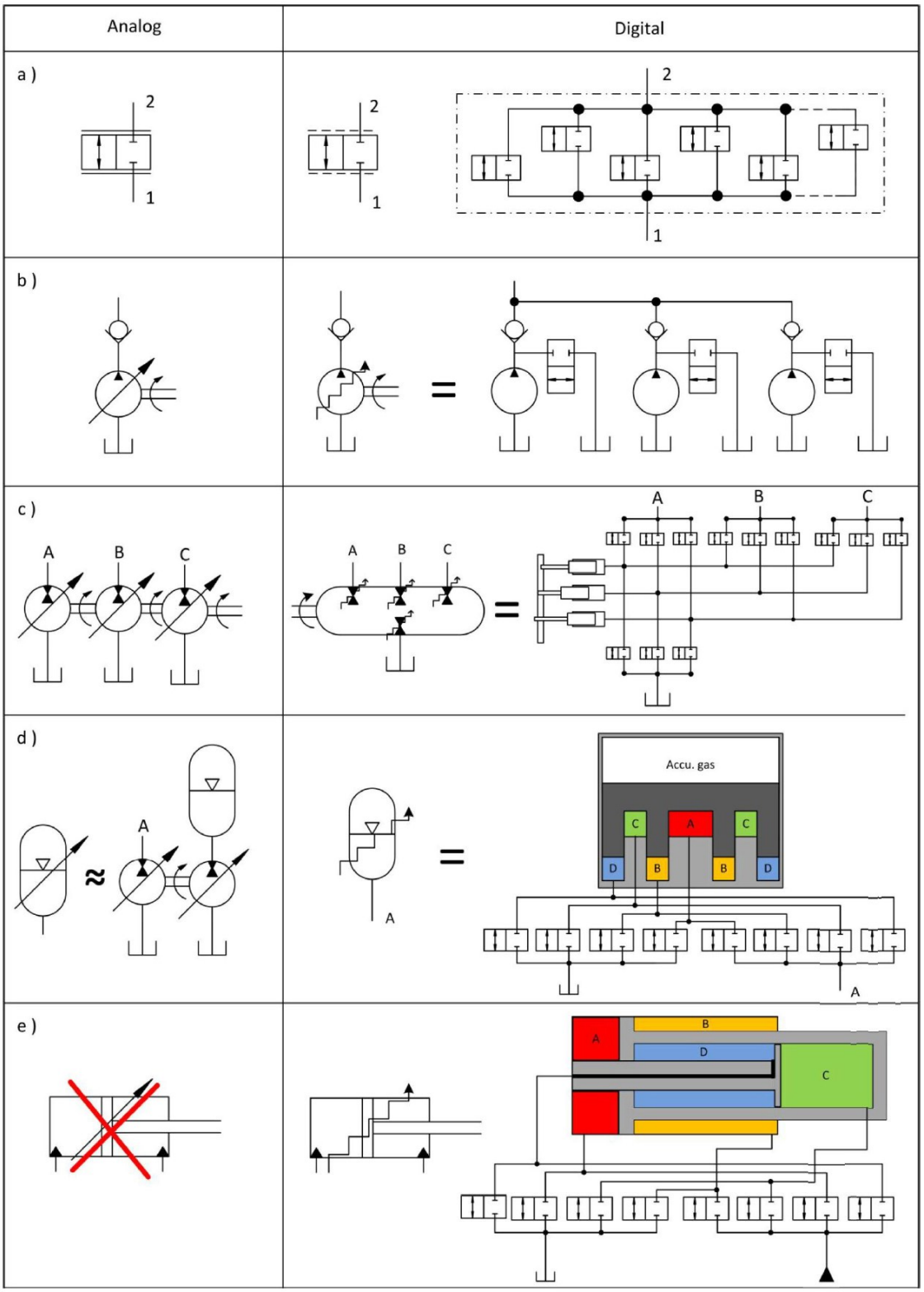

Figure 5. Analogue and digital versions of control edge, pump, power management system, variable accumulator and variable displacement cylinder [11]

As presented in Figure 5, it is possible to achieve digital control versions of each analogue component a) - d). In addition, new hydraulic components, such as variable displacement cylinder, can be invented as shown in row e). This brings a table of new opportunities with it. Next, examples of novel digital hydraulic systems utilizing these digital components are further discussed in the following sections of this chapter.

2.3.2 Hydraulic Switching Control

Hydraulic switching control techniques have been reviewed by Scheidl et al. in [17]. The concept is based on fast digital switching valves. The state of these valves can be controlled by pulse width modulation (PWM), which makes the control system simple and robust. One variation of hydraulic switching control is so called Buck converter [18]. The main idea is to produce required mean flow by rapidly switching 2-way valves on pressure and tank lines. Idealized schematic of the system is presented in Figure 6.

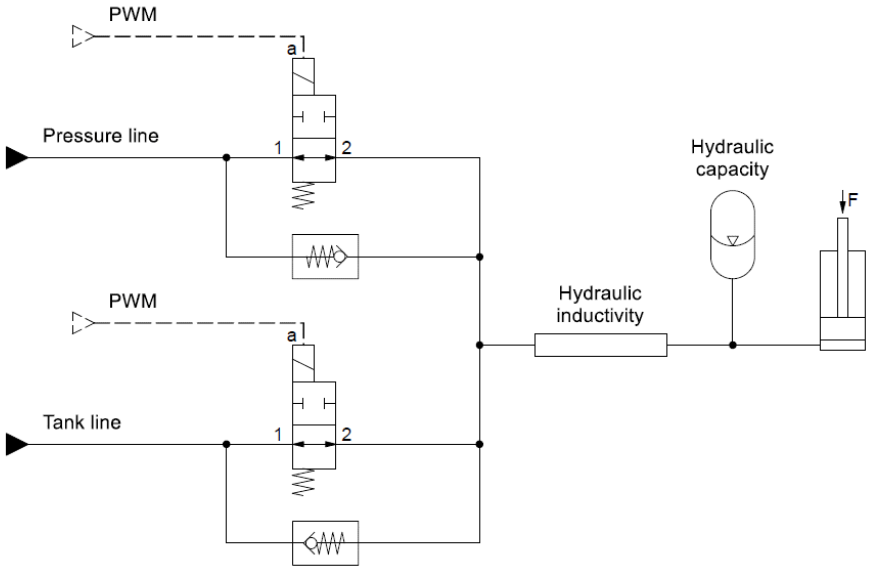

Figure 6. Hydraulic buck converter [18]

The main components of the system presented above are the two valves, inductance pipe, accumulator, and single action cylinder. Hydraulic inductivity is defined by the length of the pipe and capacity by the volume of the accumulator. The first experiments conducted in [18] show that the Buck converter can reach efficiency of 76%, thus significantly improving hydraulic system efficiency compared to proportional valve system. However, this can be achieved only if a certain level of flow rate is achieved. Too low or too high flow rate will decrease the efficiency. In addition, the two-valve setup has some significant disadvantages, including pressure losses over valves and high-speed demand for valve switching. Moreover, the timing of the opening and closing the two valves has a remarkable influence on efficiency and possibility of cavitation. Therefore, the two valves have to be very precisely controlled, which might be challenging. [18]

2.3.3 Digital Flow Control Unit

Digital Flow Control Unit (DFCU) can be considered as a basic unit in digital hydraulics [2]. The DFCU consist of multiple parallel on/off valves which can be operated by different methods. One of these methods is so-called Pulse Code Modulation (PCM). In PCM, the

valve states are defined by binary series, and if each valve has an individual flow rate capacity, the number of different outputs is 2^N, where N is the number of on/off valves. A DFCU unit with four valves is presented in Figure 7.

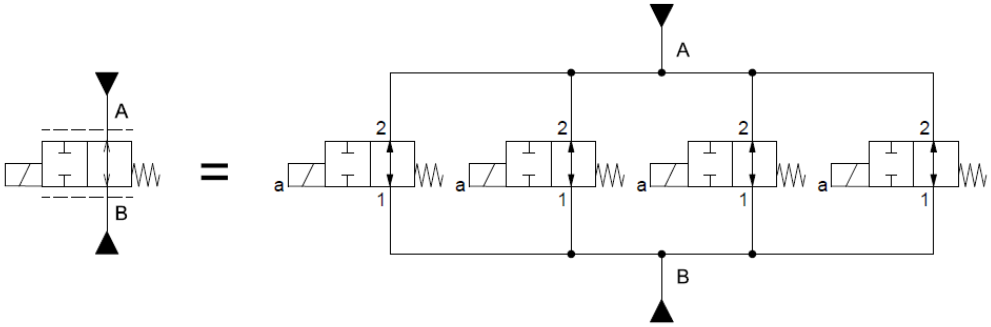

Figure 7. DFCU with four control valves [19]

The advantages in using on/off valves instead of proportional valves are low manufacturing costs, reliability, insensitivity for dirt and minimal leakage. The control electronics are also simple. However, on/off valves are also related to certain challenges, such as noise, possible pressure peaks and discrete force output. Nevertheless, combining digital on/off valves into DFCU units can provide a good motion control, even with slow-response valves, and longer lifetime compared to hydraulic switching control. [19]

DFCU can be applied to any digital hydraulic control system, and its behaviour can be defined by configuring a suitable number of valves. These can have same or different flow rate areas with each other. The main advantages of using DFCU are good fault tolerance, easy programmability, and excellent energy efficiency. The measurement analysis of four valve DFCU system in [20] show that energy losses can decrease by 53 – 71% compared to a conventional LS system, in which proportional control valves are used.

2.3.4 Digital Valve System

Digital Valve System (DVS) can be used as a digital alternative for traditional hydraulic components, such as proportional control valve. Typical DVS consists of four DFCUs and is able to control each flow path independently [9]. This is demonstrated in Figure 8.

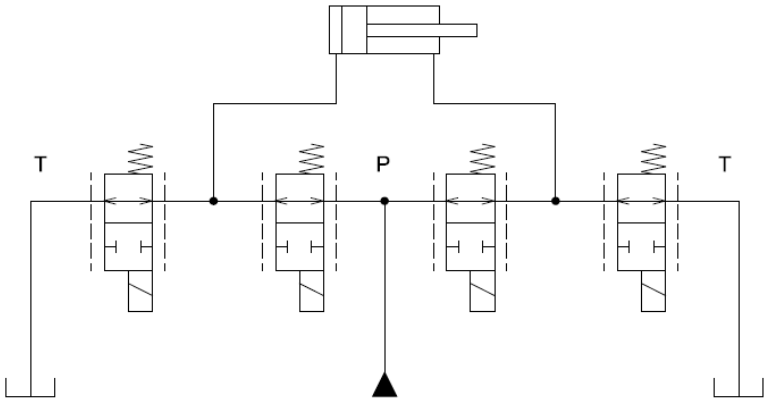

Figure 8. DVS with four DFCUs [21]

Linjama and Vilenius studied velocity control of a DVS with four DFCUs in [21]. Their test results imply that the tracking performance is comparable to traditional servo systems in high velocities, but good servo systems perform better at lower velocities. Nevertheless, the DVS has the benefits of on/off valves, as described in previous section, and performing well in this area might compensate less accuracy at lower velocities in certain applications. In addition, with robust controller and fault detection and diagnosis (FDD) tools, the DVS is able to operate even if some of the valves are not working at all [9]. This might be a superior feature in applications, in which the machine operates continuously 24 hours in a day.

Siivonen et al. experimentally tested FDD for DVS in [22]. Researchers caused some pre-defined faults in the system and tested reconfiguration of the controller for compensating the faults. Their results showed that the system was capable of working with these faults, and only small negative effect was seen in the performance. The system was also able to function even with the most serious faults. Therefore, it can be concluded that DVS with active online FDD tools can be very effective for fault compensation, and can make the system highly fault tolerant.

2.3.5 Multi-Chamber Cylinder

One way of digitalizing a hydraulic system is to replace a traditional cylinder with a multi-chamber cylinder. While the traditional cylinder is based on two pressure chambers and is controlled by a proportional valve, the multi-chamber cylinder has multiple pressure chambers and utilizes digital on/off valves in flow control. This adds the benefits of a non-throttling DVS into the system, but enables a force control as well. Linjama et al. presented secondary control method for this type of multi-chamber cylinder in [23]. The system overview is presented in Figure 9.

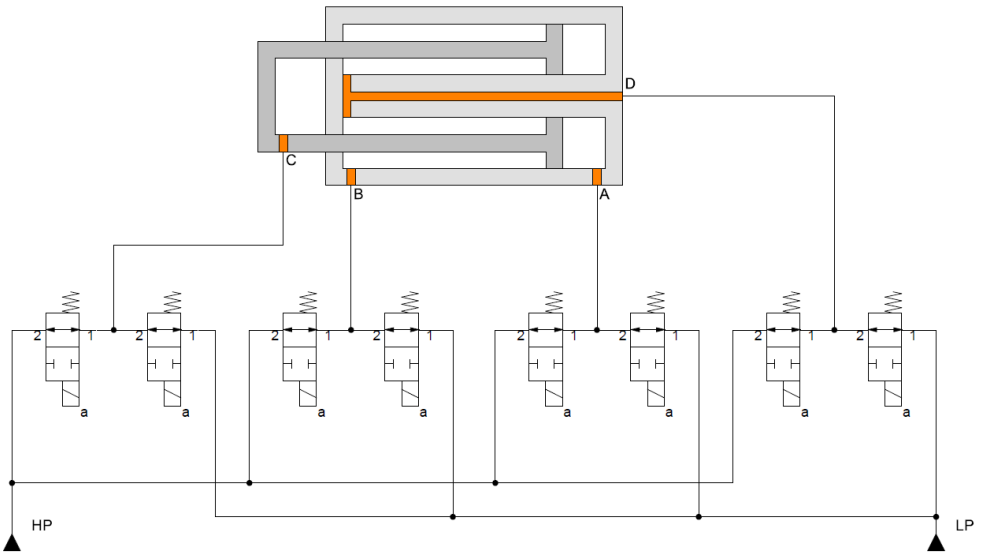

Figure 9. Multi-chamber cylinder with four chambers and two pressure levels [23]

With a multi-chamber cylinder consisting of four chambers and two pressure sources, as shown in Figure 9, it is possible to achieve 16 discrete force levels. If the number of supply lines is increased, the number of force levels becomes $N_{\text{supply}}{}^{N_{\text{chambers}}}$ [15]. Therefore, the resolution can be defined as needed for each application. According to the experimental measurement results in [23], it is possible to achieve 60% reduction in power losses with a

multi-chamber cylinder compared to a traditional LS system. In addition, it is shown that the pump can be dimensioned for the average power demand instead of peak power demand. This offers significant advantage compared to traditional systems, as less expensive and smaller components can be used in the same application. However, the controllability of the cylinder in low speed is not as good as it is with well-tuned proportional valve. Nevertheless, this can be improved with more sophisticated controller and more carefully selected system parameters such as valve sizes, chamber area ratios, hydraulic capacitances, and inductances. [23]

Huova et al. also studied multi-chamber cylinder efficiency in [24]. Their setup included three-chamber cylinder and DVS for controlling it. The DVS consisted of two DFCUs for each cylinder chambers. One is used for connecting the chamber to high pressure line and the other for connecting to low pressure line. Therefore, the system can use nine pressure states and the velocity of the cylinder is determined by DFCU setting. Results of this study indicated that energy losses could be reduced up to 66% compared to a LS system.

2.3.6 Digital Hydraulic Transformer

A Digital Hydraulic Transformer (DHT), connected to a hydraulic cylinder, operates almost similarly as the multi-chamber cylinder discussed in the previous section. Instead of using an integrated multi-chamber structure in the cylinder, the pressure series are produced with a separate DHT unit. Bishop has discussed this concept in [25] and [26]. A simplified operating principle of the DHT is presented in Figure 10.

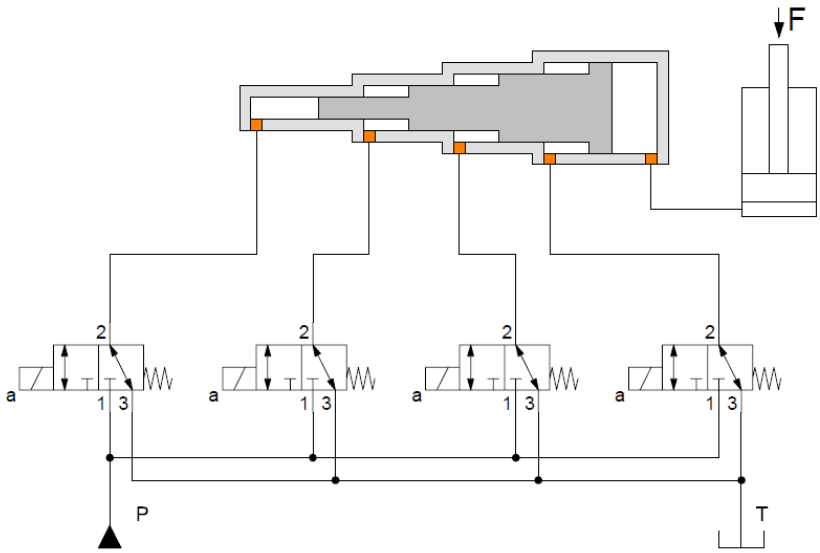

Figure 10. Digital Hydraulic Transformer [25]

As demonstrated in Figure 10, a high-pressure line is connected to four 3/2 valves, which are digitally controlled. These valves determine the state of DHT from the binary series given by controller. With this type setup, fifteen different pressure combinations can be selected for the working actuator. However, the force can be applied only in one direction. For producing force in both directions and enabling the four-quadrant actuator operation, Bishop has proposed a double acting DHT solution in [25]. The double acting DHT concept is presented in Figure 11.

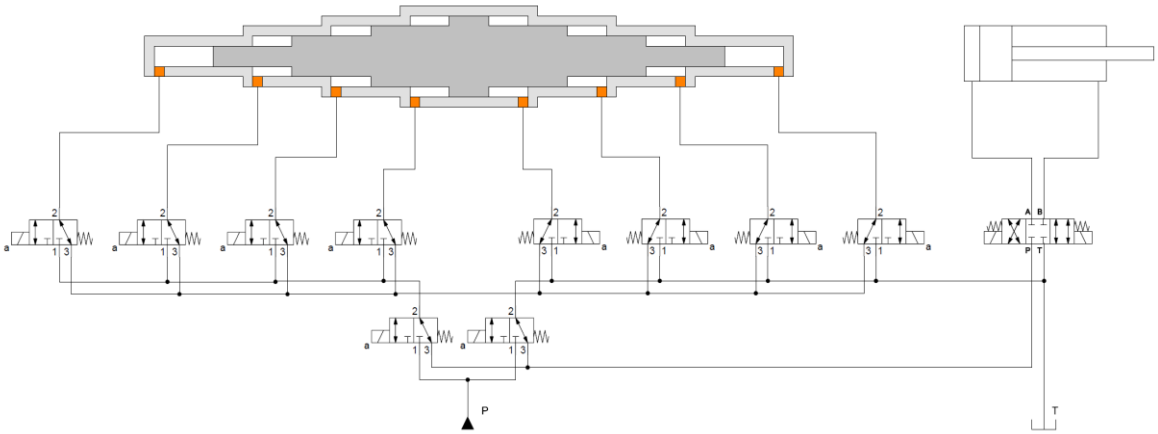

Figure 11. Double acting, four-bit DHT [25]

With this type of double acting DHT, it is possible to achieve 143 unique transformation ratios and the four-quadrant operation. If the cross-section areas are A, 2A, 4A and 8A, the transformation ratios can vary from 0.667 to 15 [26]. The main disadvantages of DHT, however, are bulky design, relatively high manufacturing costs and pressure spikes at valve switching. These problems concern both the single and the double acting DHT. Moreover, the seal friction force is quite high due to increased sliding surface area. Therefore, friction losses can consume a significant proportion of power at low working pressures. [25]

2.3.7 Independent Metering

An independent metering (IM), sometimes referred as a Separate Meter-In, Separate Meter-Out (SMISMO), is a method for an independent pressure and flow rate control of individual hydraulic ports [27] [28]. However, IM is not a very novel technology, as it has been used in heavy-duty industrial applications [27]. Nevertheless, energy efficiency study of IM with 3-way proportional valves was introduced by Mattila and Virvalo in [27]. Their test setup is shown in Figure 12. The idea was to control cylinder chambers independently for achieving more energy efficient closed-loop control system. With an independent chamber control, the pressure drop across control edges can be decreased by minimizing back-pressure on the other cylinder chamber [15]. The results showed that the tested IM design improves controllability, and thus, the supply pressure could be decreased. This leads to lower energy consumption, since conventional systems requires higher supply pressure for achieving the same accuracy. The test results showed direct 15% energy savings with independent metering compared to traditional system. [27]

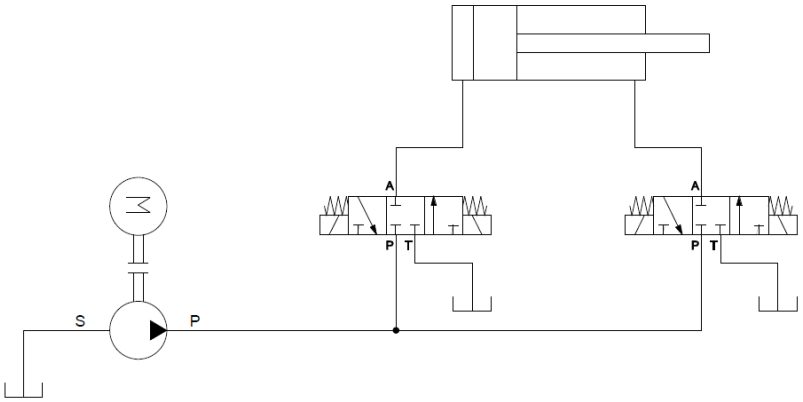

Figure 12. Independent metering with 3-way proportional directional valves [27]

Furthermore, an Independent Metering Valve (IMV) and method for controlling it was introduced in [29]. The system control was based on 2/2 valves. As described in the patent, IMV allows the valve to be controlled electronically and independently from other valves [29]. Energy efficiency of this type IMV, applied in an excavator, was studied in [30]. Schematic of the studied IMV system is presented in Figure 13. Simulation results showed that energy savings up to 44% in boom-down and 21% in arm-down motion could be achieved [30].

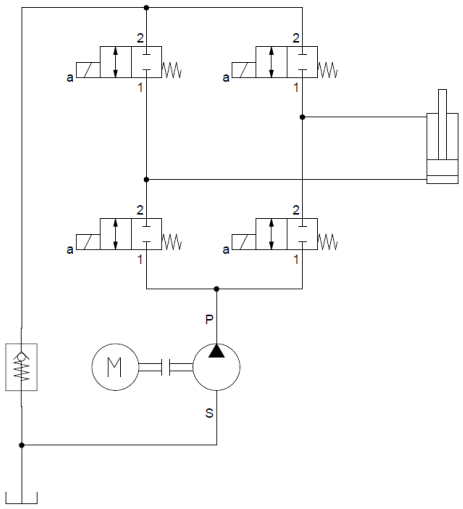

Figure 13. IMV based on 2/2-valves [30]

2.3.8 Digital Hydraulic Pump-Motor

Conventional piston-type pump operation is based on valve-plate, and the displacement per revolution is adjusted by changing the stroke of the pistons. This is done by changing angle of the plate in which pistons are attached. Thus, the change in plate angle will make corresponding adjustment to the piston stroke. The efficiency of this type conventional pump is dependent on plate angle and is usually significantly lower at small displacements. Digital version of this type of pump, however, has digitally controlled on/off valves for activating the required number of pistons. Active pistons will produce a full displacement while the other pistons idle. In addition, the concept allows independent metering the same way as discussed in previous section. An idealized schematic of a digital hydraulic pump with two independent outlets is presented in Figure 14. [4]

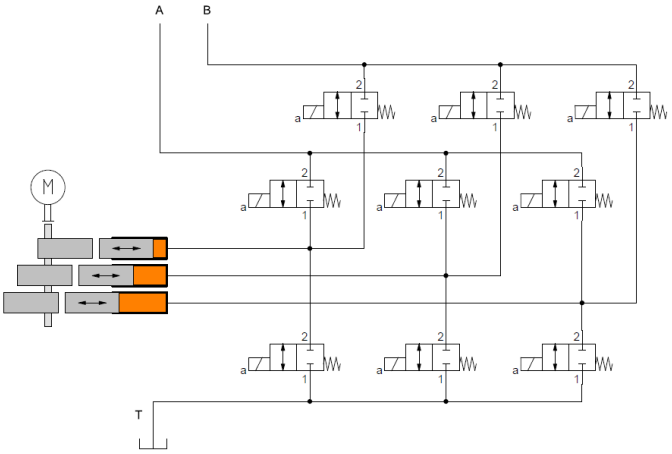

Figure 14. Digital hydraulic pump with two independent outlets [10]

The main advantage of using digital hydraulic pump is the programmability and ability to control outlets independently. The yielded energy savings can be remarkable, since unnecessary pistons can idle while only required number of pistons produce flow rate. [10]

2.3.9 Digital Hydraulic Power Management System

The Digital Hydraulic Power Management System (DHPMS) offers the IM capability by binary series. The Digital Hydraulic Pump-Motor with independent outlets (Figure 14) discussed in previous section is one version of the DHPMS. The other versions reviewed in this section are based on fixed displacement pumps. One example of fixed displacement pump DHPMS is presented in Figure 15. [31]

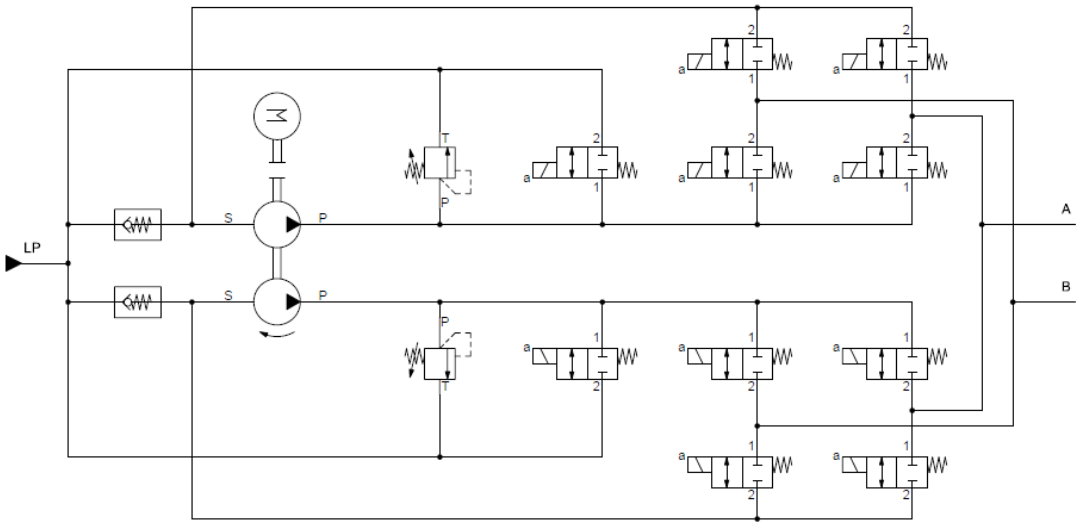

Figure 15. DHPMS based on fixed displacement pumps [31]

As shown in Figure 15, the system consists of two fixed displacement pumps and ten on/off valves for enabling required flow paths. This is the key feature in DHPMS and allows the use of independent metering. Examples of some possible flow paths are demonstrated in Figure 16.

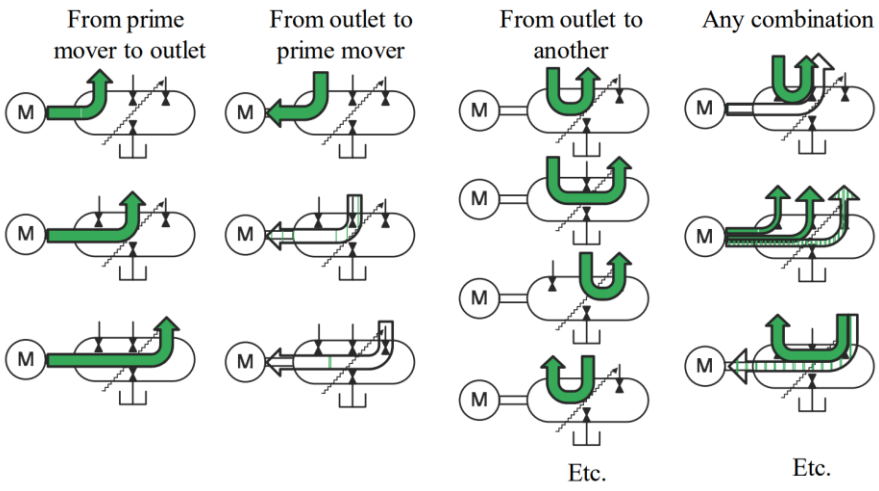

Figure 16. Flow path examples of four-port DHPMS [32]

Heikkilä et al. conducted an experimental evaluation of a piston type DHPMS in [33]. The system had similar working principle as the one presented in Figure 14. The prototype used in the study, however, consisted of six-piston boxer pump, fast on/off valves and two independent outlets. The results of this study implied that the use of DHPMS can enable significantly better efficiency compared to traditional hydraulic systems due to its extended functionality. However, the amount of this improvement is highly dependent on the application. [33]

2.3.10 Displacement controlled system

In a displacement controlled (DC) system, the actuators are controlled by variable displacement pump/motors. The concept offers potential for energy saving, since the throttling losses can be minimized and the system pressure is always close to optimal because of the load-dependent pressure setting [4]. The structure of a simple DC actuator is presented in Figure 17.

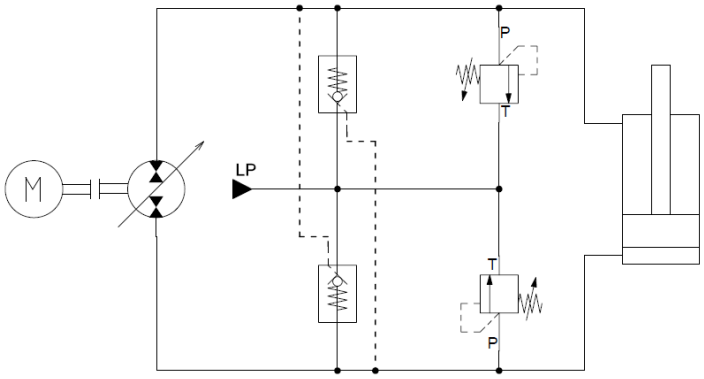

Figure 17. Concept of DC system [34]

DC actuation of hydraulic hybrid excavator has been studied in Purdue University, and several publications have been written about the topic [35]. For example, in [34], productivity and fuel consumption measurements were conducted, and the results indicated that the DC system prototype excavator consumed on average 40% less energy than a conventional LS system. In addition, the researchers found that the DC excavator had 17% better productivity in moving dirt per hour. Furthermore, the better efficiency yielded significantly lower oil temperatures, which leads to possibility for decreasing hydraulic cooling power even by 50%. [34]

After achieving promising results in [34], the following research introduced a DC series-parallel (DC S-P) hybrid configuration, which offered further energy savings in the DC system. With the DC S-P, the total efficiency was up to 50% better than that in an LS system [36]. An improved efficiency of the DC S-P system is based on an accumulator added to the system, which enables energy recovery feature. Furthermore, an advanced control algorithm for the DC actuator was investigated in [37]. The implementation was concluded to be not only effective, but also implementable for other applications than excavators.

However, one of the main disadvantages of the DC system is that each actuator needs its own pump/motor unit, which makes the system bulky and more expensive than traditional LS system [38]. To overcome this issue, Busquets and Ivantysynova proposed a pump switching technique. The system is based on flow distributing manifold, consisting of digital

on/off valves which can direct the flow to the selected actuator. The structure of this type of multi-actuator DC system is presented in Figure 18.

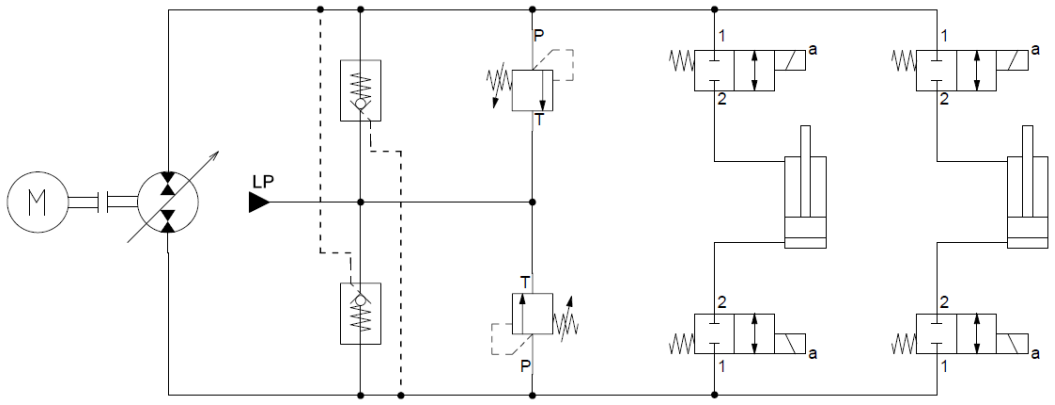

Figure 18. DC multi-actuator system [38]

The multi-actuator DC system presented in Figure 18 can offer the benefits of the initial DC system for multiple actuators without a need for separate pump/motor unit.

2.3.11 Direct Driven Hydraulic Drive

Instead of using a variable displacement pump as in DC system, a speed-controlled motor can be utilized in pump-controlled systems. The pump in this case is a constant-displacement pump and the flow rate is controlled by a frequency converter, which determines the rotational speed of the servo motor. The Direct Driven Hydraulic (DDH) concept is based on this idea. Constant displacement pump/motors are connected directly to cylinder chambers, as shown in Figure 19. [39]

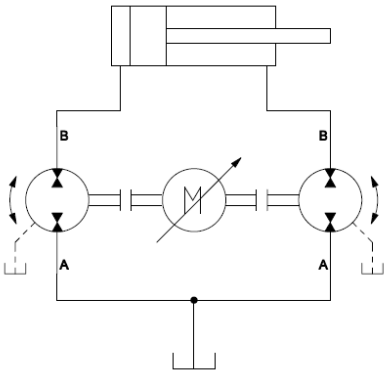

Figure 19. Working principle of Direct Driven Hydraulic Drive [39]

In the DDH with two constant displacement pump/motors, as in Figure 19, the displacement ratio of the two pump/motors must match the cylinder chambers area ratio in order to keep the system balanced. However, this might be difficult to achieve due to relatively large manufacturing tolerances in pump/motors. These displacement errors may cause unexpected pressure peaks in the system with a fast movement or long strokes. The system pressure is determined by the cylinder load, and the flow rate is controlled with a frequency converter connected to the brushless servo motor. This allows the four-quadrant operation, and it is possible to recuperate energy by using servo motor as a generator. The experiments conducted by Minav et al. in [39] show that DDH setup could work up to 73% efficiency in lifting motion. However, the lowering efficiency was only 12 – 29% due to inefficient

performance of the motor/pumps and no energy recuperation was implemented in this experiment. [39]

Further research of DDH presented improved system without a conventional oil tank. The setup was similar to the one in Figure 19, but the oil tank was replaced with an accumulator. In addition, another smaller accumulator was added to the rod side of the cylinder in order to compensate displacement errors of the pump/motors. Simulation results of the research indicate that the chosen approach was appropriate for flow compensation and significantly better efficiency can be achieved compared to traditional valve-controlled system. [40]

DDH systems could be used not only in industry, but in non-road mobile machines (NRMM) as well because of the high power density and accuracy of the electric motor [41]. Keeping that in mind, the DDH system efficiency has also been studied in sub-zero temperatures in [42] and [43]. These experimental studies showed that the energy consumption increased more than twice in sub-zero temperatures compared to the room temperature, since hydraulic losses increased from 20% to 50% and hydro-mechanical losses from 14% to 26% [42]. However, as proved in [43], the performance of a DDH system can be significantly improved in cold temperatures by utilizing a standard-quality oil to a high-performance oil.

2.3.12 Hydraulic Energy Recovery System

Hydraulic energy efficiency can also be improved by using hydraulic energy recovery systems. This is especially interesting in zero-energy processes, in which the ideal system could perform without external energy input once the system has been started. For example, in lifting-lowering applications, the same amount of energy is used for lifting, and then released in lowering. This is the case in this thesis as well. If the released energy can be fully recovered, theoretically no energy has been consumed and no output work has been done [44]. Keeping this in mind, Hänninen studied hydraulic energy recovery systems for a reach truck in [45]. One suggested solution was so-called Direct Hydraulic Recovery System (DHRS), in which energy is recovered into hydraulic accumulator during lowering phase. The stored potential energy can then be re-used for lifting motion. The DHRS operating principle is shown in Figure 20.

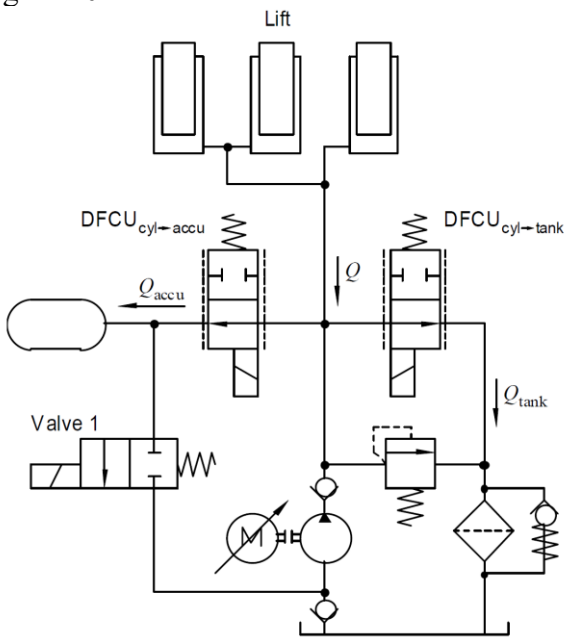

Figure 20. DHRS operating principle [45]

The DHRS is operated by a speed-variable electric motor in lifting motion and a DFCU in lowering motion. This enables an accurate velocity control with minimal leakages. In lowering motion, the DFCU guides the flow to the accumulator. If the accumulator maximum capacity is reached, the rest of the flow is guided to the tank. The maximum capacity depends on cylinder load because with higher load the cylinder is capable of charging the accumulator with higher pressure. The recovered energy can then be used to assist pump in lifting motion. The system controller was implemented in electronic control unit (ECU), and the control algorithm was based calculation of a cost function. Experimental results showed 10% reduction in power consumption compared to the original proportional control valve system of the reach truck. [45]

Another suggested energy recovery system was so-called Indirect Hydraulic Recovery System (IHRS). The system components were identical to the DHRS but the accumulator side DFCU was replaced with a hydraulic transformer as shown in Figure 21. The hydraulic transformer consists of a fixed displacement hydraulic motor, coupled with a variable displacement pump. The lifting velocity is determined by swash plate angle of the variable displacement pump. [45]

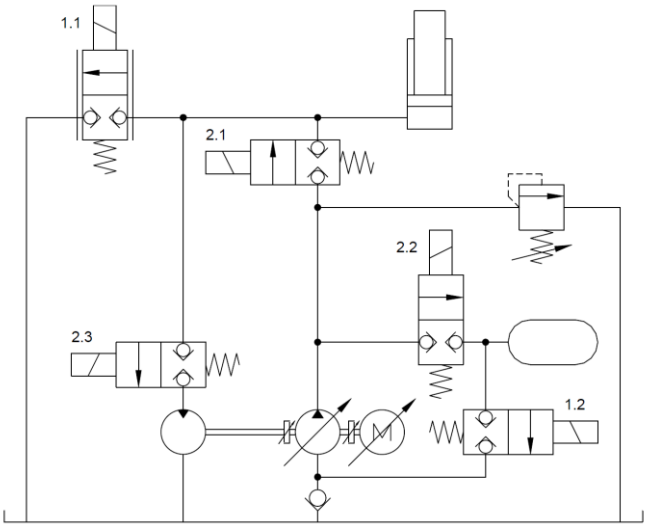

Figure 21. IHRS operating principle [45]

IHRS design allows higher lifting velocity in low load cases than DHRS, but it also offers better energy saving capability. Although the total throttling losses were higher compared to DHRS, the average reduction in power consumption was 28%. It was also noticed that the energy efficiency of IHRS was highly dependent on lifting velocity. With higher velocity, the throttling losses increased significantly. [45]

2.3.13 Digital Hydraulic Multi-Pressure Actuator

A Digital Hydraulic Multi-Pressure Actuator (DHMPA), the device studied also in this thesis, was first time realized by Huova et al. in [46]. This first practical experiment of the DHMPA was motivated by promising feasibility analysis provided by Linjama et al. in [47]. The idea of the DHMPA resembles multi-chamber cylinder and digital hydraulic transformer, since these all are based on discrete pressure levels which are selected digitally by binary series. However, the principle of DHMPA is different, as it stores energy locally to an accumulator, which is then used as a primary power source. This offers a similar energy recovery capability as discussed in Section 2.3.12. Intermediate pressures between

accumulator and tank line pressure are generated by piston type pressure converters. Only average power is required from the pump unit and it is controlled by digital on/off signal. Simplified working principle of the DHMPA concept is presented in Figure 22.

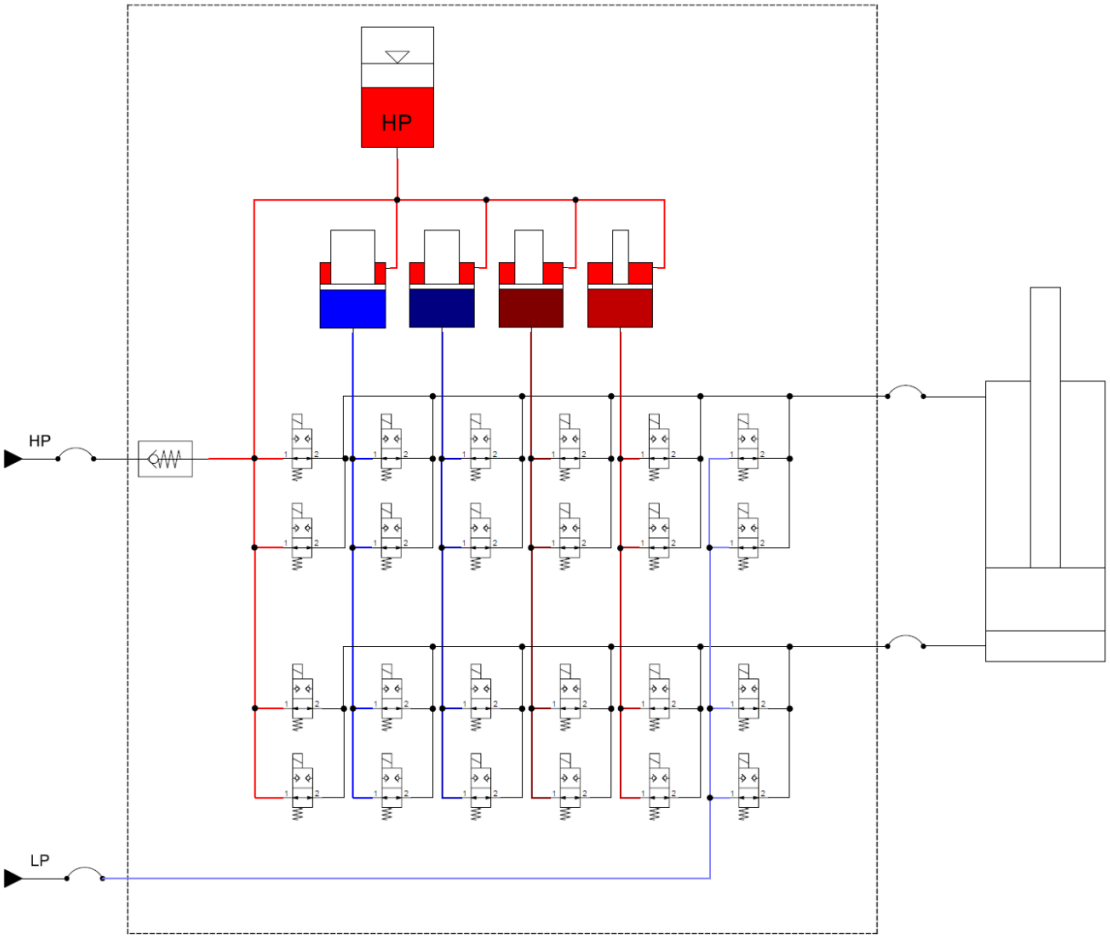

Figure 22. Working principle of DHMPA [48]

As shown in Figure 22, the DHMPA unit is connected to a high and a low-pressure source (HP, LP). The system operates in a certain working pressure area, limited by $p_{\min}$ and $p_{\max}$. HP line supplies flow rate to the HP accumulator, and once $p_{\max}$ threshold is reached and the accumulator is charged, the controller turns the HP supply off. It will be turned back on when the HP line pressure decreases below minimum pressure $p_{\min}$. The HP accumulator is the primary power source of the system, and it is connected to four pressure converters. Together with these and the LP source, the system has total of six pressure levels, yielding 36 different output force combinations by using a differential cylinder. Therefore, the cylinder velocity can be controlled with 36 discrete force steps, generated by the pressure combinations of the six pressure levels. The size of force steps is determined by the HP pressure level and area ratios of the pressure converters and the working cylinder. The flow paths are determined and set by the controller. Different control strategies for the DHMPA control have been discussed in [46], [8] and [48].

One of the main advantages of the DHMPA is the ability to provide a high peak power with minimum power losses, while only an average input power is fed to the system [46]. The power losses were further investigated through practical experiments conducted in [8]. The

results were highly promising, indicating energy losses reduction up to 77% compared to traditional four-way proportional LS-system. The experimental system setup and its partial losses are shown in Figure 23.

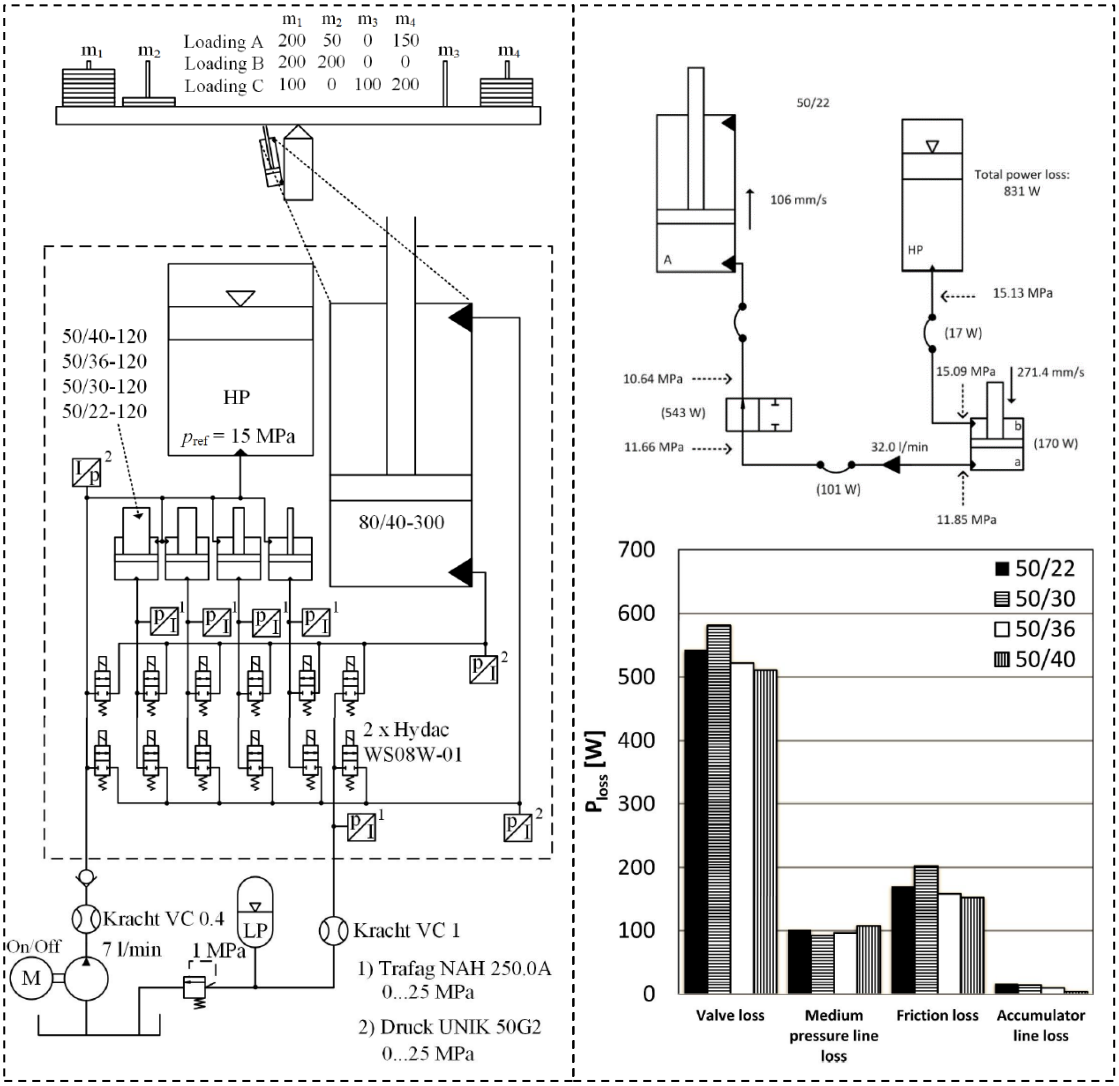

Figure 23. Experimental system setup (left) and partial losses (right) of DHMPA [8]

As shown in Figure 23, the major losses occurred in valves with proportion of 66%. This is emphasized in high actuator velocities, as valve losses are proportional to flow rate. Flow rate from the accumulator in this case was 32.0 L/min, except for 50/30 converter it was 32.6 L/min. Each bar in the loss chart represents single energy path through each pressure converter. It can be noticed that the size of hydraulic converter does not have significant effect on losses, and the difference in 50/30 cylinder can be explained with slightly different flow rate. Medium pressure line composed 12% of total losses, cylinder friction 21% and accumulator line only 1%. [8]

As the DHMPA is capable of regenerating energy, the system has to be able to utilize negative flow rate also from LP line towards HP line. Otherwise, only converter pressure levels would be available for regeneration control. The reversed flow from the LP line is enabled by pressurizing it with an accumulator. A simple and common way of implementing this is to utilize a PRV together with the accumulator, before the reservoir connection as

shown in Figure 23. However, the PRV loses energy, so for achieving better efficiency, Paloniitty et al. introduced a compact and energy efficient solution for pressurizing a tank line in [49]. Their idea was to remove the tank and PRV entirely and replace it with LP accumulator as shown in Figure 24.

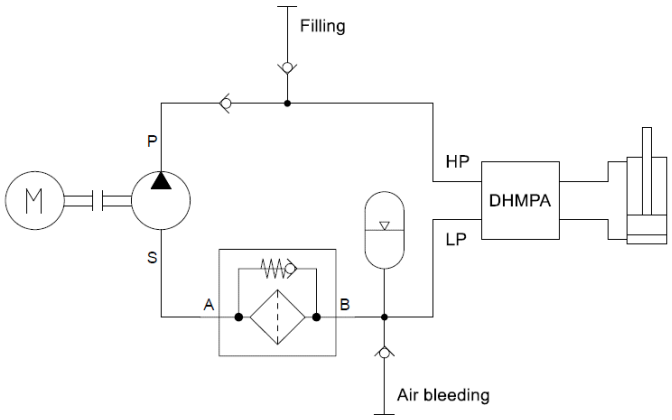

Figure 24. The tankless implementation of the DHMPA [49]

The tankless implementation of the DHMPA was shown to be more energy efficient than the PRV-tank setup. Furthermore, the system was more compact, and no unexpected problems arose in experimental tests. However, it is worth to notice that a pressurized LP line with a direct connection to pump's suction inlet requires a special sealing in the pump, which is designed for a high suction line pressure. In addition, the LP accumulator has to be able to contain all the hydraulic oil that can be discharged from the HP accumulator and working cylinder. As there is no reservoir in the system, the hydraulic fluid could be filled through a filling port and the air was removed from a separate bleeding port. [49]

The latest implementation of the DHMPA was studied in [48]. One of the main targets in this study was to improve the design by decreasing the complexity of the system. The results showed up to 79% decrease in power losses when compared to proportional valve system with constant pressure pump, and 64% when compared to LS system. However, the losses slightly increased compared to previous implementation of DHMPA due to smaller capacity on/off valves. The energy loss comparison is shown in Figure 25. This implementation was contained a tank and PRV connection, so the achieved efficiency could even be increased by using tankless LP line as described in the previous paragraph.

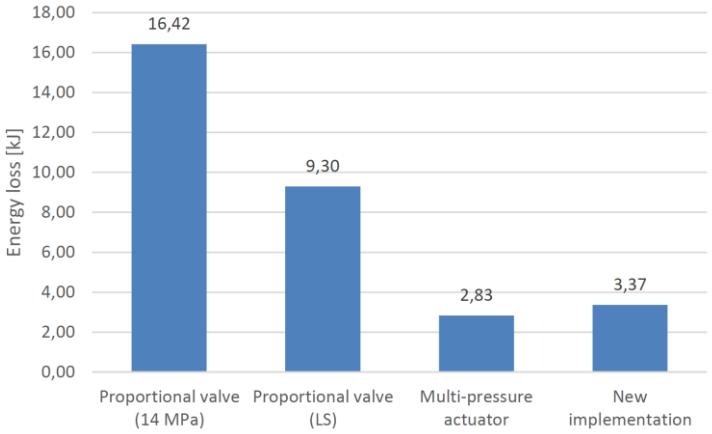

Figure 25. Energy loss comparison between proportional valve system, LS system and DHMPA unit [48]

The production costs of this type of hybrid actuator are considerably higher than those in traditional LS system, and cost reduction through fuel savings by prime mover are highly dependent on the application and its duty cycle [8]. On the other hand, the pump unit required for the DHMPA can be smaller capacity than that in the in LS system and it can a be simple constant flow rate pump, leading to considerably lower pump unit costs. Altogether, it is not clear if the DHMPA is cost-effective in any case, but it can offer excellent energy efficiency. In addition, through further development of the DHMPA, the manufacturing costs could be reduced to a lower level. For now, the energy efficiency and loss analysis have shown highly promising results, superior to other digital hydraulic solutions discussed previously in this section. However, only proof of concept device has been built and the it has been tested only with mid-size NRMM boom mock-up [8] [46] [47] [48] [50] and a swing function of a micro-excavator [51] [52]. Therefore, this thesis will further investigate the energy efficiency of the DHMPA in pure load-lifting application.

3 Setup Description

3.1 *Digital Hydraulic Multi-Pressure Actuator*

The aim of this thesis is to determine the efficiency of the DHMPA unit by measuring the energy consumption in load-lifting application. In order to achieve this aim, it is essential to understand the working principle of the test unit. Section 2.3.13 presented general operation and reviewed previous research of the DHMPA. Now, this section reviews the DHMPA unit used in this test further in detail.

Figure 26 shows the realization of the DHMPA unit with six pressure levels. This is the configuration used in this study. The main components of the system are high-pressure accumulator, pressure converters, and on/off valves. These are implemented in a common valve block. The six pressure levels consist of HP and LP inputs together with the four intermediate pressures, generated by pressure converters. The HP line is connected to a constant flow pump that provides the input power to the system. The LP line is connected through PRV to the tank. Work port A is connected to the piston-side and port B to the rod-side of the cylinder.

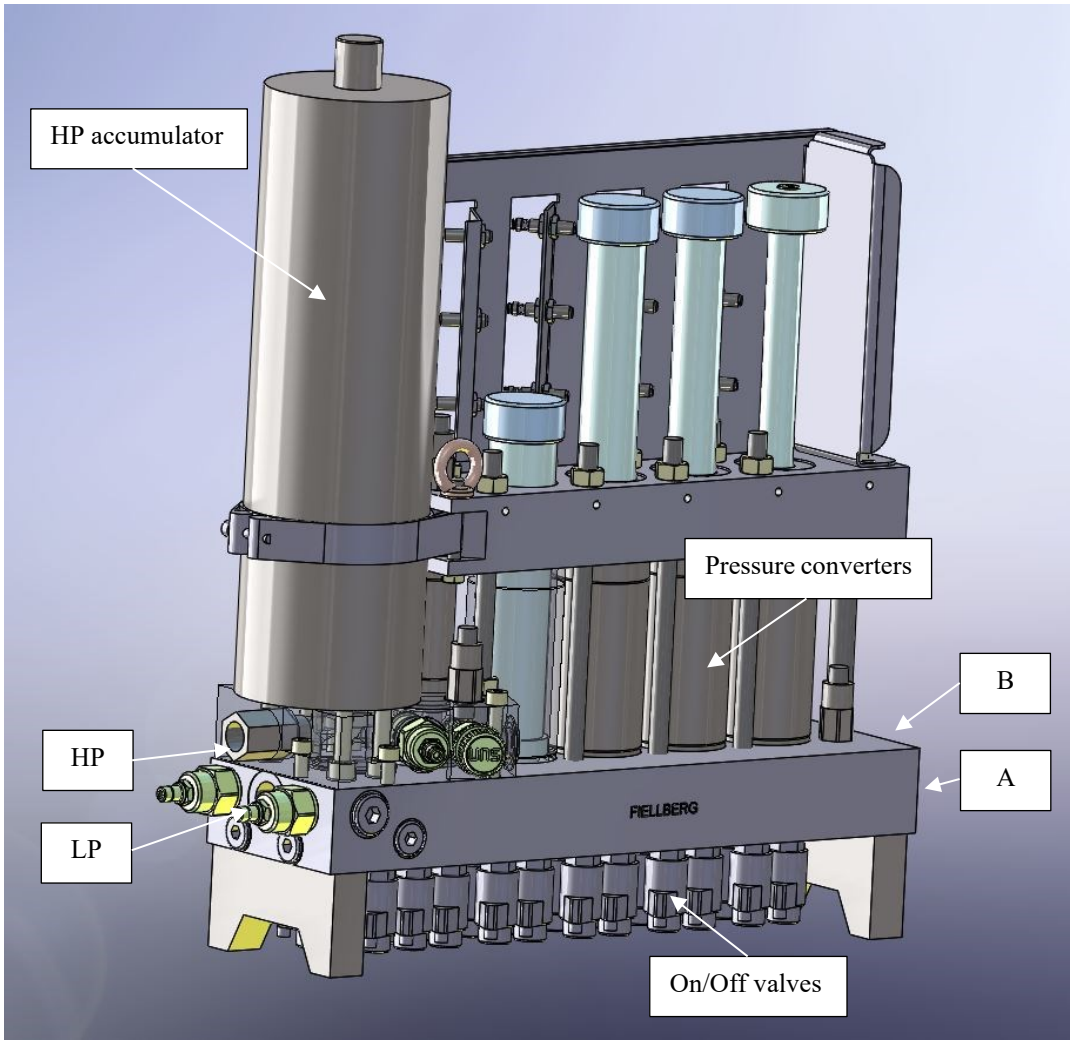

Figure 26. CAD model of the DHMPA unit [51]

Because the pressure levels generated by the pressure converters are dependent on the HP accumulator pressure, the magnitude of these changes during the work cycle as the HP pressure changes between $p_{\min}$ and $p_{\max}$. In this test case, the corresponding pressures limits are 10 and 14 MPa. As the LP line pressure is set to 1 MPa, and the converter dimensions are known, the resulting pressure series can be calculated. These pressure series are shown in Figure 27.

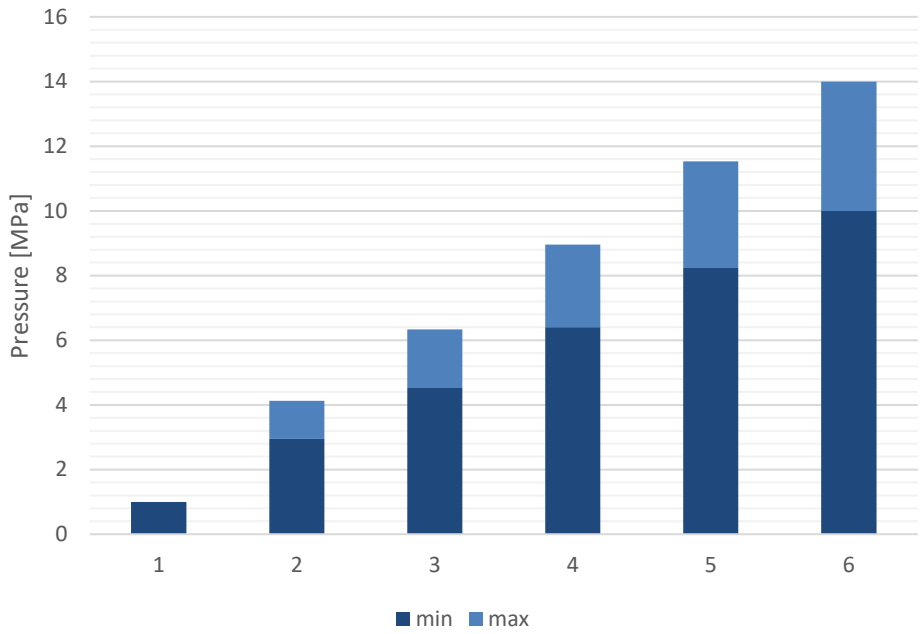

Figure 27. Pressure series of the DHMPA

The pressure series show the range of pressure variation in each pressure converter. When the HP accumulator is charged and the HP pressure level reaches 14 MPa, the maximum pressures are available in converters as well. On the other hand, as the HP decreases towards 10 MPa, the converter pressures approach their minimum pressures as well. The LP pressure is adjusted by the PRV, so it remains approximately constant while the other pressure levels change.

One of the main advantages of the DHMPA is the minimization of throttling losses in the system by utilizing non-throttling on/off valves. These digital on/off valves are used for directing the flow to the required pressure converters or directly to the working actuator. Therefore, each of the six pressure levels can be connected either to the A or B chamber of the working cylinder. As a consequence, by using a differential cylinder, the DHMPA is capable of producing 36 individual output force levels. The magnitude of these force levels depends on the HP pressure, LP pressure, area ratio of the converters and the area ratio of the cylinder. As shown in Figure 27 , the HP line pressure $p_{\max}$ is set to 14 MPa, $p_{\min}$ to 10 MPa and LP line pressure to 1 MPa. Intermediate pressures are calculated based on pressure converter area ratios, which are 3.40, 2.21, 1.56 and 1.21. The working cylinder is size of 50/36-300 mm, yielding area ratio of 2.08. Based on this information, the corresponding force series used in this thesis are determined in Figure 28.

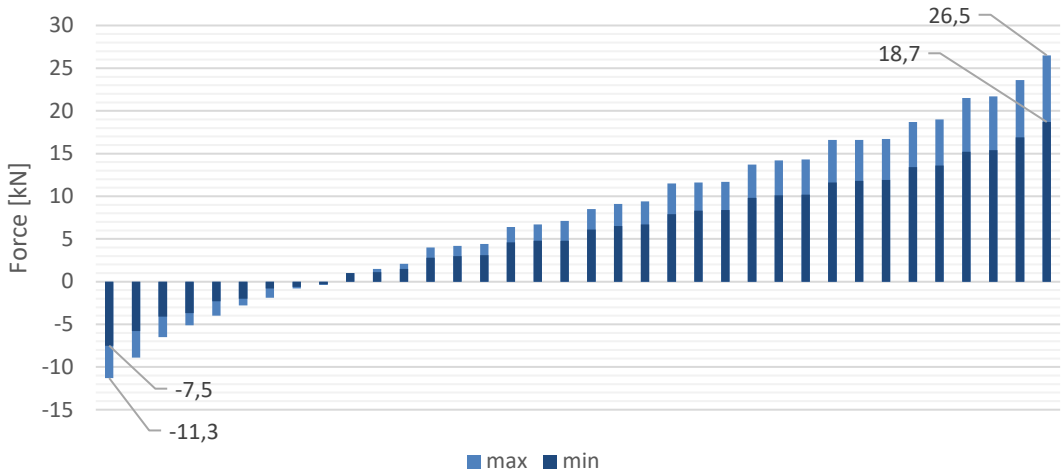

Figure 28. Force series generated by DHMPA

As shown in Figure 28, the maximum output force can be up to 26.5 kN. This is obtained in the extension of the cylinder with $p_{\max} = 14$ MPa . Maximum retraction force on the other hand is -11,3 kN. However, as the HP pressure decreases close to $p_{\min}$, the output forces are smaller as well as shown with the dark blue colour. With $p_{\min} = 10$ MPa, the corresponding output forces are divided between -7.5 kN and 18.7 kN. As the cylinder is placed in rod-up position, a positive force lifts the load-mass while negative force lowers it.

However, the calculations do not consider the effect of the load-mass. For evaluating the forces available for load-mass acceleration, so-called mass-compensated force series are calculated. As the cylinder is placed rod-up position in the test rig, the effect of load-mass can be calculated by subtracting the gravitational force from the generated force series. These compensated forces can then be used for accelerating the load-mass. However, pressure or friction losses are not considered, so the final output forces for acceleration are slightly smaller than the calculated forces. The mass of the load is 1180 kg, yielding a constant force of -11,58 kN. The mass-compensated force series are presented in Figure 29.

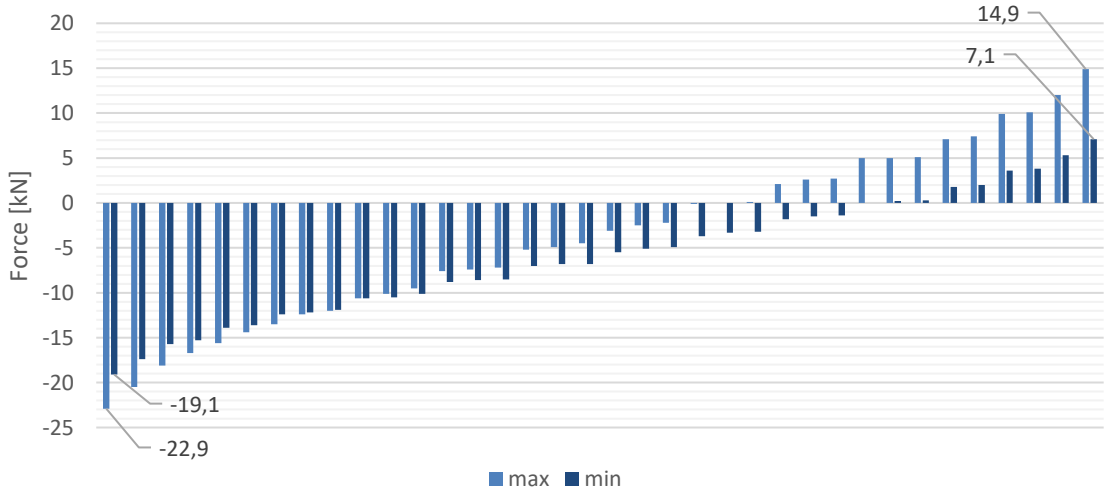

Figure 29. Mass-compensated force series

As Figure 29 shows, the forces are not quite optimally divided for this test setup as majority of the forces are negative, especially with lower accumulator pressure. For achieving an

optimal division of the force levels, the unit should be more specifically dimensioned for this test rig. Nevertheless, for testing purposes and determining the efficiency of the DHMPA unit, the generated force series are sufficient, keeping in mind that they might have some effect on the overall performance.

It is worth noticing that all force levels are not constantly available due to the limited stroke length of the pressure converters. Each pressure converter has a stroke of 120 mm, and once the piston approaches the end position, another pressure level must be chosen. That pressure level remains unavailable until the converter piston is driven backwards, closer to the neutral position. The aim is to keep the converters near these central locations. Nevertheless, as there are more than one almost similar force levels, it is possible to switch to second closest option without compromising the system performance. Furthermore, for driving converter pistons back to zero-position end, so-called crossflow connection can be utilized. This feature enables opening on/off valves so that more than one pressure source is connected to the same side of the working cylinder. This forces the lower pressure converter piston to be driven backwards until the zero position is reached. While the crossflow connection enhances controllability of the DHMPA, it also decreases efficiency as pressure is used only internally, instead of an output work. The crossflow connection is demonstrated in Figure 30. [48]

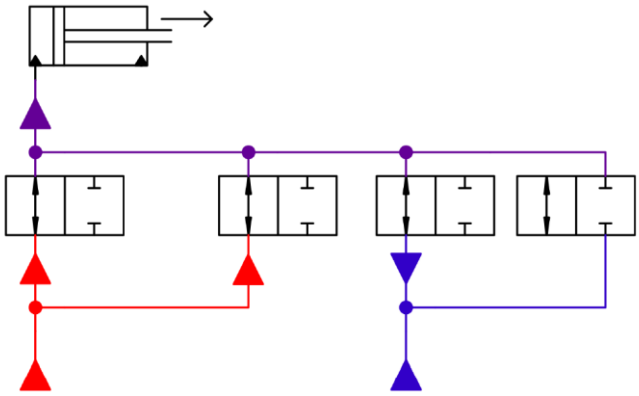

Figure 30. Crossflow connection [48]

As the operation of the DHMPA unit requires real-time calculation, a PLC based controller is utilized, and the control algorithm is implemented in structured text in the control unit. The DHMPA is controlled by EPEC 5050 controller. It is a multifunction controller with 32-bit processor and 65 I/O pins, of which most are so-called multifunction pins enabling programmable interface [53]. EPEC 5050 also includes CAN-bus communication, which in this case is used as an user interface communication for the DHMPA. The control structure of the DHMPA is presented in Figure 31.

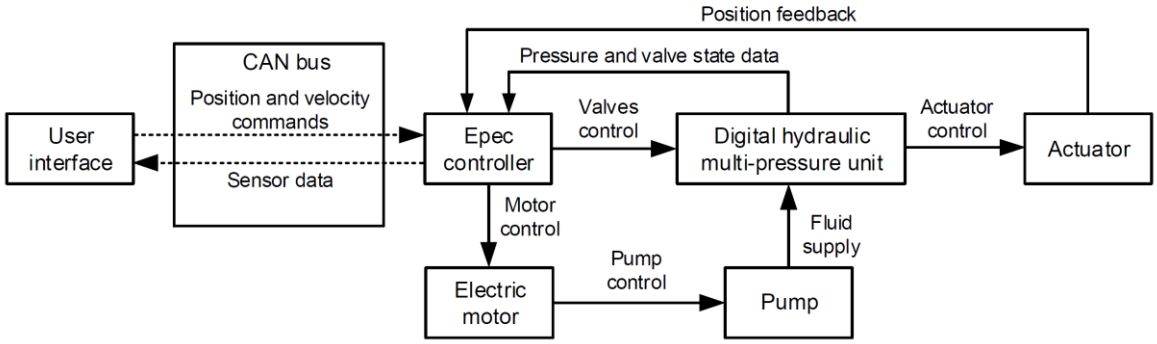

Figure 31. DHMPA control structure [51]

During the operation, EPEC 5050 observes pressures, valve states, pressure converter piston positions, actuator position and user inputs. Based on this information, EPEC 5050 determines new valve states and if necessary, charges the HP accumulator by turning the pump unit on. It will also send corresponding data to the CAN-bus for the user interface.

The DHMPA control is based on steady-state model of the system. The force controller compares pre-defined control alternatives and selects the optimal candidate from the search space. The force evaluation is made by estimating each pressure candidate for the both cylinder chambers separately. The control force candidates are then determined as follows:

$$F(\mathrm{i}) = p_{\mathrm{A_{cand}}}(\mathrm{i}) \cdot A_{\mathrm{A}} - p_{\mathrm{B_{cand}}}(\mathrm{i}) \cdot A_{\mathrm{B}}, \tag{9}$$

where $F(\mathrm{i})$ is the i^{th} control force candidate [N],
$p_{\mathrm{A_{cand}}}(\mathrm{i})$ is the i^{th} pressure candidate for chamber A [Pa],
$p_{\mathrm{B_{cand}}}(\mathrm{i})$ is the i^{th} pressure candidate for chamber B [Pa],
A_{A} is the effective area in chamber A [m^2], and
A_{B} is the effective area in chamber B [m^2]. [48]

After all the force candidates are calculated, the corresponding valve states are compared. The control candidates can be implemented either by direct valve opening to certain pressure level or by crossflow connection as discussed earlier. In the direct opening, the pressure candidates can be calculated in real-time. However, the crossflow case is not trivial; the pressure value has to be iterated, which causes considerable computational burden. In order to avoid this in real-time calculation, a pre-defined polynomial fit is used in a crossflow case. Instead of iterating the actual value, an approximation made by calculating the corresponding polynomial value. This approximation has been proven to be accurate in the most cases. The final control value is found by the calculation of a cost function. The cost function compares and rates the competing control alternatives. The affecting parameters are force tracking error, valve activity, deviation of transformer piston positions from the middle position and crossflow connection. The best performing control candidate is then implemented. [48]

The force controller is capable of selecting the most suitable force candidate by comparing the valve combinations, but it also needs the reference force input. Reference force calculation is required for achieving the desired system response. Therefore, in addition to the force controller, an upper-level controller is needed. The upper-level controller calculates the reference force based on PI-tuning parameters and the feedback position. It can operate in two modes: velocity or position reference mode. For example, it can be given a velocity reference with joystick or a position reference as a step signal. In the velocity control mode, the system is running as an open-loop PI-controller, as follows:

$$F_{\mathrm{ref}} = K_{\mathrm{P_{vel}}}(v_{\mathrm{ref}} - v) + \int K_{\mathrm{I_{vel}}}(v_{\mathrm{ref}} - v)\,\mathrm{d}t, \tag{10}$$

where F_{ref} is the force reference given to lower-level controller [N],
$K_{\mathrm{P_{vel}}}$ is velocity controller proportional term [$\mathrm{Ns/m}$],
$K_{\mathrm{I_{vel}}}$ is velocity controller integral term [$\mathrm{N/m}$],
v_{ref} is the velocity reference [$\mathrm{m/s}$], and
v is the calculated actuator velocity [$\mathrm{m/s}$]. [48]

In position reference mode, however, the position and velocity reference are given by user interface. In this case, the upper-level controller is P-type velocity controller. The value for P-controller is generated by PI-type position and velocity feedforward controller:

$$F_{\mathrm{ref}} = \left[\left(K_{\mathrm{P_{pos}}}(x_{\mathrm{ref}} - x) + \int K_{\mathrm{I_{pos}}}(x_{\mathrm{ref}} - x)\,\mathrm{d}t + v_{\mathrm{ref}}\right) - v\right] K_{\mathrm{P_{vel}}}, \qquad (11)$$

where $K_{\mathrm{P_{pos}}}$ is the position controller proportional term $[1/\mathrm{s}]$,
$K_{\mathrm{I_{pos}}}$ is the position controller integral term $[1/\mathrm{s}^2]$,
x_{ref} is the position reference [m], and
x is the measured actuator position [m]. [48]

In both modes, the upper-level controller returns the desired reference control force. As Equations (10) and (11) show, the reference force is dependent on the PI-tuning parameters and tracking error. This reference force is then given to the force controller for valve control comparison and selection. The final valve openings are determined based on the cost of the different control alternatives in terms of force tracking error, valve activity, deviation of transformer piston positions and crossflow connection. Finally, the best performing valve combination is selected and implemented.

3.2 *Components and Test Rig*

In order to determine the energy efficiency of the DHMPA unit, a test setup was built. The setup consists of the DHMPA unit, pump unit, load-lifting test rig and the data acquisition system. This section reviews this configuration in detail. The DHMPA unit installation is shown in Figure 32.

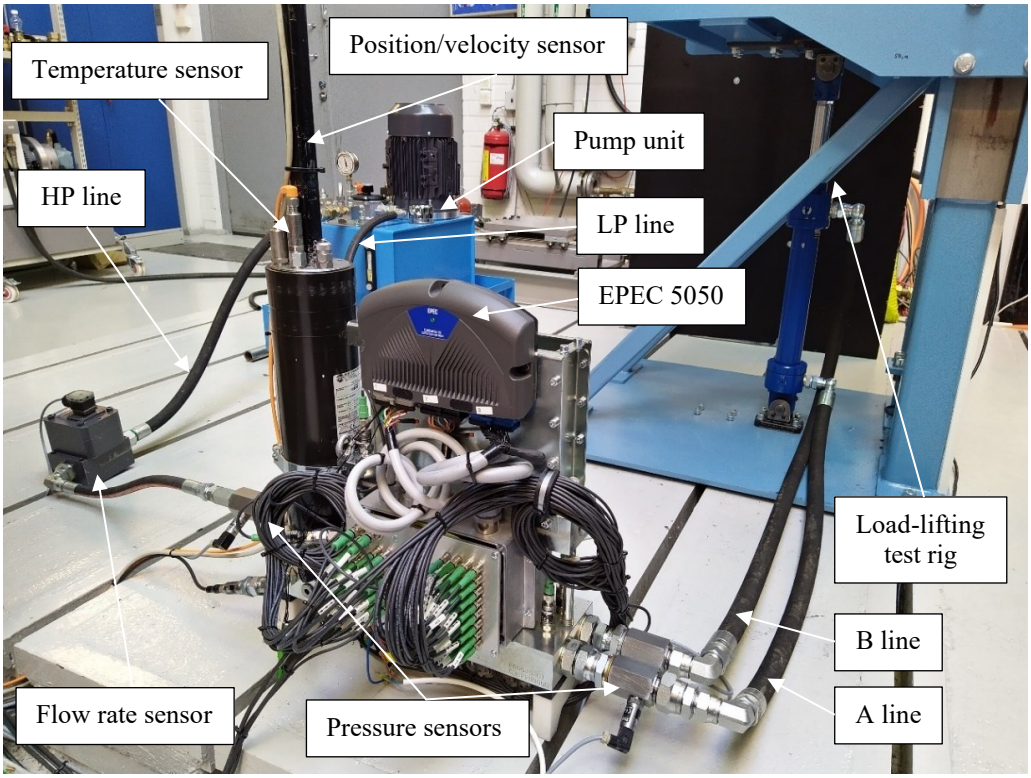

Figure 32. DHMPA test setup

In addition to the CAD-model of the DHMPA (Figure 26), the test unit in Figure 32 includes the EPEC 5050 controller and the other control electronics and wirings. The HP and LP lines are connected to the pump unit, and A and B ports to the working cylinder. HP and LP line have flow rate sensors installed for measuring the pump unit flow rates. In addition, HP, LP, A and B ports are equipped with pressure sensors. Furthermore, the HP accumulator is equipped with piston position/velocity sensor and gas temperature sensor. Finally, a hydraulic fluid temperature sensor is placed on the LP line.

As this study concentrates on the efficiency of the DHMPA in load-lifting application, the DHMPA unit is applied to the test rig that allows mass movement only in vertical direction. The mass of the load, including the frame, is 1180 kg, and it is attached to vertical rails as shown in Figure 33. The mass was measured with crane scale within ± 10 kg tolerance. The load is lifted by 50/36-300 mm hydraulic cylinder, which is directly connected to DHMPA as described in previous paragraph. The maximum stroke of the cylinder in this test rig is 240 mm. However, only 40 mm stroke is used in the test. The test rig includes a position/velocity sensor, which is used for load-mass position measurement for the DHMPA unit and the data acquisition system. Data acquisition system also utilizes the velocity output of the sensor for estimating cylinder piston velocity. This can then be also used for A and B chamber flow rate estimation.

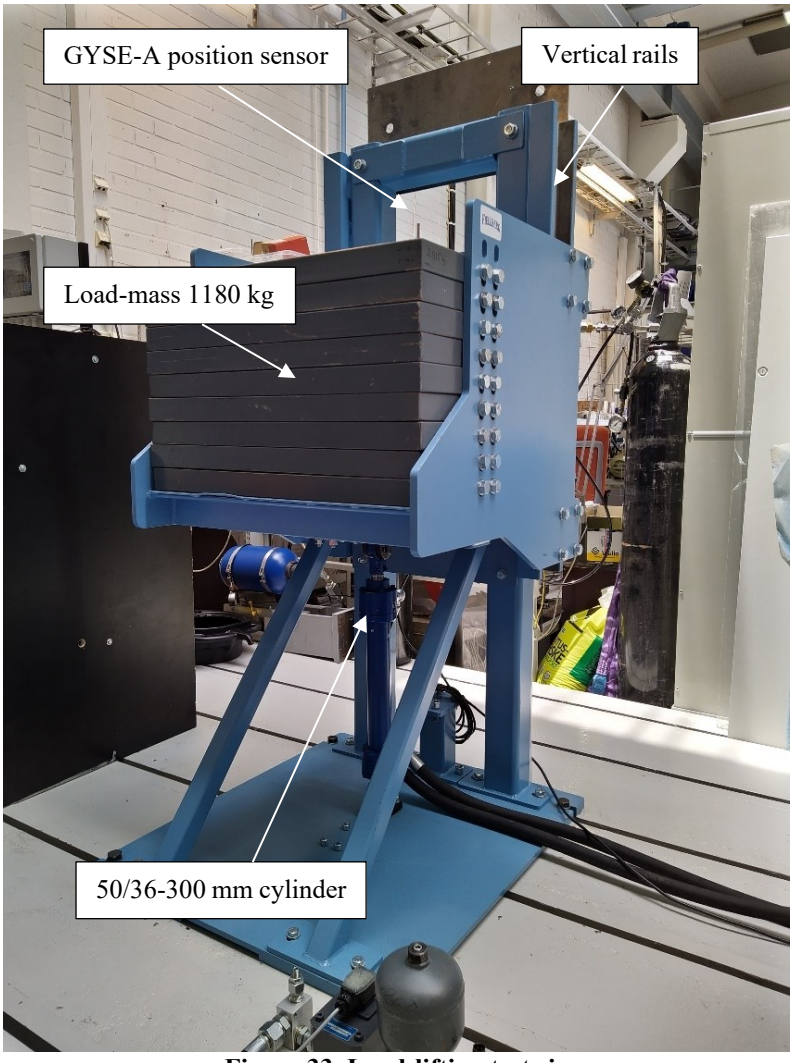

Figure 33. Load-lifting test rig

Furthermore, the detailed hydraulic diagram of the system is presented in Figure 34 and the corresponding bill of materials in Table 1. The diagram includes the hydraulic components of the system and the sensors used by the controller and the data acquisition system. The hydraulic diagram consists of the following major components: Pump unit, DHMPA unit, HP and LP line components, and the working cylinder.

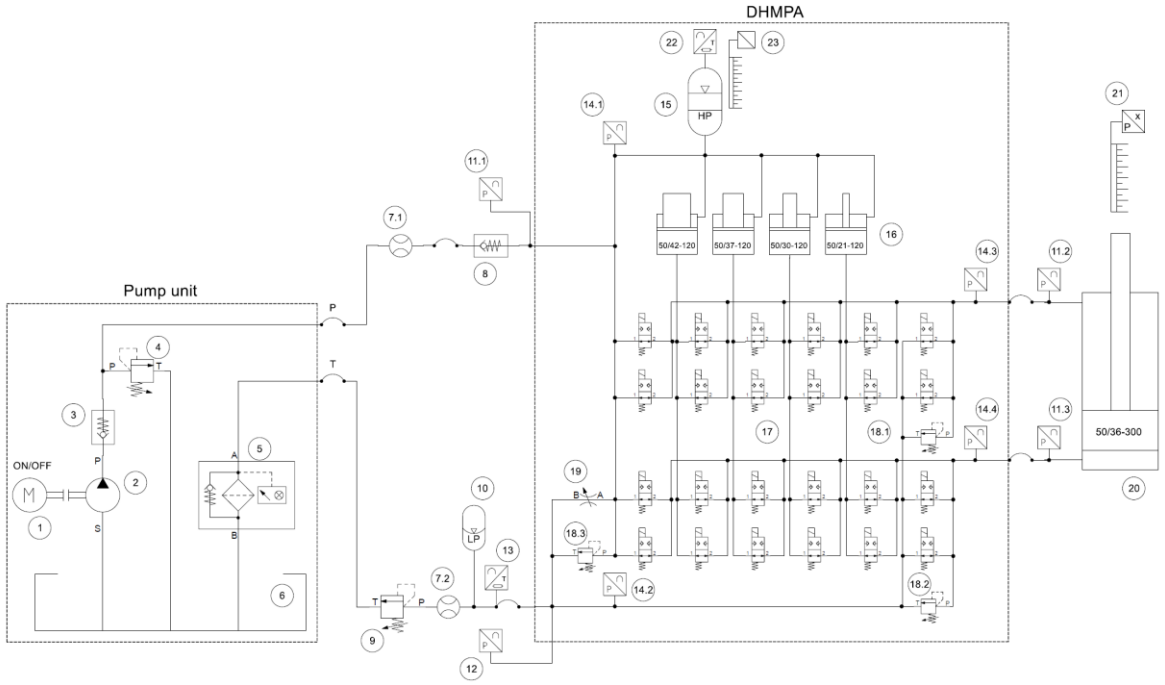

Figure 34. Hydraulic diagram of DHMPA test setup used in this study

The pump unit consists of 5.5 kW electric motor, 11 cm^3 gear pump, 20 MPa pressure relief valve and a filter unit. It can provide nominal flow rate of 16 L/min at 20 MPa pressure. In this setup, it is turned on or off by the DHMPA unit. Pump unit pressure and tank line are both equipped with flow rate sensors. These together with the pressure measurements enable determination of the hydraulic input and output power. Non-return valve on the HP pressure line ensures that flow is not inverted, and the accumulator remains pressurized while the pump unit is turned off. The tank line PRV maintains the LP pressure, and enables the use of the LP accumulator as a low-pressure energy storage. In order to recover energy with all six pressure levels, hydraulic fluid needs to be directed back to the HP accumulator from the LP line as well. The LP accumulator enables this reversed hydraulic fluid flow in the system. HP line, LP line, A-chamber and B-chamber are all equipped with internal and external pressure sensors. Internal pressure sensors are used by the DHMPA and external by the data acquisition system. The LP line is equipped with a temperature sensor for monitoring the temperature level of the hydraulic fluid and it is used by the data acquisition system. The cylinder position sensor is used by the DHMPA and the data acquisition system. In addition, the HP accumulator is equipped with position/velocity sensor and gas temperature sensor.

The DHMPA unit consists of the HP accumulator, four pressure converters, 24 on/off valves, and three PRVs. In addition, a throttling valve is included, though it is fully closed in a normal operation and does not affect the system performance. The three PRVs should also be fully closed in a normal operation, as they are installed for safety purposes. HP accumulator is a piston-type accumulator with 2 litre hydraulic capacity, and it is pre-

charged with 9 MPa gas pressure. HP accumulator is connected to pressure converters, which are used to decrease high-pressure to the intermediate pressures according to their effective area ratios. All the six pressure levels – HP, LP and four converter pressures – are connected to two pairs of on/off valves each. One valve pair is for connecting the pressure to the cylinder A-chamber and the other for B-chamber.

Table 1. DHMPA test setup bill of materials

No	Qty	Description	Type	Manufacturer
1	1	Electric motor (5.5 kW, 400V, 1440 r/min)	MS112BM-4	MOVES
2	1	Gear pump (11 cm3)	OT200 P11 D/G 28 P2	OT
3	1	Non-return valve with spring	VU38	-
4	1	Pressure relief valve (20 MPa)	VMP 3/8”	-
5	1	Return filter with bypass valve	MPF1002AG2A10 HPB01	MP-FILTRI
6	1	Reservoir	S30 (30 L)	HYDRASPECMA
7	2	Flow rate sensor	VC 1 + AS 8	KRACHT
8	1	Non-return valve with spring	HBS ½” 0.5 bar	-
9	1	Pressure relief valve (2 MPa)	VSC-30	BOSCH-REXROTH
10	1	LP accumulator	1 L	-
11	3	Pressure sensor 0…25 MPa	8252.74.2517	TRAFAG
12	1	Pressure sensor 0…1.6 MPa	8252.74.2517	TRAFAG
13	1	Temperature sensor -25…100°C	ETS 4144-A-000	HYDAC
14	4	Pressure sensor 0…25 MPa	NAH 8254	TRAFAG
15	1	HP accumulator	2 L	-
16	4	Pressure transformers	50/42-120 mm 50/37-120 mm 50/30-120 mm 50/21-120 mm	-

No	Qty	Description	Type	Manufacturer
17	24	On/off valves	W22-D-5	BUCHER
18	3	Pressure relief valve (22 MPa)	VSC-30	BOSCH-REXROTH
19	1	Throttle valve	-	-
20	1	Differential cylinder	50/36-300	BOSCH-REXROTH
21	1	Position/velocity sensor	GYSE-A	SANTEST
22	1	Temperature sensor -50…150 °C	TA2135	IFM
23	1	Position/velocity sensor	RH 0…10 V	MTS

Data acquisition system is implemented fully separately from the DHMPA for achieving accurate and independent measurement results. Furthermore, the measurement results can be validated by comparing collected data from data acquisition system and DHMPA. The sensor locations were presented in the hydraulic diagram (Figure 34).

The hardware for data acquisition, excluding sensors, is provided by Beckhoff Automation. The system consists C6920 real-time industrial PC, EK1100 coupler for EtherCAT terminals and data acquisition terminals, as listed in Table 2.

Table 2. Data acquisition system bill of materials

No	Qty	Description	Type	Manufacturer
1	1	Control cabinet Industrial PC	C6920	Beckhoff
2	1	EtherCAT Coupler	EK1100	Beckhoff
3	2	4-channel analog input terminal 4…20 mA, differential input, 12 bit	EL3024	Beckhoff
4	1	Potential distribution terminal, 8 x 24 V DC	EL9186	Beckhoff
5	1	Potential distribution terminal, 8 x 0 V DC	EL9187	Beckhoff
6	1	2-channel analog input terminal ±10 V, ±5 V, ±2.5 V, ±1.25 V, differential input, 24 bit	EL3602	Beckhoff

No	Qty	Description	Type	Manufacturer
7	1	2-channel analog input terminal -10…+10 V, differential input, 16 bit	EL3102	Beckhoff
8	1	HD EtherCAT Terminal, 5-channel input, potentiometer measurement with sensor supply	EL3255	Beckhoff
9	1	CANopen master/slave terminal	EL6751	Beckhoff
10	1	Power supply, 24 V DC	BAE0002	Balluff

The data acquisition system operation in based on Programmable Logic Controller (PLC) program, that is written as structured text in the industrial PC. The program is developed in Visual Studio based TwinCAT 3 programming environment. The program consists of three main components:

1) PLC Project
2) Scope Project
3) Human-Machine Interface (HMI) Project

The PLC project is the core project of the system and it is used to read terminal inputs, write CANopen terminal outputs and control other data acquisition system features. The Scope project is used for recording the sensor data and it is controlled by the PLC project while HMI project acts as a user interface. Therefore, PLC project variables can be accessed from the user interface, that is implemented as HMI project. As the PLC project is capable of controlling the Scope project, the whole test program can be implemented as a combination of these three projects. The data acquisition view of the HMI project is presented in Figure 35.

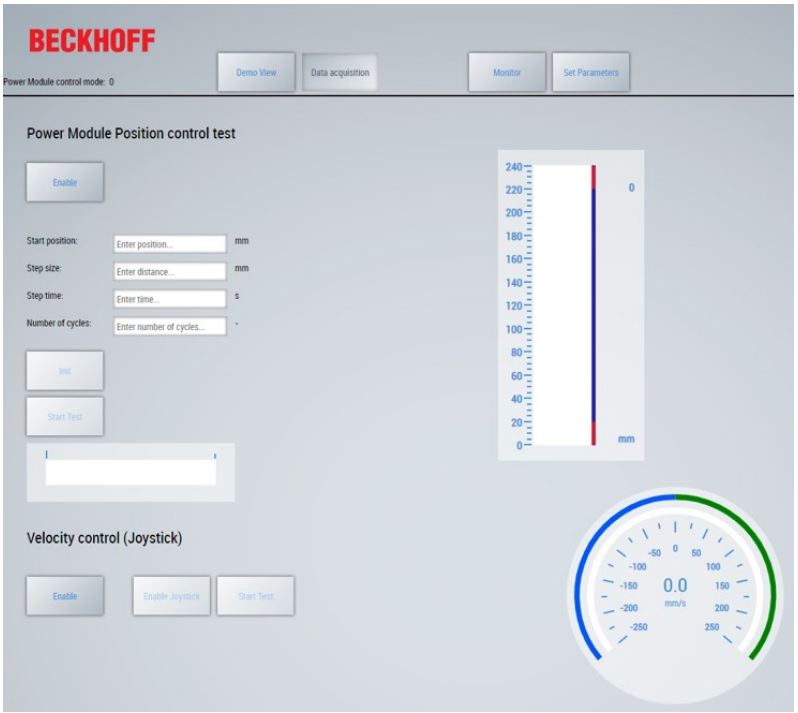

Figure 35. Beckhoff HMI, data acquisition view

As shown in Figure 35, the data acquisition view consists of position control and velocity control test. These two modes correspond to the EPEC 5050 position and velocity control modes, which were presented in the end of Section 3.1. However, only position control test was used in this study. As Figure 35 shows, the test parameters, such as starting position, step size, step time and the number of cycles can be given via the data acquisition interface. During the test, each cycle executes one new position step. The sign of step size in reversed in each cycle, leading to an up-down movement with given step size. The first step is positive, so with starting position of 120 mm and step size of 40 mm the load-mass will be moved between 120 and 160 mm so that one cycle duration is as long as defined in the step time field.

In addition to the data acquisition view, the user interface contains demo, monitor and set parameters views. Demo view can be used for position or velocity control similarly as the data acquisition view, but without data recording. Monitor simply shows the sensor values so that user can observe them without data acquisition mode. Set parameters tab allows the user to set the DHMPA tuning parameters, such as P and I gains, positioning tolerances, $p_{\min}$ and $p_{\max}$, and the cost function partial weights.

3.3 *Test Case Parameters*

In this thesis, DHMPAs efficiency is determined in position control test. The reference position is given as step signal, repeating an up-down movement for 500 cycles between 120 and 160 mm. As each cycle includes one new reference position, the load-mass is lifted total 250 times, as well as it is lowered. Each step position is hold for two seconds, leading to total of 17-minute test time. As discussed earlier, HP pressure limits are set to $p_{\min} = 10$ MPa and $p_{\max} = 14$ MPa, meaning that the pump is turned on below $p_{\min}$ threshold and turned off above $p_{\max}$ threshold. The LP line PRV is adjusted to 1 MPa. HP accumulator was loaded with pre-charge pressure of 9 MPa and LP accumulator with 0.7 MPa. The position tolerances of the controller were set so that the positioning is stopped if position error is decreased below $x_{\text{tol},1} = \pm 2$ mm and it is started again if position error increases above $x_{\text{tol},2} = \pm 3$ mm. In addition to these parameters, position controller gains and force controller cost function weights are presented in Table 3.

Table 3. Test parameters in the load-lifting test

Symbol	Parameter	Value
n	Number of cycles	500
x_0	Start position	120 mm
Δx	Step size	40 mm
Δt	Step time	2 s
t_0	Start time	0 s
t_1	Stop time	1000 s
$p_{\max}$	HP accumulator upper threshold	14 MPa

Symbol	Parameter	Value
$p_{\min}$	HP accumulator lower threshold	10 MPa
p_{LP}	LP PRV opening pressure	1 MPa
$p_{\mathrm{pre,HP}}$	HP gas pre-charge pressure	9 MPa
$p_{\mathrm{pre,LP}}$	HP gas pre-charge pressure	0.7 MPa
$x_{\mathrm{tol},1}$	Stop positioning tolerance	± 2 mm
$x_{\mathrm{tol},2}$	Start positioning tolerance	± 3 mm
$K_{\mathrm{P_{pos}}}$	Controller position P-gain	5 $1/\mathrm{s}$
$K_{\mathrm{I_{pos}}}$	Controller position I-gain	9 $1/\mathrm{s}^2$
$K_{\mathrm{P_{vel}}}$	Controller velocity P-gain	29 000 $\mathrm{Ns/m}$
W_{sw}	Switching cost weight	0.0003
W_{V}	Volume cost weight	50 000 000
W_{cf}	Crossflow cost weight	4 000

The selection of test parameters was based on initial testing of the system. However, as this is the first time when the DHMPA unit is applied to a vertical load-lifting test rig, these tuning parameters might not be completely optimised. As shown in Table 3, several tuning parameters are selected, and they all have their own effect on the system response. Therefore, it is possible that with a careful optimisation, more sufficient parameters could have been found. Nevertheless, for now these parameters were selected as the best compromise between efficiency and controllability.

In this chapter, the DHMPA and its operation principle was investigated further in detail in order understand how the system performs and how different factors affect energy efficiency and performance of the DHMPA. Furthermore, the test setup was reviewed together with the data acquisition system. Finally, the test parameters used in this study were presented. The next chapter presents the experimental results of the test and analyses the data.

4 Results

4.1 *Performance Analysis*

4.1.1 Positioning

The data reviewed and analysed in this chapter was collected with Beckhoff data acquisition system described in Section 3.2. Data points were collected in 10 ms time intervals. The exported data was then analysed and plotted in MATLAB R2020a.

In the test case of this thesis, the load-mass was moved periodically in 40 mm steps, up and down. The position was controlled with the position controller presented in Section 3.1. Figure 36 shows the given reference position and system response during 580 – 700 s timeframe. The load-mass reference position is given in blue colour and the measured position in orange.

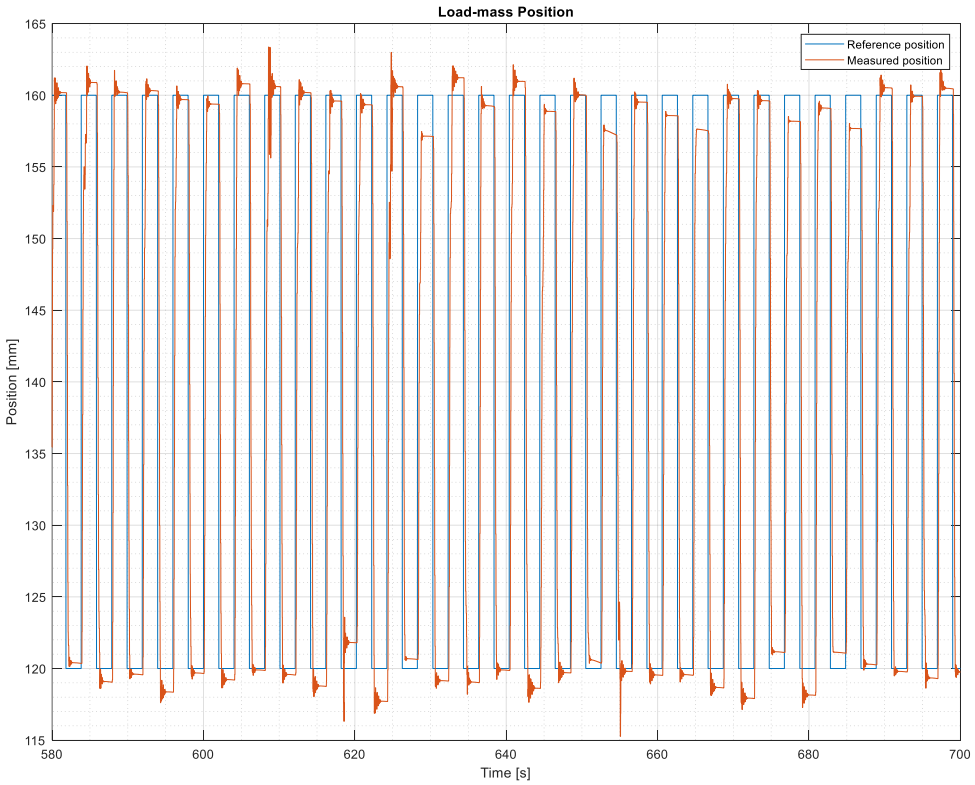

Figure 36. Position of the load-mass

As the measured position in Figure 36 shows, the response is quite repeatable, but some unexpected errors and oscillations occur. Some of these errors can be seen for example at 609 s, 619 s and 625 s. These unexpected oscillations can be affected by changing the tuning parameters, though in this test case the errors could not be entirely avoided. Furthermore, after each step, small oscillations are present due to bending of the test rig structure, as the mass of 1180 kg is quickly decelerated. These oscillations could be affected with more rigid structure of the test rig, and by choosing lower gains in the controller. Nevertheless, an

overall accuracy is good, especially when these unexpected oscillations are not present. The total position error during 580 – 600 s time interval is presented in Figure 37.

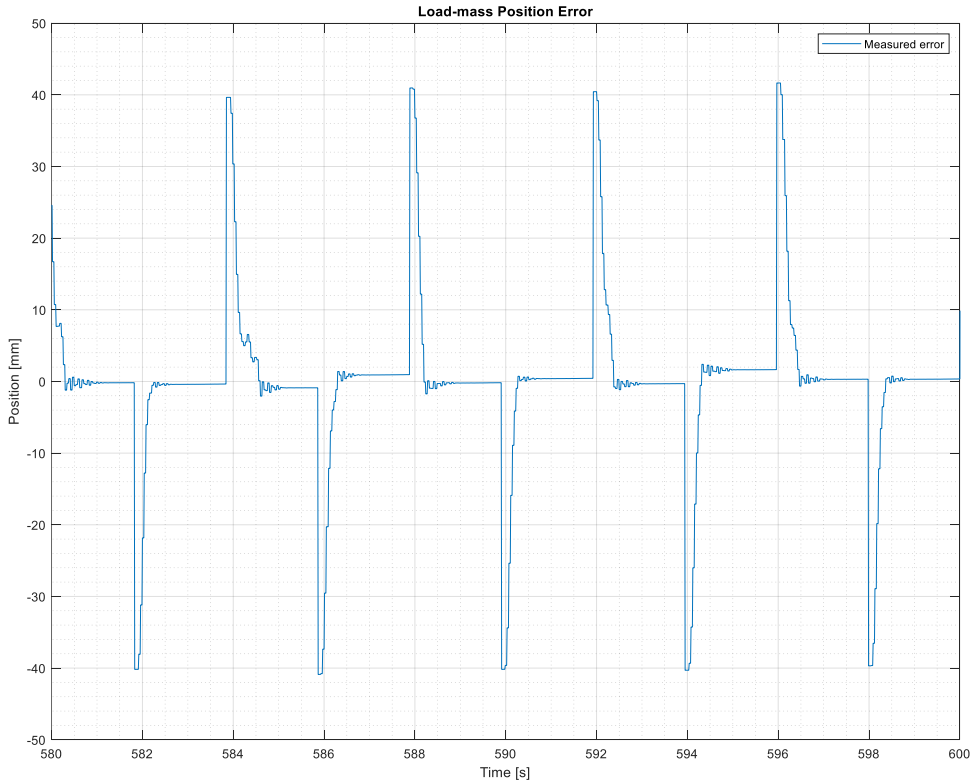

Figure 37. Position error of the load-mass

As the position error in Figure 37 shows, it takes approximately 0.1 s to start the movement and total 0.4 – 0.6 s to reach the given position within given tolerance. In this test case, the tolerance limit for stopping the movement was ± 2 mm. Majority of the positionings are performed with good accuracy, even less than 1 mm error, but some cycles are end with 2 mm error, or the final position is never reached before the next step due to unexpected position errors in the system. Nevertheless, if the unexpected cases are neglected, the final position is always reached within approximately ± 2 mm accuracy. The accuracy can be affected with the selection of tuning parameters, and the ones used in this test were selected in terms of balanced controllability and good energy efficiency. However, for achieving a better performance in terms of stability and repeatability, a more careful study in the controller tuning is needed.

4.1.2 Pressure Levels

As the load-mass is moved up and down, it utilizes potential energy both in HP and LP accumulators. The HP accumulator acts as a primary power source while LP accumulator is used for enabling the use of lowest pressure level in energy regeneration. Both HP and LP pressures were measured in the test. The HP pressure shows whether the HP accumulator is charged or discharged, and the LP pressure gives an indication of the operation in the LP PRV and accumulator. These both pressures are presented in Figure 38 between 580 and 700 s.

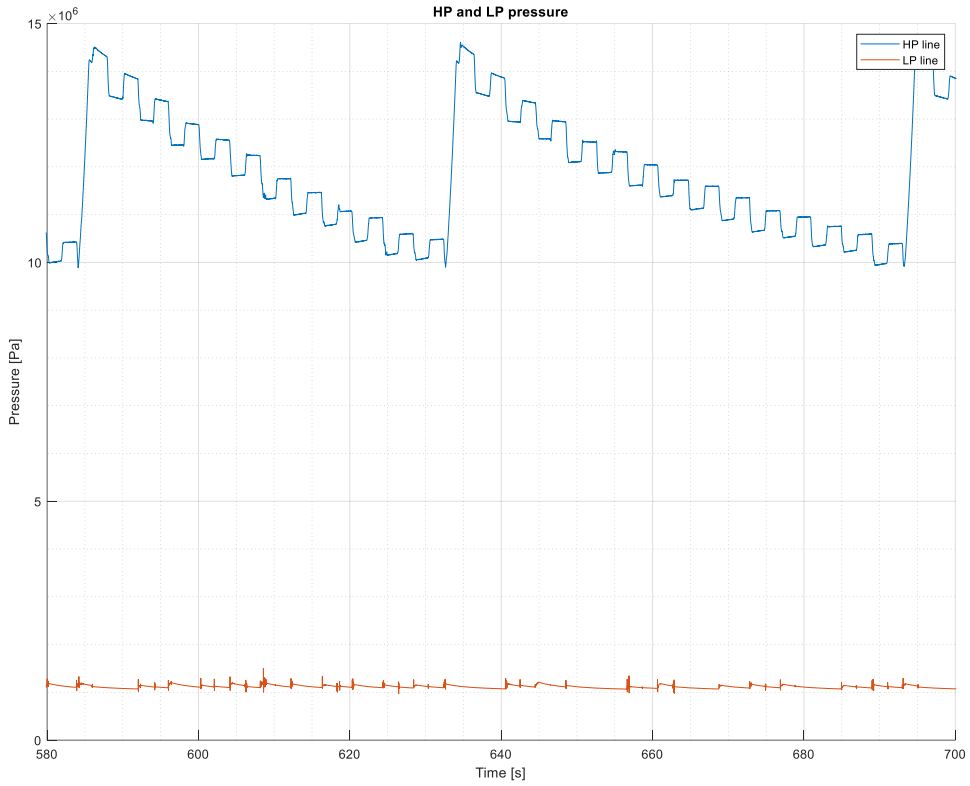

Figure 38. HP and LP line pressures

The HP pressure in Figure 38 demonstrates the working principle of the DHMPA: The system is loaded to $p_{\max}$ pressure by an external pump unit. In this case $p_{\max}$ is set to 14 MPa. During the work cycle, this stored energy can be used as an output work to the actuator, or energy can be restored to the system. This can be seen as an increase or decrease in the pressure level. In this test, the same amount of potential energy was lifted and lowered periodically. An ideal system could therefore operate infinitely without an external pump unit. However, as losses are always present in real-life applications, the potential energy cannot be fully restored. This leads to that the HP pressure decreases over time, and once the $p_{\min}$ level is reached, the system needs to be charged again. In this kind of zero-energy process, the charged energy can be pointed to cover all the energy losses in the system, as the load-mass is always lowered to the start position.

The LP accumulator gas volume is smaller, and the operating pressure is considerably lower than that in the HP accumulator. The opening pressure of the PRV in the LP line is set to 1 MPa. Therefore, LP pressure cannot indicate charge level of the LP accumulator as clearly as HP pressure does. However, small pressure spikes in the LP line can be observed. The spikes occur if the flow rate to LP line is rapidly increased. The spikes are then quickly smoothened due to opening of the PRV. In addition, it can be seen that the LP pressure level does not decrease below the set 1 MPa pressure. Theoretically, this could happen if the volume required for the regeneration is greater than the amount of stored hydraulic fluid in the LP accumulator. In this case, the maximum amount of fluid that could be required from the LP accumulator equals to the cylinder B-chamber fluid volume with 40 mm stroke. This corresponds to volume of 0.038 L, while usable volume of the 1-litre LP accumulator with

0.7 MPa pre-charge pressure is approximately 0.3 – 0.4 L at 1 MPa pressure. Therefore, the required amount of hydraulic fluid for regeneration is always considerably lower than the available volume in the LP accumulator, and the DHMPA unit cannot decrease the LP pressure below 1 MPa by using the fluid for regeneration.

Next, Figure 39 shows pressure levels in cylinder A and B chambers. For achieving clearer view of the pressures and behaviour during the duty cycle, time interval is set shorter than previously, from 580 to 600 s.

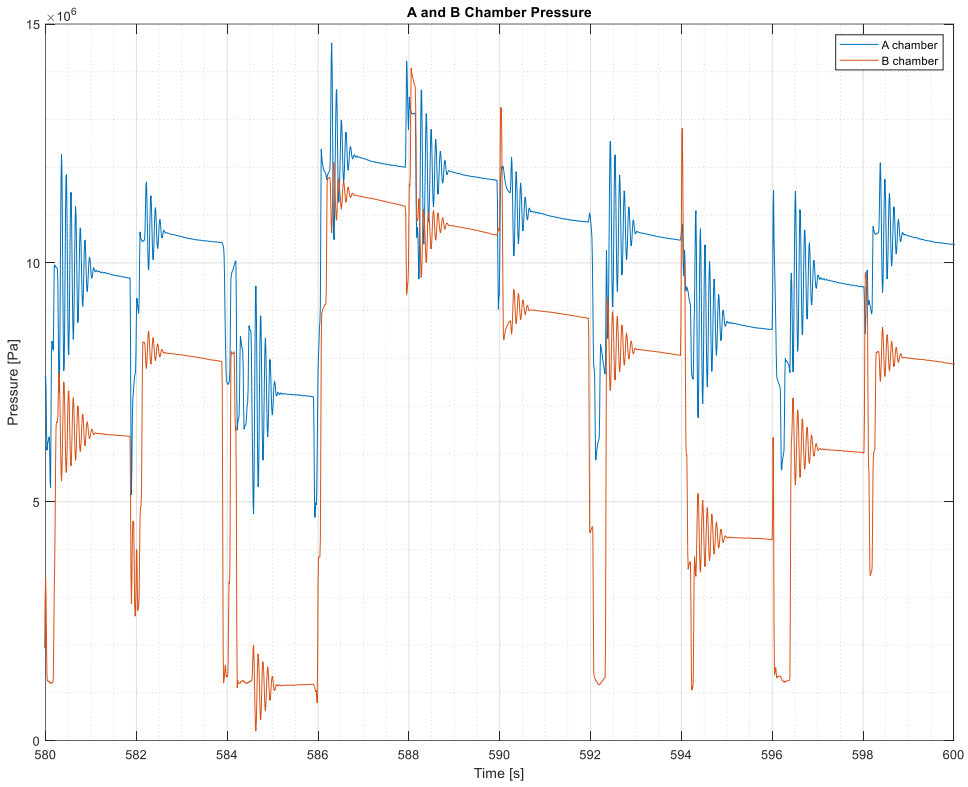

Figure 39. A and B chamber pressures

The pressures in A and B chambers show oscillations after reaching each reference position. Oscillations are magnitude of 4 MPa in A chamber and 2 MPa in B chamber. This can be considered as a natural response as the system has no hydraulic damping elements while the load-mass is quickly decelerated by on/off valves after reaching reference position. Oscillations in the A chamber are higher, as the effective piston area is 2.08 times higher than in B chamber.

4.1.3 Flow Rates

Figure 40 shows the input and output flow rates of the DHMPA. Positive flow rates indicate input flow and negative rate output flow from the DHMPA. The HP flow rate equals directly to the flow rate from the pump unit, so it indicates when the pump is on or off. HP and LP flow rates can be used to describe how hydraulic fluid can be utilized in the system. Based on the continuity equation, the average flow rates should be equal but opposite signs to each other, as the same amount of fluid has to flow out as there has flown in, assuming that the charge level of the accumulators remain constant. However, it should be noticed that average

flow rates will equal to each other exactly only after very long test time, as HP line flow rate is cyclic. As Figure 40 shows, with 500 cycles the averages do not have enough time to approach each other but they get relatively close. Furthermore, the magnitude of flow rate averages gives an indication of the efficiency, as described in the previous section. With lower averages, the system internal losses are smaller. In other words, if the average flow rate through the DHMPA unit is smaller, the same amount of work is done with less input energy. If the average flow through the DHMPA unit approaches zero, the energy-efficiency approaches 100% because less energy is consumed into internal losses.

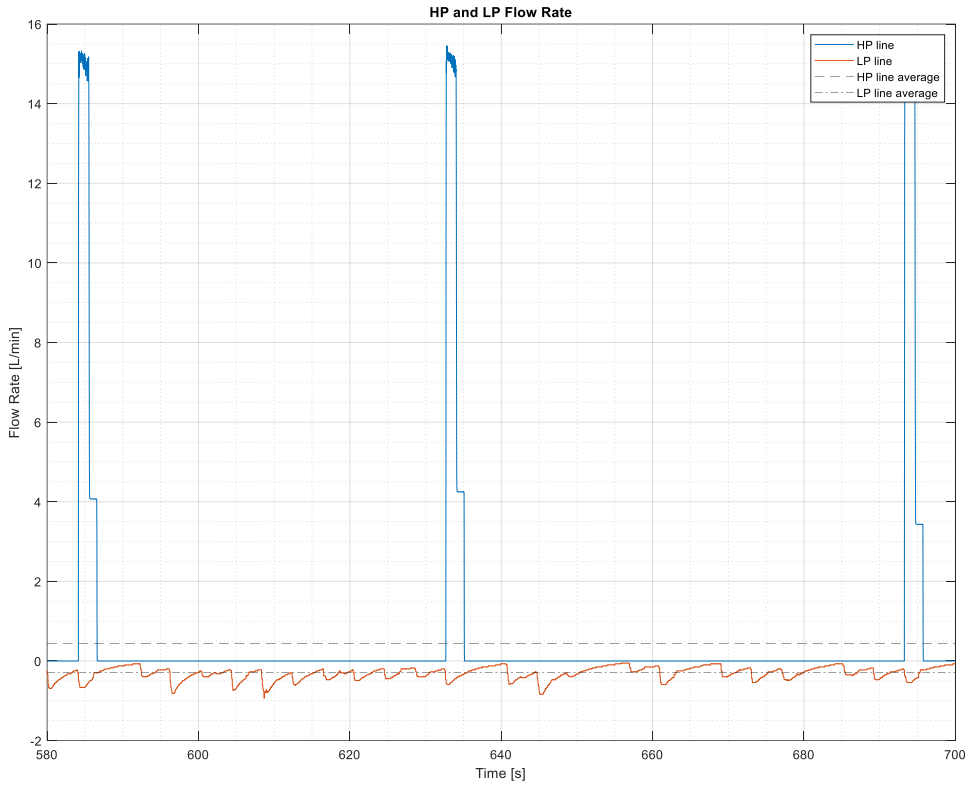

Figure 40. HP and LP line flow rate

The pump unit is rated to produce flow rate of 16 L/min at 20 MPa. As shown in Figure 40, the actual flow rate is approximately 15 L/min, while the average flow rate input is only less than 0.5 L/min. Therefore, it would be possible to use significantly lower flow rate pump. On the other hand, the pump unit is switched on only every 45 – 50 s, and otherwise, the DHMPA operates with the energy charged and regenerated in the accumulator. For achieving better energy-efficiency, it would be better to use smaller flow rate pump as the thermal losses in the HP accumulator would decrease. With fast charging, the gas temperature in HP accumulator rises significantly, which leads to thermal energy losses as discussed further in Section 4.1.4.

Next, Figure 41 presents the A and B chamber flow rates of the working cylinder. A positive flow rate indicates flow into the chamber and negative out of the chamber. A and B chamber flow rates are calculated from measured cylinder velocity and effective chamber areas, as follows:

$$q_{\mathrm{v,chamber}} = v_{\mathrm{cyl}} A_{\mathrm{chamber}}, \tag{12}$$

where $q_{\mathrm{v,chamber}}$ is the flow rate to the cylinder chamber $[\mathrm{m}^3/\mathrm{s}]$,
v_{cyl} is the velocity of the cylinder piston $[\mathrm{m}/\mathrm{s}]$, and
A_{chamber} is the effective chamber area $[\mathrm{m}^2]$.

Therefore, the two chamber flow rates are proportional and opposite to each other. The ratio of flow rates is equal to cylinder chamber area ratio as the velocity is the same in both chambers. Flow rates in Figure 41 are converted from m^3/s to L/min.

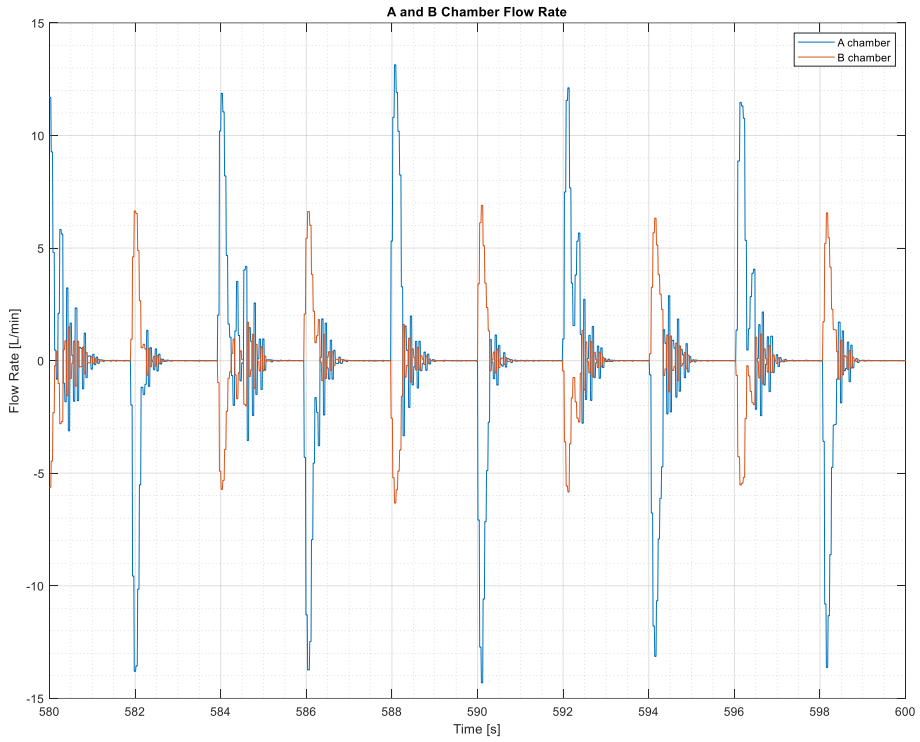

Figure 41. A and B chamber flow rates

As Figure 41 shows, the maximum actuator flow rates are approximately 12 – 14 L/min. The maximum flow rate is in A chamber due to larger effective piston area. In B chamber the maximum flow rate is 5 – 7 L/min. Cylinder size in this test was 50/36 mm, having area ratio of 2.08. This corresponds well to the ratio of the maximum flow rates, as the flow rate calculation was based on piston velocity and effective chamber areas.

Hydraulic fluid flow is directed to the A and B chambers from the pressure converters, or HP and LP accumulator. In this experiment, HP accumulator was equipped with position/velocity sensor that can be used for flow rate calculation. On contrary, flow rate from LP accumulator back to the cylinder was not measured, as it is considered as an internal energy storage as well as the pressure converters. Therefore, flow rate from the LP accumulator is not observed for determining the energy balance. Nevertheless, the LP accumulator is used in order to enable backwards flow in the system during energy regeneration. The amount of recovered energy can be measured by pressure and flow rate of the HP accumulator. The pressure was measured with pressure sensor as was shown in Figure 38 and the flow rate can be calculated as follows:

$$q_{\mathrm{v,accu}} = v_{\mathrm{accu}} A_{\mathrm{accu}}, \tag{13}$$

where $q_{\mathrm{v,accu}}$ is the flow rate to the accumulator [m^3/s],
v_{accu} is the velocity of the accumulator piston [m/s], and
A_{accu} is the accumulator piston area [m^2].

This calculated flow rate of the HP accumulator is shown in Figure 42 during 580 – 600 s. Again, positive flow rate indicates flow into the accumulator and negative out from the accumulator. Flow rate is converted from m^3/s to L/min.

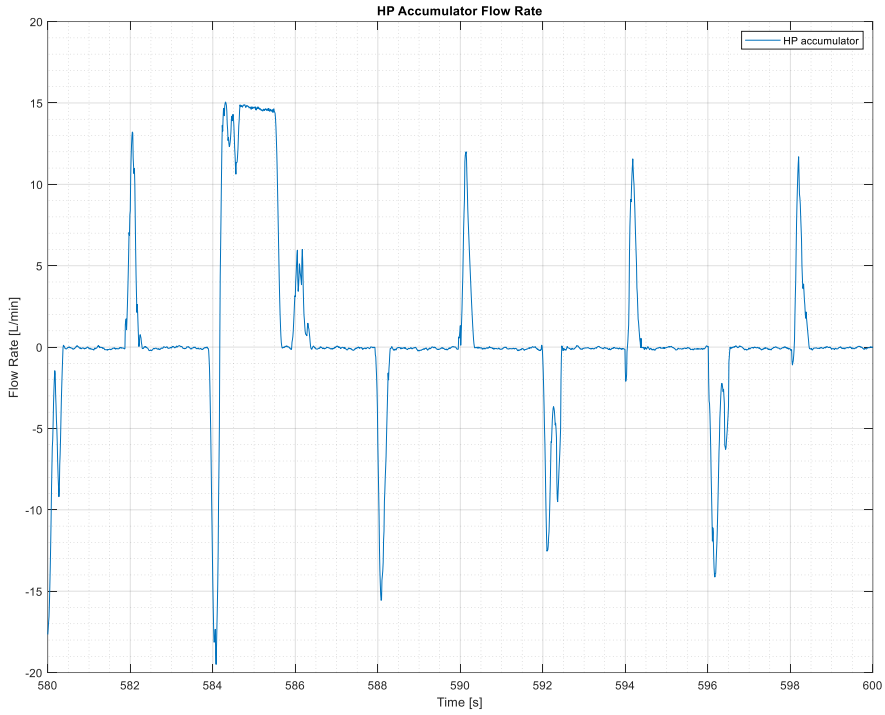

Figure 42. HP accumulator flow rate

As the HP accumulator is the primary power source in the system, it is essential to observe its flow rates in order to determine the energy balance of the system. In Figure 42, three different flow cases can be detected:

1) Charging with pump unit
2) Charging with recovered energy
3) Discharging for output work

Charging with pump unit can be seen at 584 – 586 s, as 15 L/min flow rate is put into the accumulator for almost two seconds. In the beginning of the charging, some interruption is seen as the last lifting movement is not yet finished. When the load-mass reaches its reference position, the flow rate into the HP accumulator settles to 15 L/min. The other positive flow rates represent recovered energy, as the pump is turned off, and no other energy sources exist. It can be seen that the maximum flow rate in energy recovery is slightly smaller as charging with the pump unit and the duration is shorter. On the discharging case, the output flow rate shows much more variation. The difference can be explained with the fact that not all potential energy, and thus, not all hydraulic fluid can be recovered, as the power losses consume energy. The consumed energy can be seen as an output flow in LP line. It

was shown in Figure 40, that the LP line has some flow all the time and therefore it is logical that the recovered flow rate to the HP accumulator is lower than output flow rate to the actuator. The differences in each output flow maximums on the other hand can be explained with the use of pressure converters. The control logic in the EPEC 5050 decides the use of converter individually in each work cycles, and it is normal that differences in converter usages over work cycles exist. The different usage of converter cylinders leads to variation of flow rate requirement as the cylinder area ratios are different. HP accumulator hydraulic fluid flow can also be observed as stored fluid volume. The amount of stored hydraulic fluid can be calculated as follows:

$$V_{\text{accu}} = x_{\text{accu}} A_{\text{accu}}, \tag{14}$$

where V_{accu} is the hydraulic fluid volume in the accumulator [m^3],
x_{accu} is the position of the cylinder piston [m/s] and
A_{accu} is the accumulator piston area [m^2].

Figure 43 presents the amount of hydraulic fluid in the HP accumulator during 580 – 700 s, converted from cubic meters to litres. The position sensor of the accumulator piston was calibrated to zero when accumulator was empty, and thus, the figure shows the absolute amount of hydraulic fluid in the accumulator.

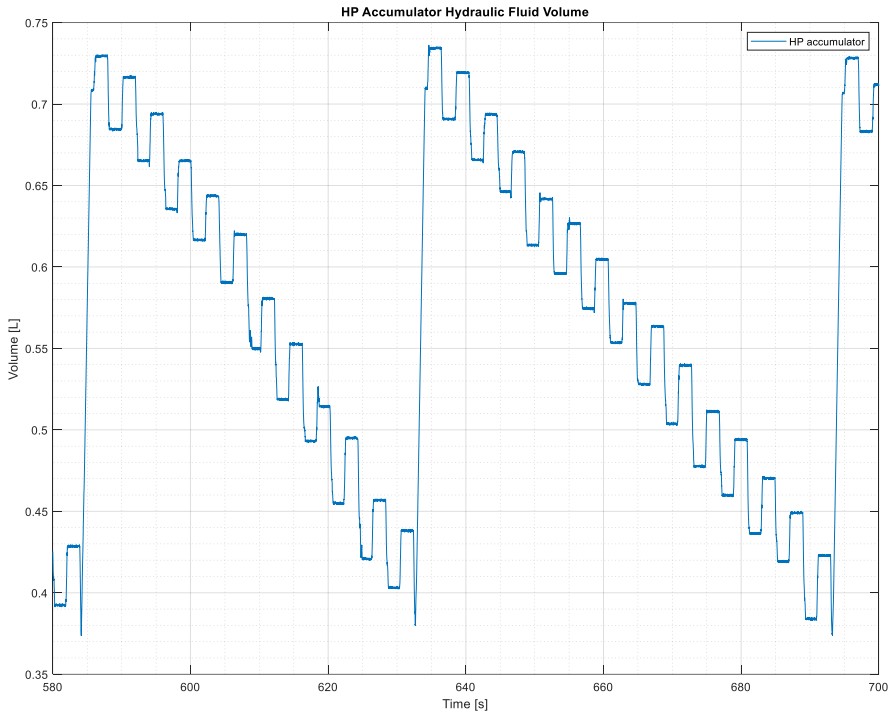

Figure 43. HP accumulator hydraulic fluid volume

As Figure 43 shows, the amount of hydraulic fluid in the accumulator is approximately 0.73 L when charged to p_{max} and 0.39 L when charge is decreased to p_{min}. With the pressure limits of 10 and 14 MPa, the amount of utilized fluid is therefore only 0.34 L. During one lifting cycle, the amount of utilized fluid changes between 0.05 and 0.06 L. In order to provide the same energy output, the amount of used fluid is increased as the pressure level is decreased. During regeneration, the amount fluid in one step changes similarly between

0.03 and 0.04 L. This indicates that approximately 70% of the used fluid can be recovered, but the exact regeneration efficiency needs to be defined through energy balance. This will be accomplished in Section 4.2.

4.1.4 Temperature

Temperature is measured in two locations for evaluating the system performance. LP line hydraulic fluid temperature is measured in order evaluate the overall temperature in the system. If the overall temperature rises significantly, major hydraulic losses might exist in the system. On the other hand, if the oil temperature does not rise significantly there cannot be significant throttling losses in the DHMPA unit. The second temperature sensor measures the HP accumulator gas temperature. This can be used to evaluate accumulator energy losses in terms of thermal losses. The exact amount cannot be measured, but the aim is to minimize temperature rise of the gas volume as the accumulator is not thermally isolated, allowing the energy to conduct out of the system. The measured temperatures are presented in Figure 44. In order to remove noise, temperature data is filtered with 100 sample moving average.

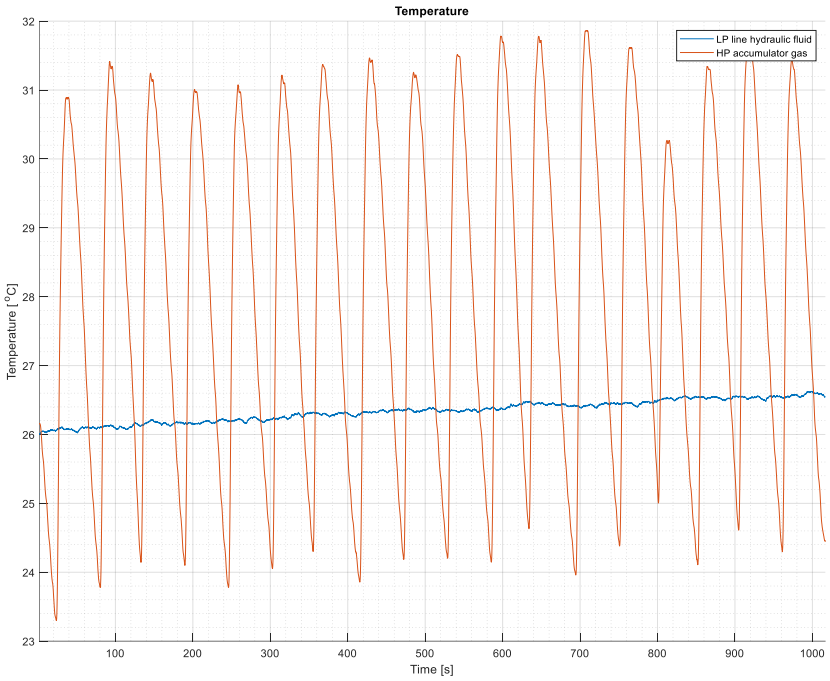

Figure 44. LP line hydraulic fluid and HP accumulator gas temperature during the test

As Figure 44 shows, the hydraulic fluid temperature rises only about 1 °C during the 17-minute test run. Initial oil temperature was 26 °C while the room temperature was 22 °C. Hydraulic fluid was therefore already heated 4 °C in previous test runs. For determining the final settling temperature, significantly longer test time would be needed. During this test, the hydraulic fluid temperature rose only slightly, which is an indication of low valve losses.

The HP gas temperature on the other hand shows significant changes during the test cycle. The temperature rises notably as the accumulator is charged fast from 10 to 14 MPa. This leads to thermal losses as excess heat is conducted to the accumulator shell and through it out of the system. On the other hand, as the pressure in the accumulator decreases, the temperature decreases as well and finally, it falls below hydraulic fluid temperature. In this state, some thermal energy actually flows into the accumulator and the average thermal

losses in the accumulator are decreased. The effect of temperature change can be seen for example in the HP accumulator pressure (Figure 38). Once the HP accumulator is charged, pressure level in it decreases even when the load-mass is not moving. The pressure is lost due to thermal leakage. Then, just before the pump unit is turned on again, an opposite reaction can be seen. The HP pressure rises even when the load-mass is stationary. In this case accumulator gas temperature has fallen below hydraulic fluid temperature and thermal energy flows back to the gas. As a consequence, the HP accumulator pressure rises. However, the overall effect of temperature changes cannot be exactly determined in this study, as the DHMPA's frame temperature was not measured. Nevertheless, it can be concluded that thermal losses occurred and further study will be needed in order to minimize these losses.

4.1.5 Cylinder Force

As the DHMPA's operation is based on pressure levels and selection of the sufficient force levels, it is interesting to observe how real output work corresponds to the optimal and selected force levels. The output force can be calculated based on chambers' pressures and effective piston areas as follows:

$$F_{\text{out}} = p_{\text{A}} A_{\text{A}} - p_{\text{B}} A_{\text{B}}, \tag{15}$$

where F_{out} is the net output force without friction losses [N],
p_{A} is the pressure in the cylinder chamber A [Pa],
p_{B} is the pressure in the cylinder chamber B [Pa],
A_{A} is the effective A chamber area [m^2] and
A_{B} is the effective B chamber area [m^2].

As the cylinder is placed in a rod-up position, a positive force points up and negative force down. The calculated cylinder output force together with DHMPA's reference and optimal force are presented in Figure 45.

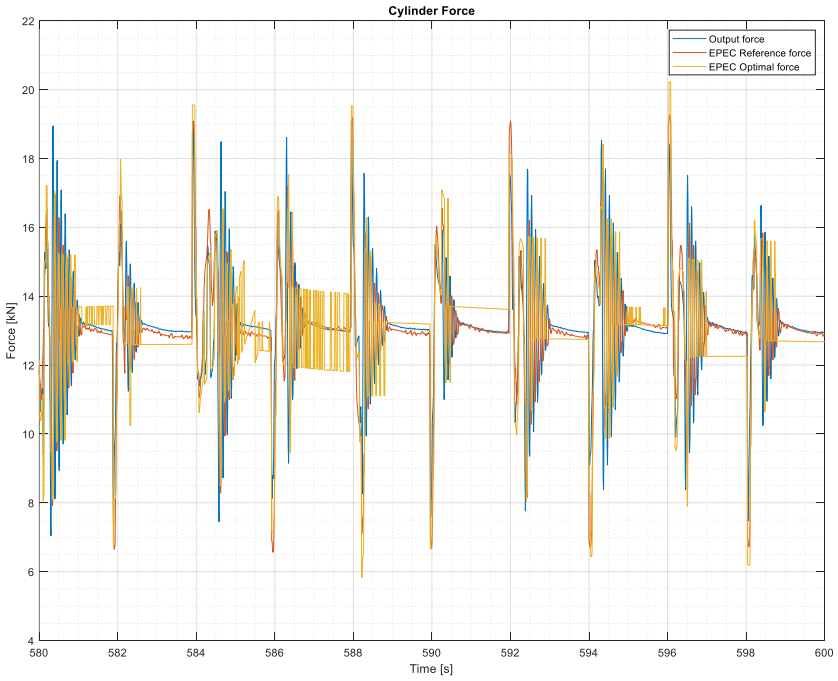

Figure 45. Cylinder output force and EPEC optimal and reference force

In Figure 45, EPEC reference force is calculated as described in Equation (11) in Section 3.1, and it is obtained in real-time from EPEC 5050 via CANopen interface. EPEC optimal force is the selected control force, determined by the cost function.

As Figure 45 shows, the output force follows the reference force quite well, especially in steady-state phases. However, the selected force level notable differs from the real output force. This is somewhat surprising result but can be explained with the fact that the selected force levels are based on position error as described in equation (11) instead of the measured output force. The DHMPA observes the system response in terms of position, and hence the error in force output does not affect the controller. In addition, the position controller is always stopped when the position is reached within $x_{\mathrm{tol},1}$= ± 2 mm tolerance, and will not be turned back on until the position error is greater than $x_{\mathrm{tol},2}$= ± 3 mm. Therefore, the optimal force can differ significantly from the output force as long as the position error is within the stopping tolerances. However, it can be seen that that the force selection does not perform in fully optimal way, as the optimal force levels are changed rapidly in certain times. For example, at 587 s, the load-mass is stationary but the optimal force does not settle in one value, but toggles between two values. Without stopping the position controller, this would lead to unnecessary valve switching as the systems toggles between the different control alternatives. As for this, it would have a negative effect on the overall efficiency and performance.

It can also be noted that the real output force, together with reference and optimal force are oscillating when the load-mass is approaching the desired position. Moreover, the output force occasionally shows notably higher peak values than the controller-based reference force. No obvious reason was found to cause this. However, for achieving the optimal performance and efficiency, these oscillations should be minimized. Again, as the force selection is highly dependent on the controller and cost function tuning parameters, a careful optimization could improve the force selection and thus system performance. However, for achieving this, the controller adjustment requires further investigation.

4.2 *Energy Efficiency Analysis*

4.2.1 Power Consumption

The previous section discussed the performance of the DHMPA unit. Now, the following sections analyse power consumption and energy balance in the system. In order to achieve the aim of this thesis and determine the efficiency of the DHMPA unit, power consumption in the system is utilized for obtaining the cumulative energy balance of the system. This can then be used for determining the three characteristic efficiencies as described in Section 2.1.

First, hydraulic input and output powers are calculated in HP and LP lines. The hydraulic power can be calculated as follows:

$$P_{\mathrm{h}} = p \cdot q_{\mathrm{v}}, \tag{16}$$

where P_{h} is the hydraulic power [W],
p is the measured pressure [Pa], and
q_{v} is the measured flow rate [m^3/s].

This hydraulic power in HP and LP line is presented in Figure 46. Positive power represents input and negative output energy. In general, HP line contains only positive input energy to the DHMPA as the non-return valve prevents backwards flow. The LP line power represents negative lost power as the potential energy of the fluid is transformed into thermal energy in the LP line PRV.

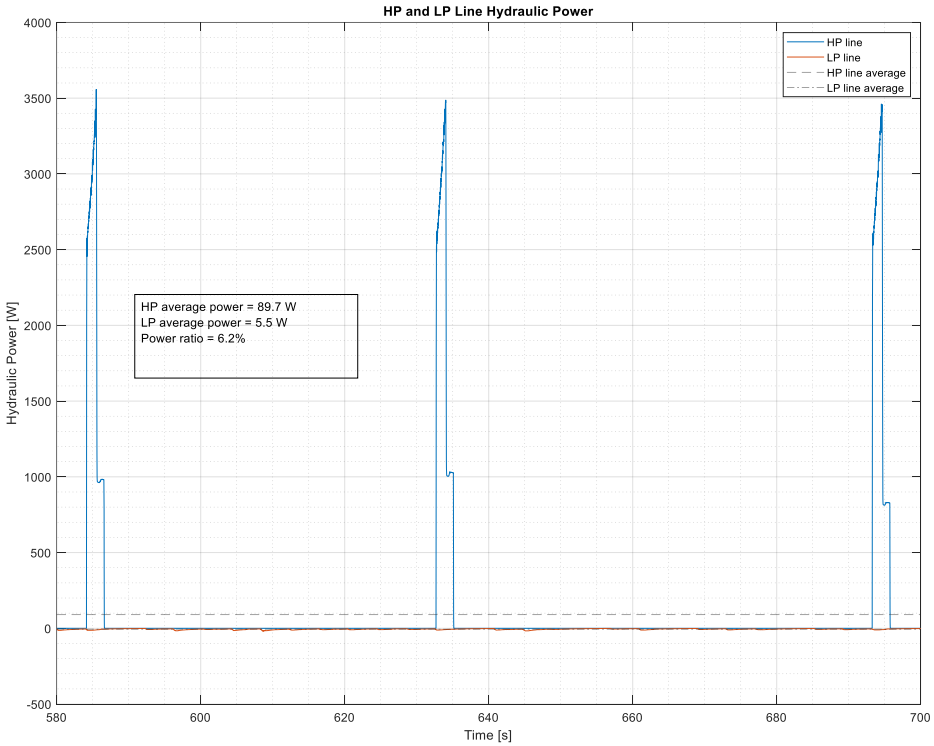

Figure 46. Hydraulic input and output power in HP and LP line

The HP line power in Figure 46 shows the hydraulic power provided by the pump unit. The peak this pump power reaches 3.5 kW, while the average input power is only 89.8 W. This supports the discussion in Section 4.1.3 that the pump could be dimensioned with smaller capacity if short pumping times are not critical. On the other hand, the LP line power is relatively small, but quite constant. The peak power in LP line reaches only 18 W, keeping the average of 5.5 W. The LP line power represents wasted energy, as the fluid is guided through LP line PRV to the tank, transforming potential energy from pressurized fluid into thermal energy. Nevertheless, as the LP line PRV is adjusted only to 1 MPa, these power losses are relatively small, only 6.2% of the input energy. However, this lost energy could be avoided by utilizing tankless structure described in Section 2.3.13.

Next, Figure 47 shows the actuator chamber powers, calculated by flow rates and pressures. Positive power represents flow into the cylinder and negative out from the cylinder. Therefore, positive actuator power corresponds the output power from the DHMPA and negative actuator power can be used for regenerating energy back to the DHMPA unit.

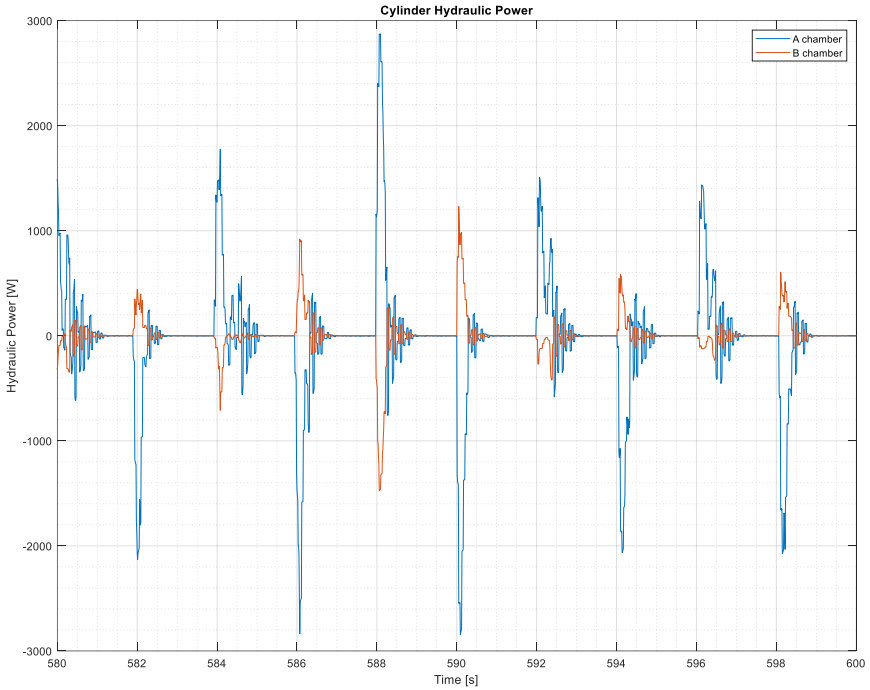

Figure 47. Hydraulic power of the cylinder chambers

As Figure 47 shows, the maximum cylinder chamber power is approximately 2850 W. This is significantly less than the maximum charging power of 3.5 kW into the DHMPA. Moreover, the net output power to the actuator is even less, as some power is always guided back to the DHMPA from the other chamber. The net output power can be determined by summing A and B chamber powers. This net power is shown in Figure 48.

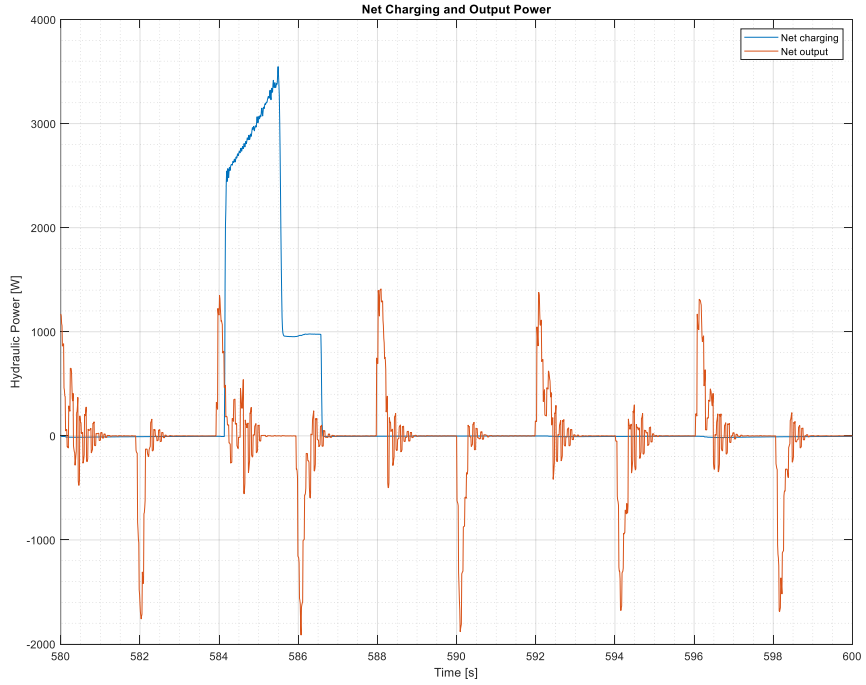

Figure 48. Net input power of the DHMPA and net cylinder power

In addition to the net cylinder power, the net charging power determined as well. The net charging power is calculated by summing HP and LP powers. These were presented in Figure 46. As Figure 48 shows, the net charging power mainly consists of pumped fluid as the LP line power is relatively low, only 6.2% of the HP line power as was shown in Figure 46. On the other hand, net actuator power clearly consists of the two components, A and B chamber powers. The positive net power of these two is used for lifting the load-mass while the negative portion can be used for energy recovery. However, the amount of regenerated energy cannot be determined based on the net actuator power as DHMPA's internal power losses consume some of the energy. Nevertheless, it can be integrated from HP accumulator hydraulic power. This power is presented in Figure 49 and it is calculated based on the accumulator's flow rate and pressure as shown in Equation (16).

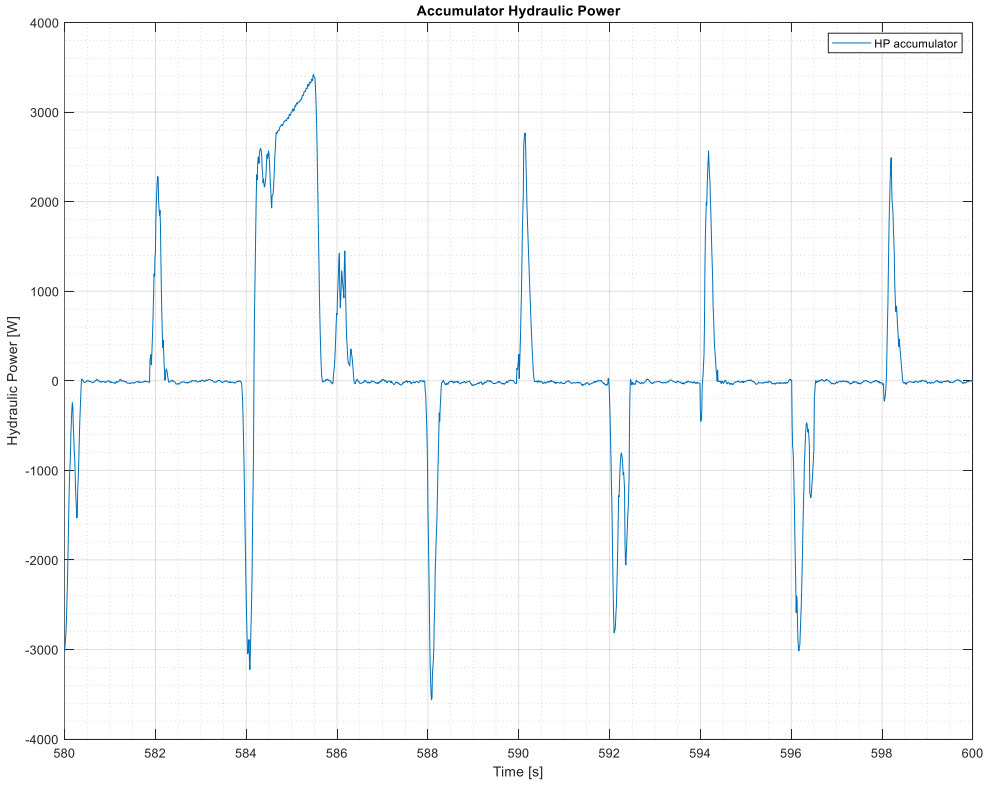

Figure 49. HP accumulator hydraulic power

HP accumulator hydraulic power is presented in Figure 49. The same three flow cases can be separated from the figure as discussed in Section 4.1.3:

1) Charging the accumulator with pump unit
2) Charging with recovered energy
3) Discharging for output work

Again, charging with the pump unit can be seen between 584 and 586 s. The other positive power values indicate regenerated potential energy from the load-mass. Negative values on the other hand represent output power for lifting the load-mass.

The powers presented in this section are utilized in the next section for determining the overall energy consumption in the system. By determining energy consumption in the system, the overall efficiency can be determined.

4.2.2 Energy Balance

This section reviews the energy balance of the system in order to determine the efficiency of the DHMPA unit. As this thesis determines traditional, overall and regeneration efficiency, the following cumulative energies are needed:

1) Net input energy
2) Net potential energy
3) Net regenerated energy

First, the net input energy is calculated from net charging power (Figure 48) by integrating it over the work cycle. As the test was a zero-energy process, the amount of net input energy represents the total amount of energy needed for overcoming the losses of the system. The net input energy is shown in Figure 50. If a reference energy consumption data was available, this net input energy could be compared with it.

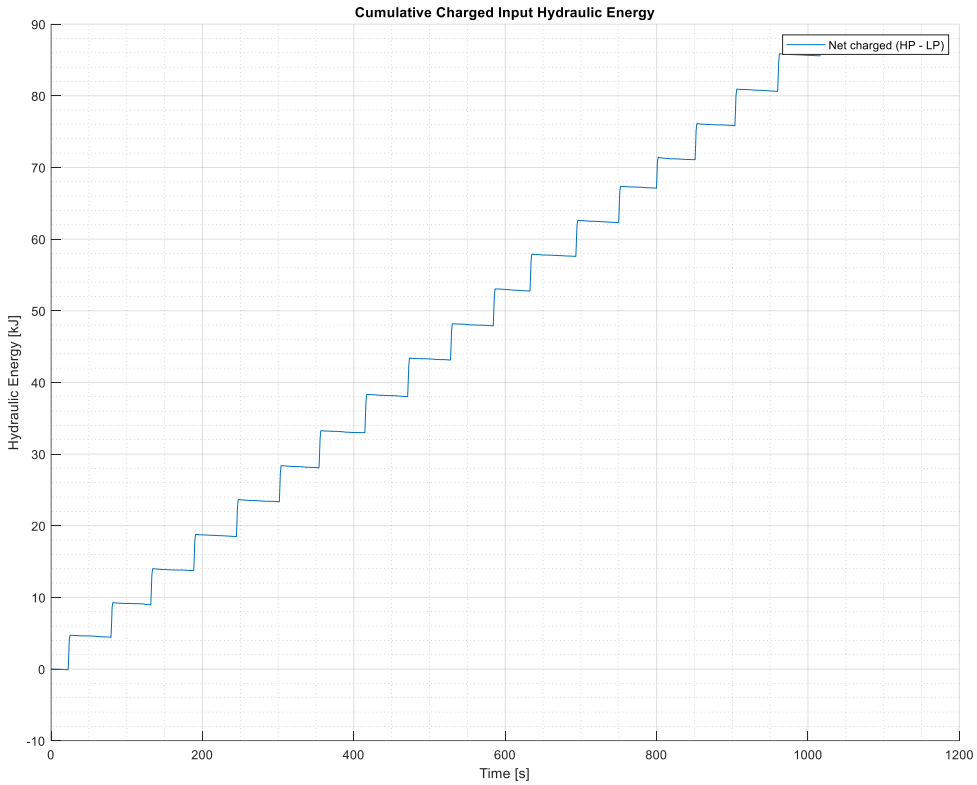

Figure 50. Cumulative hydraulic net input energy

In Figure 50, each step corresponds to one charge with the pump unit. Between each step, the cumulative energy input decreases slightly as small amount of energy flows through LP line PRV back to the tank. In the end of the test, total amount of cumulative input energy is 85.59 kJ.

Next, the amount of output potential energy is calculated. As this zero-energy process does not have a real output work, a cumulative amount of potential energy used for lifting is used instead. In addition, the amount of this cumulative lifting energy equals to the amount of recoverable potential energy. The amount of cumulative output lifting can be calculated as follows:

$$E_{\text{pot}} = n_{\text{lift}} \cdot mgh, \tag{17}$$

where E_{pot} is the total potential energy lifted during the test [J],
n_{lift} is the number of lifts [-],
m is the mass of the lifted load [kg],
g is the gravitational acceleration [m/s^2], and
h is the lifting height in one cycle [m].

This cumulative output load-lifting potential energy is presented in Figure 51. As the load-mass remains constant, the cumulative lifting work increases steadily in steps over the test run. One step represents one lifting cycle. The height of these steps equals to the load-mass potential energy in 40 mm height.

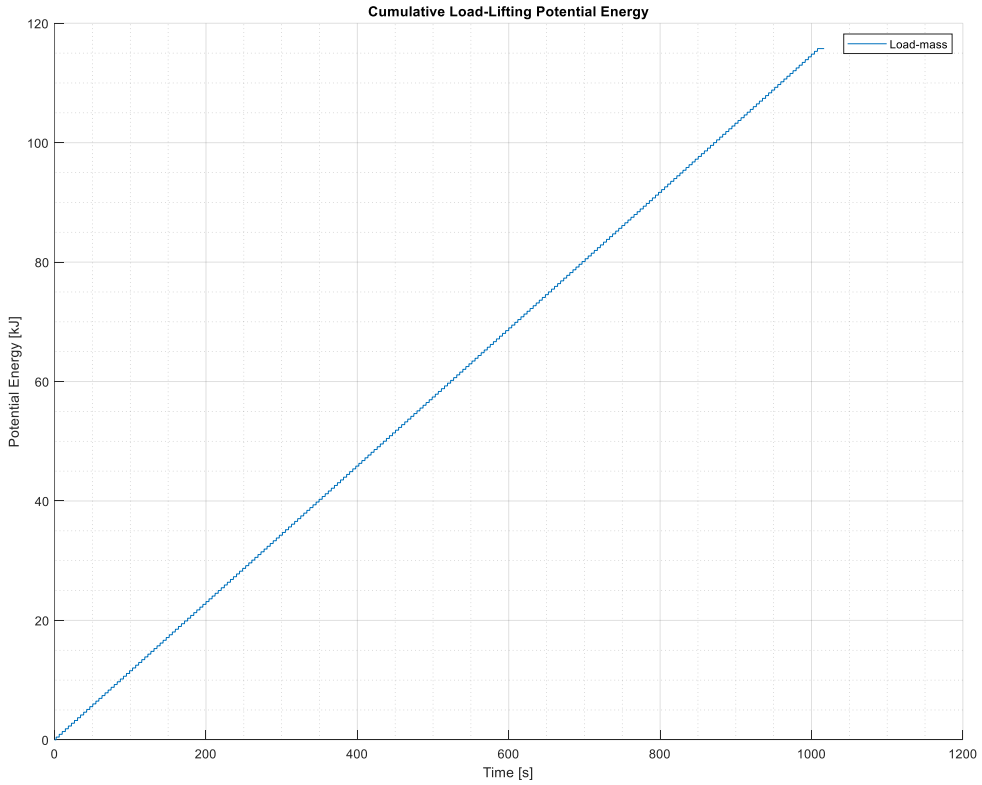

Figure 51. Cumulative load-lifting potential energy

As Figure 51 shows, the cumulative potential energy used for lifting the load-mass rises steadily over the test time as the load-mass, cycle time and lifting height per cycle are kept constant. In the end of the test, the cumulative load-lifting potential energy reaches 115.8 kJ. This is the amount of output energy used in this study.

Finally, the amount of regenerated energy is determined. The amount of regenerated energy equals to the input energy of the HP accumulator once the amount of HP line pumped input energy is subtracted from it as follows:

$$E_{\mathrm{reg}} = E_{\mathrm{accu,pos}} - E_{\mathrm{HP}}, \tag{18}$$

where E_{reg} is the total amount of regenerated energy during the test [J],
$E_{\mathrm{accu,pos}}$ is the total amount of input energy into the accumulator [J], and
E_{HP} is the total amount of input energy through HP line [J].

The amount of regenerated energy based on Equation (18) is presented Figure 52. The final amount of it reaches 73.04 kJ in the end of the test.

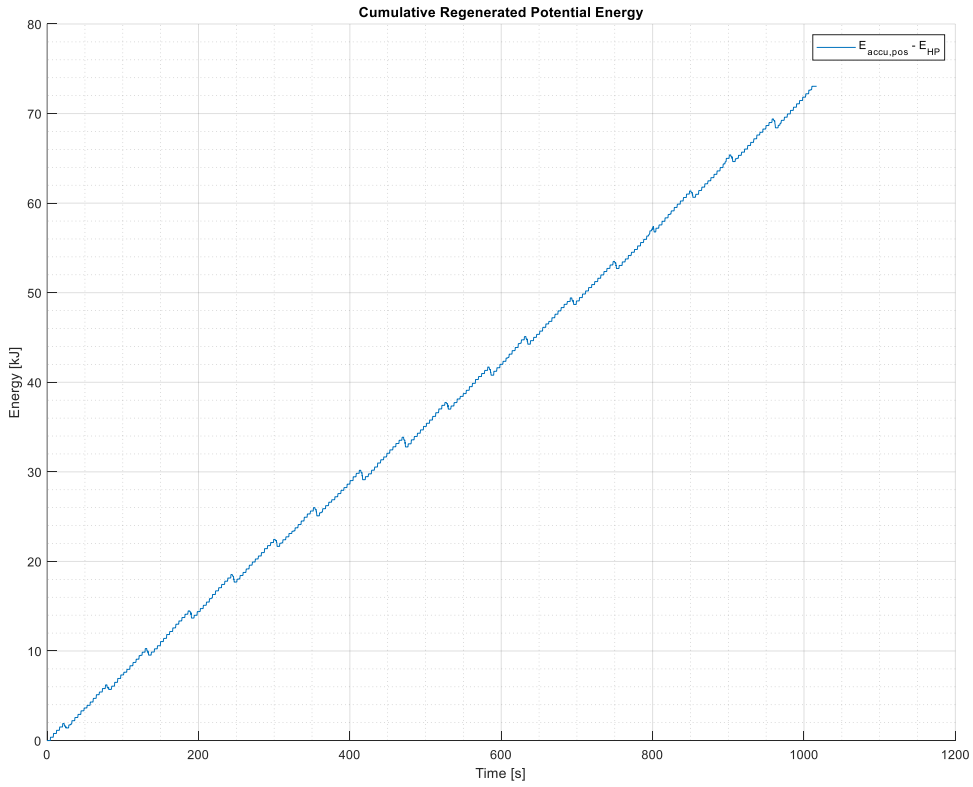

Figure 52. Cumulative recovered energy

However, as Figure 52 indirectly shows, this regenerated energy does not consider thermal losses in the accumulator. These thermal losses can be seen as a small decrease at every time the accumulator is charged with the pump unit. The major portion of these thermal losses are due to charging with pump unit, and these should not be considered in regeneration losses. Therefore, the final amount of regenerated energy is higher than presented in Figure 52. The correct amount can be estimated by calculating the average recovered energy per one cycle and multiplying it by the total number of lowering cycles. The equation for this is as follows:

$$E_{\mathrm{reg,est}} = n_{\mathrm{low}} \cdot E_{\mathrm{reg,ave}}, \tag{19}$$

where $E_{\mathrm{reg,est}}$ is the estimated amount of regenerated energy during the test [J],
n_{low} is the number of lowering cycles [-], and
$E_{\mathrm{reg,ave}}$ is average regenerated energy per one lowering cycle [J].

For calculating the average regenerated energy per cycle, the total regenerated energy (Figure 52) was investigated between the pump charges. The amount of regenerated energy was calculated from these time intervals and the total number of investigated time intervals was 10. Each of these time intervals contained 12 regeneration cycles, leading to a total amount of 120 steps from which the average regenerated energy was determined. The average regenerated energy calculated this way was 369.7 J. The resulting amount of estimated total regenerated energy, based on Equation (19), is presented in Figure 53.

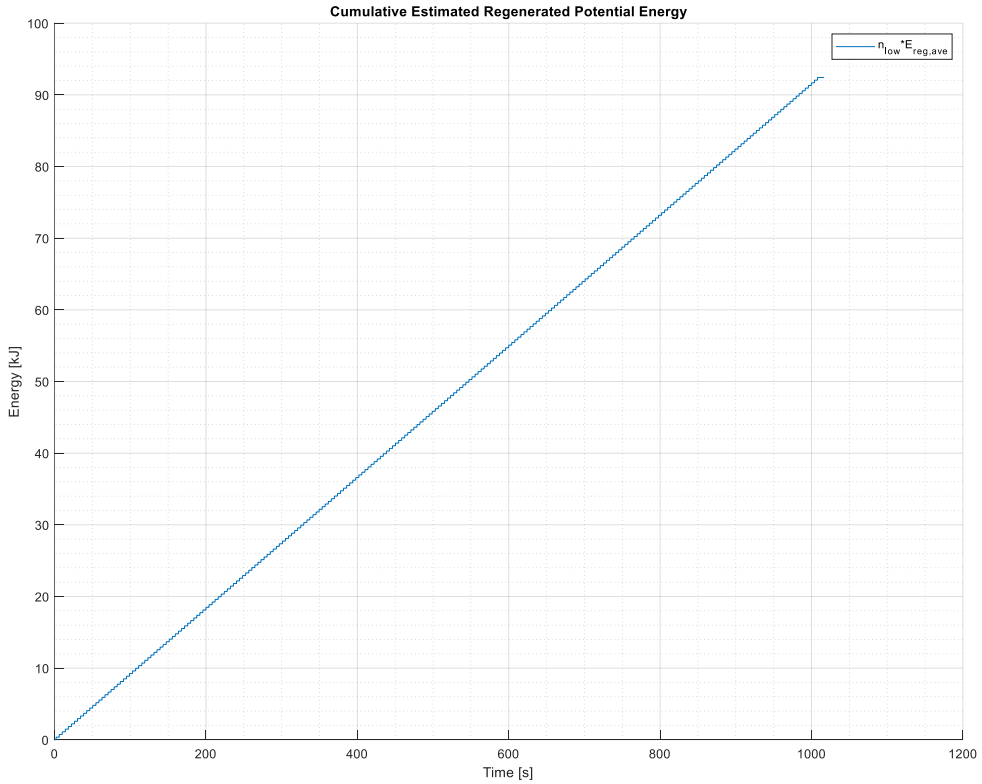

Figure 53. Estimated amount of regenerated energy

In this estimation, the final value of regenerated energy reaches 92.42 kJ, which is 26.5% more than the original calculation. Nevertheless, this estimation is more accurate as the effect of thermal losses in the HP accumulator is neglected by observing recovered energy only between the charging cycles. This value is therefore used in the next section for determining the regeneration efficiency.

As a summary, Figure 54 presents the three required energies for determining the efficiency of a DHMPA. These values are utilized in the final energy-efficiency calculations.

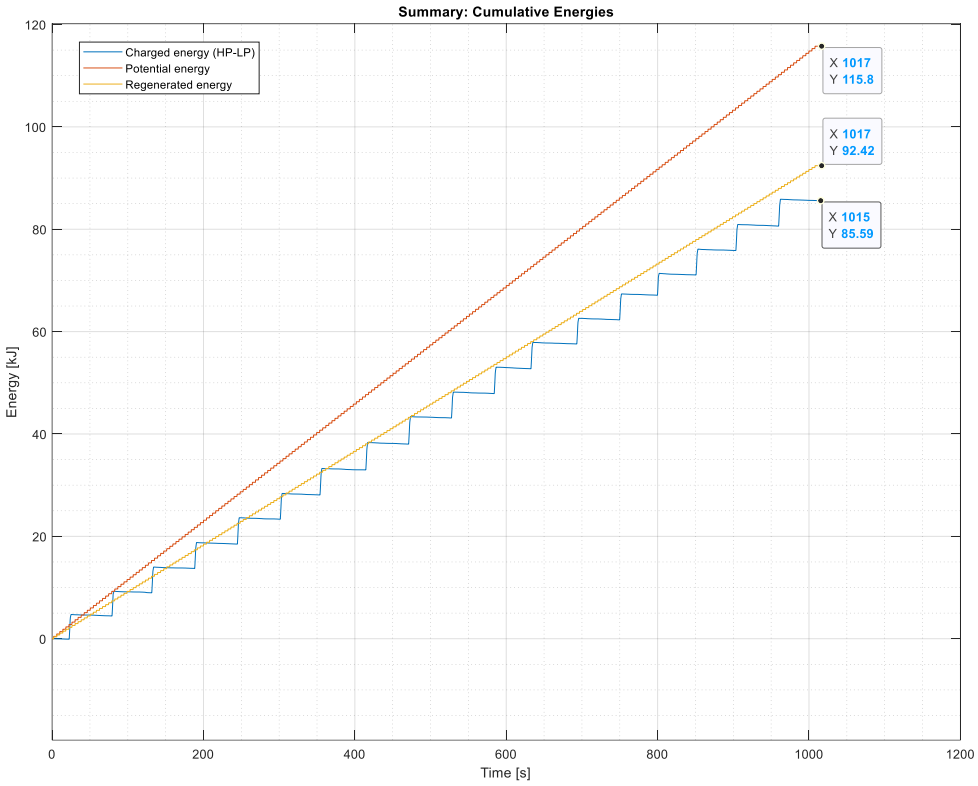

Figure 54. Summary: Cumulative energies

As shown in Figure 54, the amount of potential energy used for lifting the load-mass is the highest. This energy represents an output work of the DHMPA unit because in this type zero-energy process no actual output work is done. At the same time, this energy equals to the amount of recoverable potential energy since the load-mass is always lowered back to the starting height. On the other hand, the energy used for lifting the load-mass consists of the two other components: Net input energy (HP – LP) and net regenerated energy. The amount of the charging energy increases with steps as the pump is turned on only every 45 – 50 s while the amount regenerated energy increases more steadily, by 369.7 J per each lowering of the load-mass.

4.2.3 Energy Efficiency

As described in Section 2.1, the system efficiency can be calculated by dividing the amount of output energy by input energy. This ratio describes how efficiently input energy can be utilized in the system. This observation works well in traditional case, but it does not consider recovered energy or what happens in zero-energy process like the one in this thesis. In order to show how energy is utilized in the DHMPA unit, three different efficiency figures are calculated:

1) Traditional efficiency
2) Total efficiency
3) Regeneration efficiency

Next, the calculation of these efficiencies is presented. However, as the operation of the DHMPA in test is cyclic, one value for the efficiency cannot be presented. Therefore, the

efficiencies are presented in the end of this section as a function of time. The determination and calculation of these efficiencies are presented next.

First, the traditional efficiency is presented. It simply describes the ratio of input and output work as shown in Equation (20). However, this is not the true efficiency of the DHMPA as it does not consider the regeneration energy.

$$\eta_{\mathrm{trad}} = \frac{E_{\mathrm{pot}}}{E_{\mathrm{in}}}, \tag{20}$$

where η_{trad} is the traditional system efficiency [-],
E_{out} is the amount of the output energy [J], and
E_{in} is amount of the charging input energy [J].

The traditional system efficiency is determined as it is comparable with traditional hydraulic systems. The input energy in this case is the net charging energy by HP and LP lines. The amount of this energy was shown in blue in Figure 54. The output work is the total potential energy, cumulated from lifting the mass. This output work was shown in orange in Figure 54. As the traditional efficiency does not consider regenerated energy, it can get values over 100%. In this case, regenerated energy acts as an extra input energy, which is not seen by the Equation (20). Therefore, this traditional efficiency value cannot be used as the efficiency of the system. Nevertheless, the benefit in calculating this figure is that it is comparable with traditional hydraulic systems. Traditional hydraulic systems cannot utilize potential energy as an extra input and therefore the efficiency for a traditional system could be determined this way. Therefore, an ideal traditional system could achieve traditional efficiency of 100%. However, in real-life applications this efficiency is typically maximum of about 30% as discussed in Section 2.2.

Next, the total efficiency is calculated. This efficiency considers the amount of regenerated energy as well, so this figure can be used for evaluating the efficiency of the DHMPA. The calculation of it is performed as shown in the following equation:

$$\eta_{\mathrm{tot}} = \frac{E_{\mathrm{pot}}}{E_{\mathrm{in}} + E_{\mathrm{reg}}}, \tag{21}$$

where η_{tot} is the total system efficiency [-],
E_{out} is the amount of the output energy [J],
E_{in} is amount of the input energy [J], and
E_{reg} is amount of the regenerated energy [J].

Unlike the traditional efficiency, the total efficiency cannot be over 100% as the regenerated energy is considered as an input energy. The amount of regenerated energy used in the efficiency calculation is shown in yellow in Figure 54. The total efficiency represents the ratio of cumulative lifting work and cumulative accumulator charging energy. Therefore, this is the most important figure in investigation of the DHMPA's efficiency for use in load-lifting applications.

Finally, the regeneration efficiency is determined. This is interesting figure as well, as it describes how efficiently potential energy from the load-mass can be utilized as recovered energy. The regeneration efficiency is calculated as follows:

$$\eta_{\mathrm{reg}} = \frac{E_{\mathrm{reg}}}{E_{\mathrm{pot}}}, \tag{22}$$

where η_{reg} is the regeneration efficiency [-],
E_{out} is the amount of the output energy [J],
E_{in} is amount of the input energy [J], and
E_{reg} is amount of the regenerated energy [J].

Now, as the calculation of these three efficiencies are introduced, the efficiency values can be presented. Figure 55 shows traditional, total and regeneration efficiency over the 17-minute test cycle.

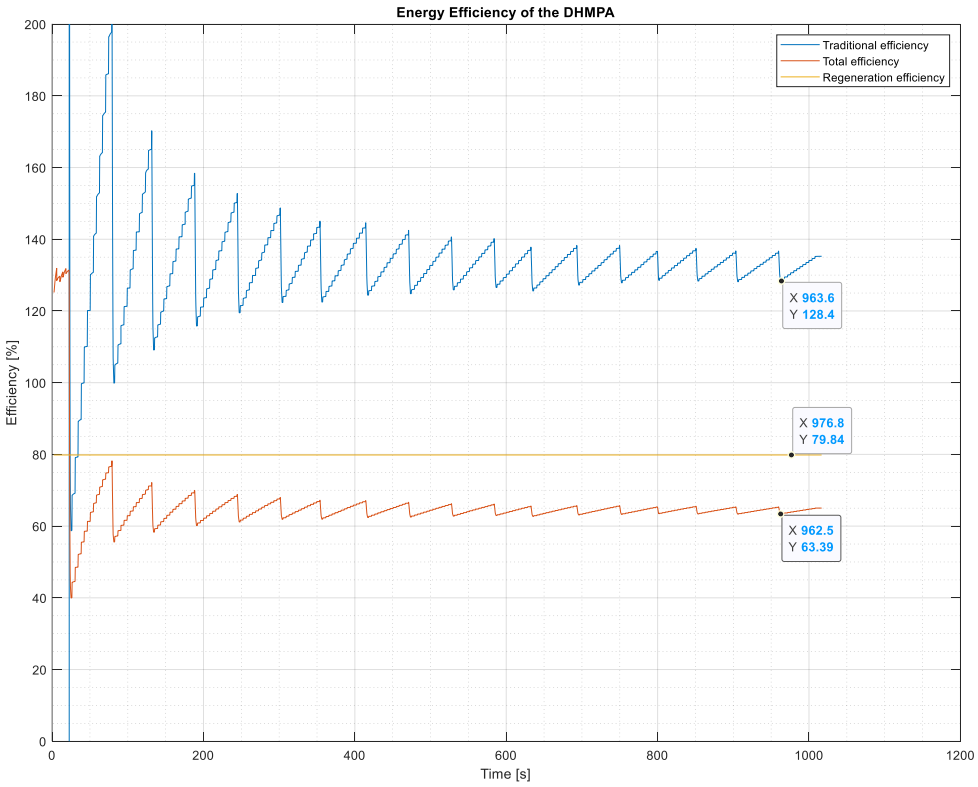

Figure 55. Traditional, total and regeneration efficiency of a DHMPA

As Figure 55 shows, during this test the efficiency calculations do not have enough time to settle to a certain value. It is obvious that significantly longer test time would be needed in order to determine an exact efficiency. Nevertheless, the lowest points of efficiency figures can be used to estimate the final efficiencies. This can be justified by the fact that unevenness in the efficiency originates from the pump input energy. The efficiency is at its worst when the pump has charged the accumulator, but that energy has not been used yet. It is certain that the final efficiency will not be lower than the lowest value in the end of the test period.

The traditional efficiency is found to be 128.4 – 135.2%. This overperforming efficiency can be justified by an extra input energy from the regenerated potential energy as discussed earlier in this section. In practise, this means that the DHMPA unit performs 28.4 – 35.2% better than an ideal conventional system.

The most important figure, the total efficiency, was found to be 63.4 – 65.0%. The amount of regenerated energy has not been measured earlier, so this is the first time when the total hydraulic efficiency could have been determined for the DHMPA unit. Nevertheless, the acquired total efficiency seems to be in line with earlier results, which were discussed in Section 2.3.13.

As the amount of regenerated energy was measured, it was also possible to measure the regeneration efficiency for the first time. The regeneration efficiency was found to be 79.8%. This implies that 20.2% of the recoverable energy is consumed in cylinder friction and valve throttling losses.

In this chapter, the measurement results of the test were presented and analysed. First, the analysis concentrated on performance of the system. Although the overall performance of the system was quite good, it was found that some oscillations and errors occurred in positioning control. For better performance, further investigation of the controller tuning is needed. The rest of the chapter concentrated on energy-efficiency analysis. The energy balance of the system was determined in order to calculate traditional, total and regeneration efficiency. These efficiencies were then determined and the results implied promising results compared to traditional hydraulic systems. However, the results cannot be directly compared to previous studies of the DHMPA as these have concentrated on energy consumption instead of efficiency calculation. As for this test setup, no reference data from the other systems or simulations were available. Nevertheless, the aim of this thesis was achieved as the efficiency of the DHMPA unit was determined in load-lifting test, and the results can be generalized to the other similar applications as well. Furthermore, the next chapter discusses the results more in detail.

5 Discussion

5.1 *The Effect of Operating Pressure Range*

In the test case of this thesis, the DHMPA unit was operated with HP pressure range of 10 – 14 MPa. However, the range can be selected otherwise as well, and the only limitation is the maximum pressure of 22 MPa, which is determined by safety PRVs in the DHMPA. In addition, the minimum pressure has to be above the one needed for lifting the load-mass. As for reference for selecting another pressure range, the DHMPA was also tested by completing the same test run with pressure range of 10 – 18 MPa. The effect of this selection is discussed in this section.

With the new HP pressure range, the system response was approximately similar as in the original test, but the final efficiencies decreased slightly. Less efficient performance is probably due to an inefficient operation at higher pressure levels and higher thermal losses in the accumulator. Nevertheless, the corresponding force series should be even slightly better, as the forces available for accelerating the load-mass are more evenly divided into positive and negative sets, which should lead to an improved performance. In order to review the system response more carefully, the next paragraphs will discuss the main differences between the new and original test.

First, the position response in the original and the new test is shown in Figure 56. It can be seen that the response is approximately similar in the new test, though the original included more small oscillations at each step. However, during the full test cycle, the new test included an increased amount of severe position errors, such as the one seen at 590 s.

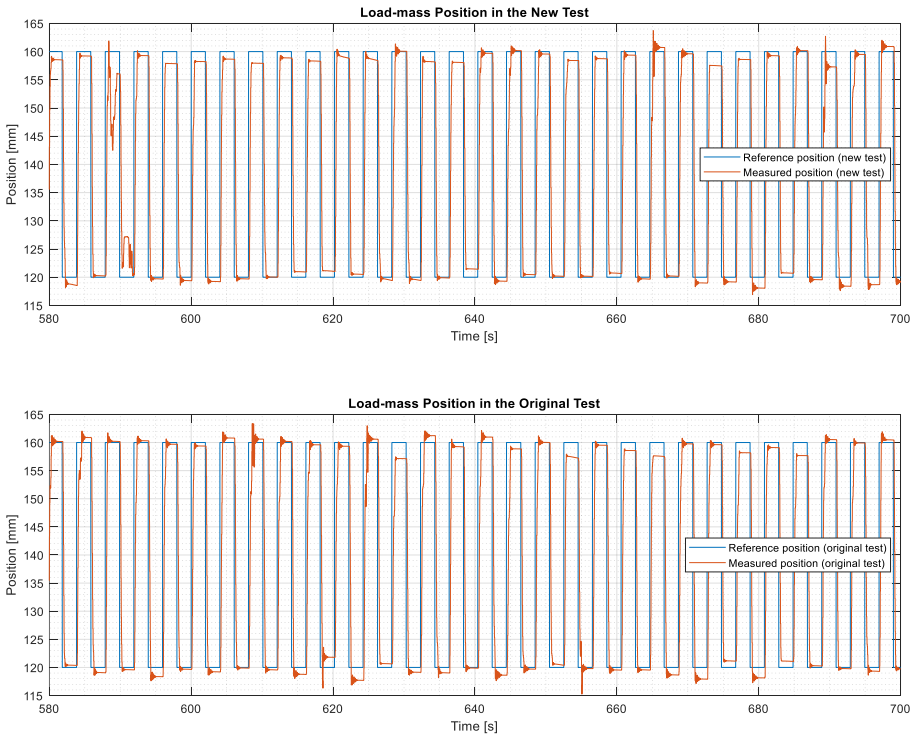

Figure 56. Position response of the load-mass in the new test

As the Figure 56 shows, the position response of the system was actually slightly better than in the original test. This should lead to an improved efficiency as well, but for some reason, it was decreased. This could be partly due to an increased amount of severe position errors, such as the one seen at 590 s. One reason these errors and decreased efficiency could lie in the tuning of the system: It might be that the same tuning parameters cannot be sufficiently applied to both ends of the operating pressure range. However, in order to justify this, a study concentrating on the tuning of the system would be needed.

Next, Figure 57 shows the pressure response in the cylinder A and B chambers between 580 and 600 s. The upper chart contains the pressures from the original test and the lower chart shows the response of the new test.

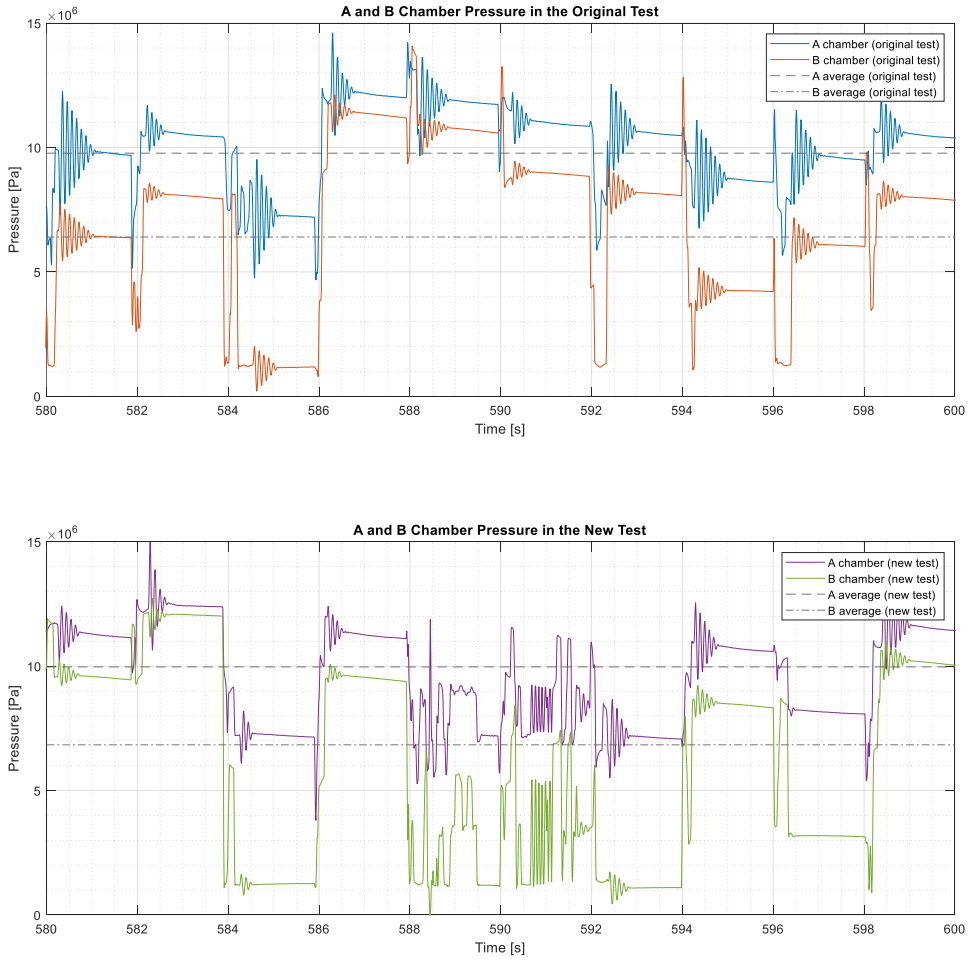

Figure 57. A and B chamber pressure level comparison between the two tests

As seen in Figure 57, the positioning error at 590 s causes significant oscillation in the chamber pressures. Nevertheless, the pressure oscillations during the normal operation are slightly smaller in the new test. This is in line with the results shown in Figure 56, in which the positioning oscillation were smaller as well. Additionally, it can be noticed that the pressure averages of the cylinder chambers are slightly higher in the new test than in the original test.

Furthermore, the load-mass velocity is observed in order to confirm that the efficiency was not affected by an altered positioning response. The velocity of the load-mass in Figure 58 shows that the velocity response, and the averages of it, remain approximately the same in the new test. If the average velocities would significantly differ from each other, the throttling losses would be affected directly, as these are dependent on the flow rate of the cylinder.

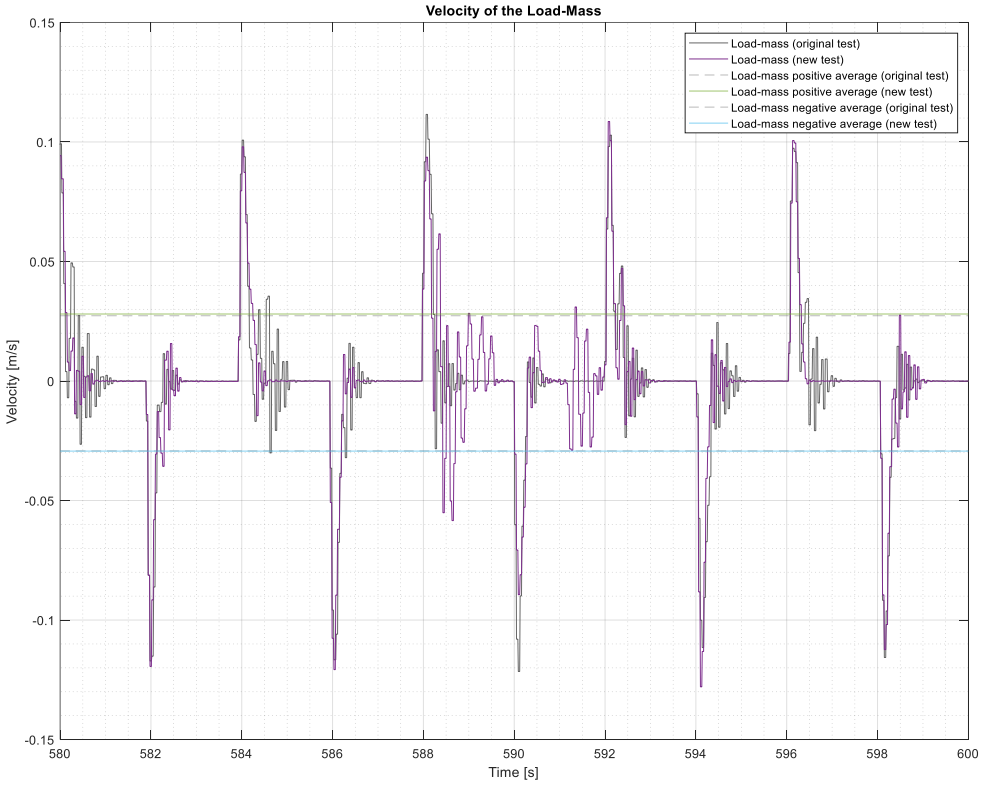

Figure 58. Velocity of the load-mass in the two tests

As Figure 58 shows, the velocity averages of the working cylinder are almost identical to each other. Thus, the flow rate averages of the cylinder in the two test cases are similar to each other as well. However, the throttling losses are not linearly proportional to the load-mass velocity, and thus, the flow rate averages cannot explicitly reveal the differences in total losses. Nevertheless, as the lifting cycle is the same in both tests and the movement is symmetrical, there is not much space for major velocity differences to occur. Thus, the velocity differences by themselves cannot fully explain the decreased efficiency. In order to accurately determine the effect of the load-mass velocity into valve losses of the system, a further energy loss analysis is needed.

One possible reason for the decreased efficiency at high pressure range might be an insufficient force level selection and an increased gap between two adjacent force levels. Although, the load-compensated force series should be more evenly divided, the difference between the two adjacent forces might be too wide. The reason for these gaps is that as the pressure level of the HP accumulator is set higher, the pressure levels of the converters also get higher. This leads to increased gaps between the available force levels. In addition, as all the force levels are not always available, the errors in force selection might increase. For

example, if one or more cylinder converters are near to their end points, the corresponding pressure levels cannot be utilized on one direction before the converter is driven back, towards to the neutral point. In order to observe the utilization of the force levels, Figure 59 first shows the force series generated by the DHMPA in the new test.

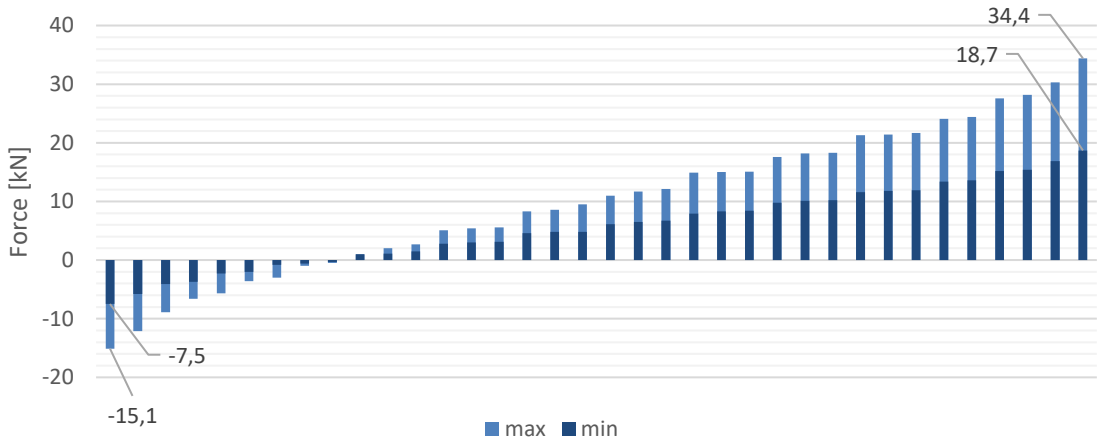

Figure 59. Force series in the new test

As Figure 59 shows, force levels are divided between -15.1 and 34.4 kN, at HP pressure of 18 MPa. Force series with the minimum pressure of 10 MPa are the same as in the original test, since the $p_{\min}$ threshold pressure was not changed. For achieving the optimal performance, a vast majority of the available force levels should be utilized. However, as shown in Figure 60, only the force levels between 5 and 20 kN were selected, and majority of those were between 11 and 15 kN.

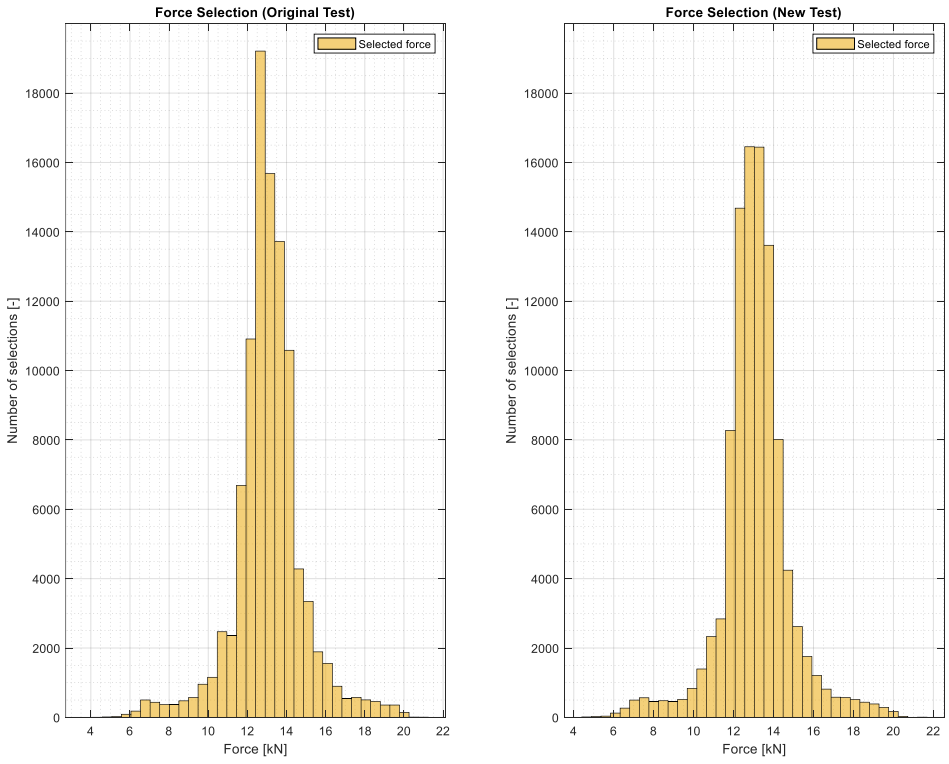

Figure 60. Histogram of the selected forces in the original and new test

As Figure 60 shows, the force selection in the new test is almost similar to the original test. However, as the force selection excludes a significant number of available force levels in both tests, it can be concluded that the system is not operating optimally in this load-lifting test rig. Especially, in the new test the force levels are divided more widely, which leads to a narrowed selection of available force levels. This problem is partly due to that the DHMPA unit was not originally designed for the test rig used in this study, and thus, the converter cylinders, on/off valves and the HP accumulator may not be optimally dimensioned. Additionally, all of the force levels are not constantly available, if some of the pressure converters are driven near to their end positions. This combined with a higher HP pressure level can lead to a forced utilization of insufficient force levels. In order to achieve a better performance of the unit, the DHMPA components should be dimensioned based on the load-lifting application. This could probably increase the efficiency as well.

Thermal losses in the accumulator are higher because the charge volume and pressure are higher in the new test. In Section 4.1.4, it was noticed that the gas temperature of the HP accumulator rose significantly during the pumping. In this new test, this effect was emphasized as the pressure range was wider, while the charging flow rate was kept the same. This led to an increased maximum gas temperature in the accumulator as shown in Figure 61.

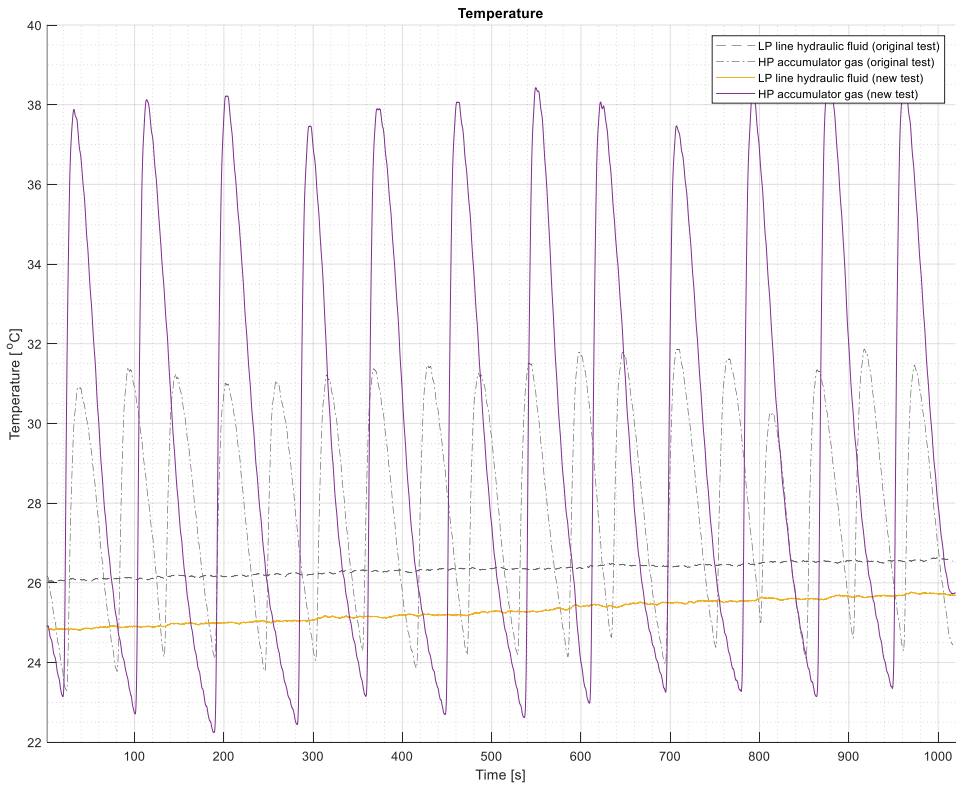

Figure 61. Temperature with higher operating pressure range

In the new test, the initial hydraulic fluid temperature was 24.8 °C, about 1 °C lower than in the original test. However, as Figure 61 shows, the difference of the temperatures between the two tests slightly narrows towards the end of the test. This implies that more internal throttling losses might occur in the system, as the hydraulic fluid temperature rises slightly

faster. However, as discussed earlier, it cannot be concluded whether the flow rates, and thus the throttling losses, through the valves were significantly higher in the new test. Thus, without a further energy loss analysis, the effect of pressure range into throttling losses cannot be directly stated. The small increase in the rising rate of the hydraulic fluid temperature might also be due to the conducted thermal energy, as the average gas temperature is higher in the new test than in the original test.

As was shown in Figure 61, the difference between gas temperatures in the two tests is notable, as the gas temperature in the HP accumulator rises up 38.5 °C, instead of 32.9 °C. It also decreases lower, but in this case the difference is only about 1 °C. Higher gas temperature after each charge causes the system waste more hydraulic potential energy into thermal energy. This can be seen as a pressure drop in the HP accumulator, as shown in Figure 62. As the gas temperature is decreased due to thermal conducting through the accumulator walls, the hydraulic fluid pressure is decreased as well. Naturally, the pressure is also decreased when the accumulator potential energy is used, but some part of it is due to thermal conductivity, and it can be seen as lost HP accumulator pressure when the load-mass is stationary, as shown in Figure 62. This thermal conduction also occurs during the lifting or lowering motion, though it cannot be observed from the figure.

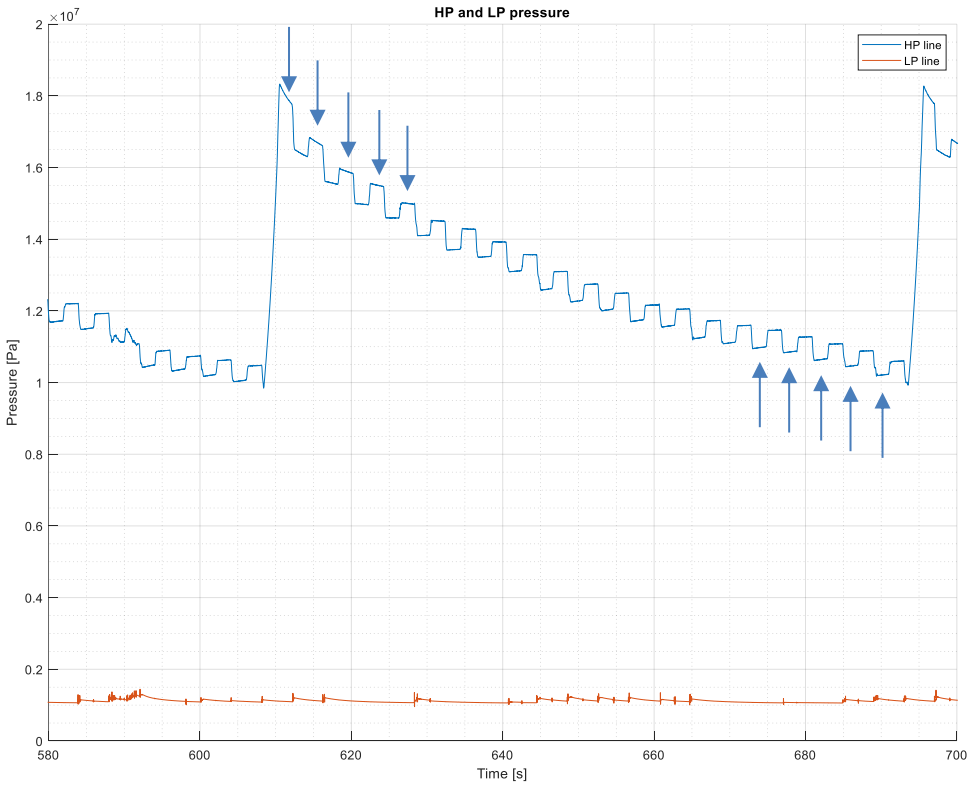

Figure 62. HP and LP pressure with higher operating pressure range

As Figure 62 shows, after the HP accumulator has been charged, a steep decrease in HP pressure can be seen, even when no hydraulic energy is taken from the accumulator. Therefore, based on the temperature and HP pressure, it can be concluded that a notable amount of hydraulic energy might be lost as thermal losses because the gas is quickly pressurized. The amount of lost thermal energy could be decreased by charging the accumulator slower. This would lead to lower peak temperatures, and thus, lower conduction

rates. However, the pumping time would be increased, which might be unwanted in certain applications. Therefore, the pumping flow rate must be chosen as a compromise between pumping time and optimal charging of the accumulator. Nevertheless, as shown in Figure 62, a few cycles before a new charge, the pressure level actually rises when the load-mass is stationary. This occurs when gas pressure is decreased below hydraulic fluid temperature. In this situation thermal energy is restored from the fluid back to the gas, which increases HP accumulator pressure, and thus, the amount of stored energy. In an optimal, isothermal case, the variation of the gas temperature would be minimized, and the average of it would be close to the environment temperature. In this case the amount of lost thermal energy would be low and the amount of restored temperature would be maximized as the temperature variates on both sides of the environment temperature. Alternatively, in an adiabatic case, the thermal losses could be decreased by utilizing a thermally isolated accumulator, which could minimize the thermal conductivity regardless of the pumping cycle.

In the new test, the increased operating pressure also affects the amount of utilized fluid from the HP accumulator. As the $p_{\max}$ threshold pressure is set higher, the accumulator is filled fuller during one charging cycle, as shown in Figure 63.

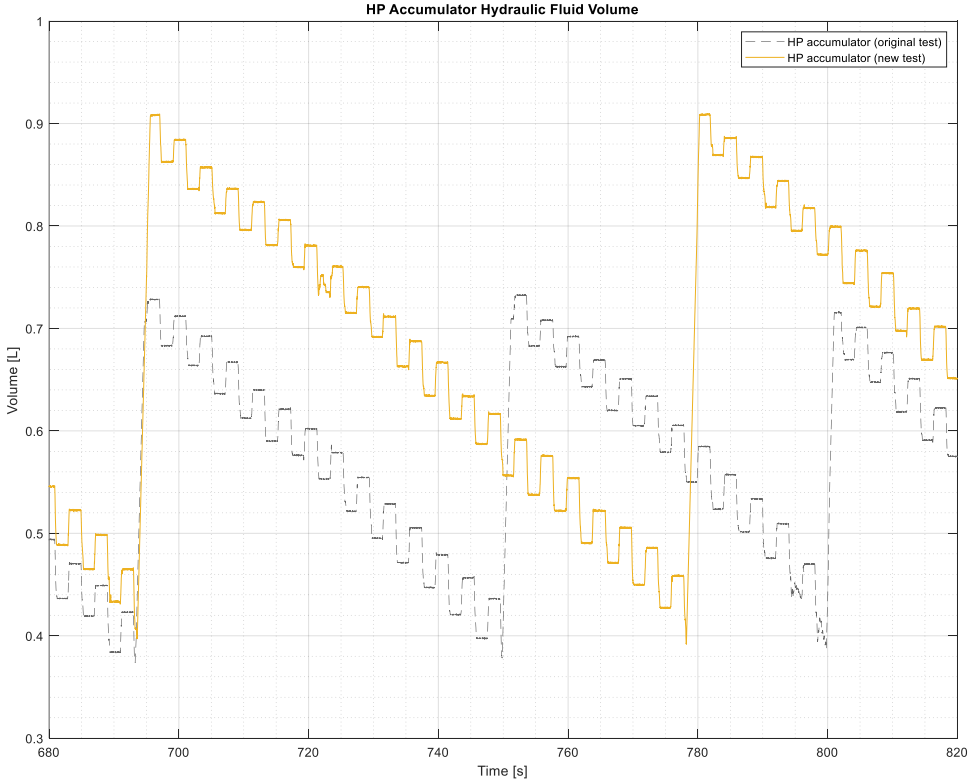

Figure 63. HP accumulator hydraulic fluid volume in the two tests

As the operating pressure range is increased from 10 – 14 MPa to 10 – 18 MPa, the amount of utilized fluid is increased from 0.33 L to 0.51 L, as shown in Figure 63. Therefore, while the pressure range was doubled, the amount of utilizable fluid increased to 150%. As a result, the pausing time between two charging cycles increased as well, approximately to 150% of the original pausing time.

Finally, as a summary, the cumulative energies of the DHMPA are presented in Figure 64. These are calculated similarly as in the original test. It can be seen that the amount of charged energy is increased 9.3%, from 85.59 kJ to 93.55 kJ, while the amount of regenerated energy decreased 6.2%, from 92.42 kJ to 86.69 kJ. Since the test cycle was identical to the original test, the cumulative potential energy was the same as in the original test, 115.8 kJ.

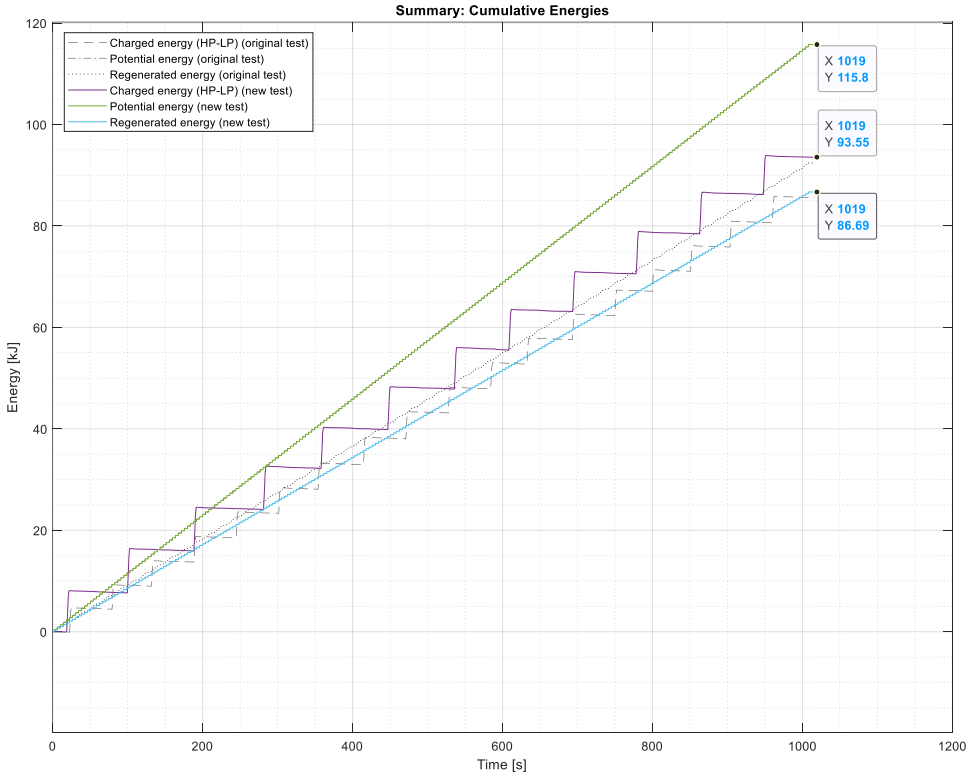

Figure 64. Cumulative energies in the two tests

As the amount of charged input energy is consumed into covering the energy losses in the system, it can be concluded that the energy losses were higher in the new test. However, in addition to increased thermal losses, it is not clear what caused higher energy consumption. One reason might lie in the velocity of the load-mass. Although it was shown that the average velocities were almost identical in the two tests, the temporal changes might cause some unexpected differences as the throttling losses are not linearly dependent on the load-mass velocity. In order to determine this effect, a further analysis is needed. Another reason might be related to insufficient selection of the force levels due to increased gaps between adjacent force alternatives. This might lead to an increased valve switching, thus affecting the valve losses. However, without further investigation, this cannot be explicitly justified. Nevertheless, it can be seen, that the amount of the regenerated energy was decreased in the new test, while the amount of the recoverable potential energy remained the same as in the original test. Because during the regeneration, the hydraulic energy is directed only through on/off valves and pressure converters, it can be concluded that during the regeneration, the throttling losses in the valves, converters and pipes were higher in the new test than in the original test. This can be justified by the study conducted in [8], which analysed the energy losses of the DHMPA. Furthermore, it was concluded that the majority of internal losses occur in on/off valves, as discussed in Section 2.3.13. Therefore, it can be concluded that the valve throttling losses were higher in the new test, though the reason for this remains unclear.

Naturally, the increased amount of throttling losses together with higher thermal losses in the HP accumulator decrease system efficiency. The three characteristic efficiencies of the DHMPA in the new test are shown in Figure 65. The figure includes the efficiencies of the original test as well.

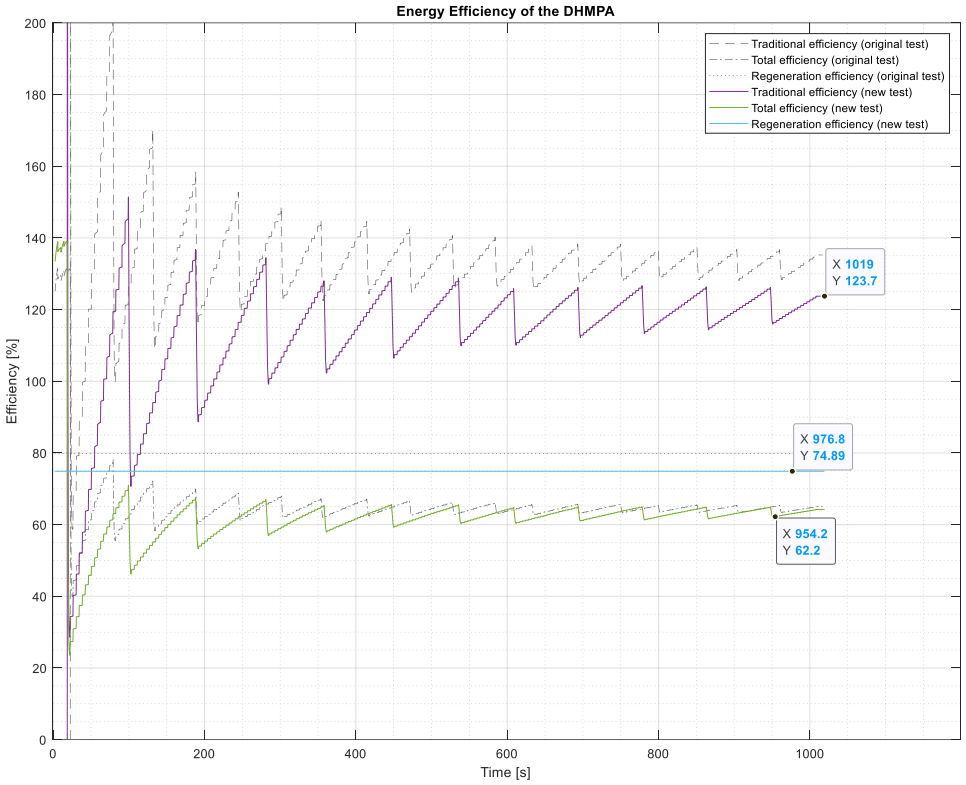

Figure 65. Efficiencies in the two tests

As Figure 65 shows, each of the three efficiencies were decreased, as $p_{\max}$ was changed from 14 MPa to 18 MPa. Since $p_{\min}$ was 10 MPa in both cases, the operational pressure range was doubled. Otherwise the test parameters were kept the same as in the original test. The traditional efficiency decreased from 128% to 116%, total efficiency from 63% to 62% and regeneration efficiency from 80% to 75%. The decreased efficiencies were concluded to be mostly due to an increased throttling and thermal losses, as discussed earlier in this section.

5.2 *Performance and Efficiency Evaluation*

On average, the positioning response is good and repeatable, but as discussed in Section 4.1.1, the positioning of the load-mass contained some unexpected errors. As for now, the position response was not as smooth as could be achieved with a well-tuned proportional valve system. The positioning was sometimes delayed, oscillated or in the worst cases the final position was not reached during the 2 s step time. An obvious reason for these errors was not found, but the tuning parameters affected significantly on the behaviour of the system. Especially cost function terms can have a great effect how the force levels are selected and implemented. For example, it is possible that the pressure converters were occasionally drifted near close to their end points. This might cause unexpected behaviour as there might not be enough fluid left, though EPEC 5050 tries to operate as there was.

However, different cost function terms were tested and no combination showed a flawless position response. Nevertheless, it is possible, that suitable tuning parameters were not found and it is the reason for positioning errors. Also, the possibility of a hardware failure, such as halted on/off valve cannot be excluded.

The efficiency was proven to be excellent compared to the traditional systems. As the total efficiency was over 63% and regeneration efficiency 80%, it is obvious that throttling losses have been successfully minimized. The traditional efficiency was found to be 128%, which can be achieved by the regeneration of the potential energy. Although it does not reflect the correct efficiency of the system, it can be compared to the traditional hydraulic systems as the regeneration of energy is not considered. For example, LS systems were reported to perform with energy-efficiency up to 36% [7]. This corresponds to approximately 3-4 times higher energy consumption than the one measured in this test. However, for an accurate comparison, a measured reference data from the same test setup or corresponding simulation model would be needed. Moreover, the efficiency of the pump unit was not considered in these efficiency calculations.

Compared to the other energy saving solutions, the DHMPA offers a competitive potential. As discussed in Section 2.3, the Buck converter could reach efficiency up to 76% at optimal flow rate, while the DDH could perform up to 73% in lifting motion. However, the Buck converter efficiency excluded the pump efficiency while the DDH efficiency includes it, which makes the comparison difficult. Moreover, either of these efficiencies does not reflect the total efficiency in a duty cycle, as the Buck converter was measured only with different flow rates and the DDH efficiency was excellent only in lifting motion. Therefore, it is not clear whether the DHMPA performed more efficiently than these systems, though it can be concluded that the total efficiency of 63% is remarkably better than those generally reported in hydraulics. The other energy saving hydraulic studies concentrated on energy consumption comparison instead of a direct efficiency analysis. Most of the other solutions were compared to a corresponding LS system, and these energy savings were up to 71%. If the energy efficiency of an LS system is 36%, the 71% reduction in energy losses corresponds to efficiency up to 80%. However, this is the best-case-scenario with up-rounded values. In addition, the test cases are not equalized, and thus, significantly lower efficiency value, for example 60 – 70% could probably be more accurate. Therefore, it can be concluded that the DHMPA can offer probably one of the best efficiencies among energy-saving hydraulic systems, especially in load-lifting applications. This is in line with the previous studies, in which up to 77% reduction in power losses were achieved compared to the traditional four-way proportional valve LS-system, as described in 2.3.13. However, a further energy consumption analysis and reference data with other technologies from the same test rig would be required in order to compare the efficiency to the other solutions. Nevertheless, the DHMPA gains a significant advantage compared to the other solutions in zero-energy processes, as it is capable of regenerating energy with efficiency up to 80%, as the results of this thesis show. It also indicates, that the throttling losses in the system are minimal. In addition, a significant proportion of energy losses are probably related to the charging of the DHMPA. For example, if the charging losses were negligibly small, the total efficiency of the DHMPA should be close to the regeneration efficiency, as the both efficiencies describe how efficiently the unit operates. However, in this test the total efficiency was 63%, which is notably lower than the regeneration efficiency of 80%. As the regeneration efficiency does not consider the unit charging at all, the lower total efficiency is most probably related to the unit losses in the input energy. These charging related losses

mostly consists of the HP accumulator thermal and LP line PRV losses. Therefore, the following research should concentrate on minimizing these losses, which could further improve the efficiency of the DHMPA. Nevertheless, it can be concluded that the efficiency of the DHMPA unit can be excellent in load-lifting applications.

5.3 *Result Validation*

This section reviews the validation of the achieved results. As the efficiency analysis on this thesis was based on real-time measurements during the test cycle, it is essential that the measurement data is correct. Therefore, the result validation is based on validating the measurement data. In this study, the data was measured with the following sensors:

1) 2 x flow sensor
2) 4 x pressure sensor
3) 2 x position/velocity sensor
4) 2 x temperature sensor

The flow sensors used are Kracht VC 1 sensors, equipped with AS 8 display units. The operation of Kracht VC 1 is based on pulse detection in the gear-measurement unit. These pulses are counted by AS 8, which is then used to send the corresponding 4…20 mA current signal to the data acquisition system. This signal can be calibrated by using a separate pulse generator in place of the flow sensor. The calibration was done for both flow sensors and therefore the measured flow rates should be reliable.

The operation of the pressure sensors can be checked by comparing the sensor data from EPEC 5050 to the ones in data acquisition system. The pressure was measured from the same locations with DHMPA's and data acquisition system's pressure sensors. Figure 66 shows the measurement error between EPEC 5050 and the data acquisition system at 0 – 2 s.

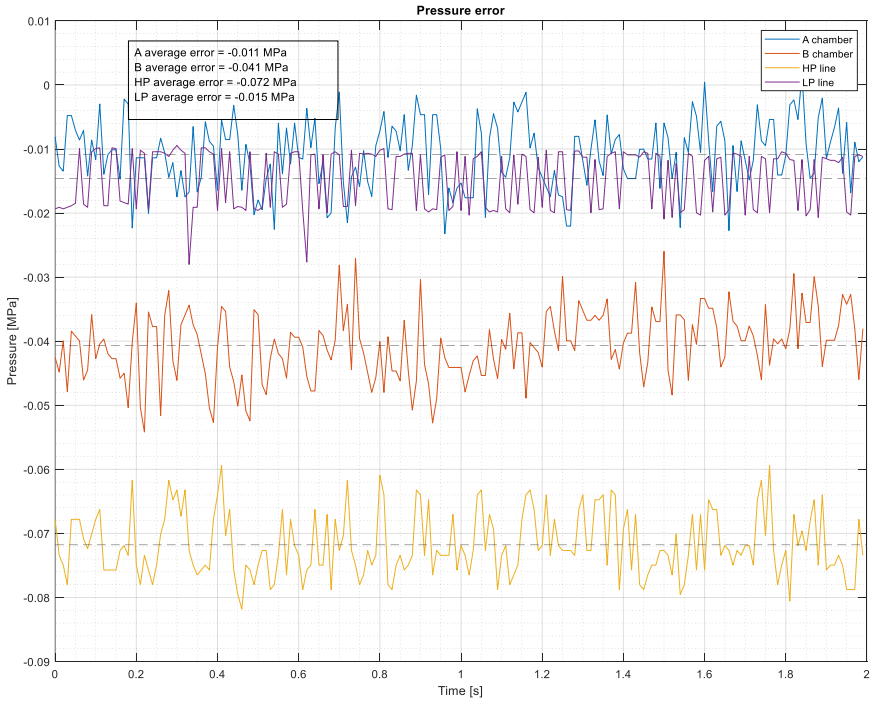

Figure 66. Pressure measurement validation

The measurement error presented in Figure 66 shows that all data acquisition system pressure values are a bit higher than the values measured by EPEC 5050. Nevertheless, as all the pressure sensors, except LP sensor, have range of 0…25 MPa, the relative error is small. The highest error occurred between HP line pressure sensors, and the relative error to the range is 0.29%. The LP line pressure sensor has range of 0…4 MPa, leading to relative error of 0.38%. For evaluating the energy efficiency in the DHMPA, these errors are acceptable. However, it should be noted that this does not reflect the absolute error, but only error between the data acquisition system and EPEC 5050.

The position and velocity sensors were used to measure the position and velocity of the load-mass and HP accumulator's piston. Sensors were calibrated based on manufacturer data sheet, and the reading was compared to an approximate distance measurement. More accurate position or velocity validation could not be completed as there were no double sensors. Nevertheless, position and velocity offsets were zeroed when stationary, at zero-position. Furthermore, it can be concluded that the position and velocity readings are reasonable because otherwise the results of the two different sensors had caused inconsistencies in the energy analysis.

The temperature sensors were not utilized in the efficiency analysis and therefore the accuracy of these is not as critical. However, in the sense of evaluating system performance, temperature readings are important. Nevertheless, the accuracy of temperature sensors was evaluated to be sufficient as both sensors displayed approximately the same value, 22 °C, in the room temperature before the DHMPA unit was operated. This value corresponds also well to the ambient room temperature in the laboratory.

5.4 *Future work*

This section reviews the future work and potential improvements for the DHMPA. As the DHMPA unit utilized in this test was a proof-of-concept device, it still has more to offer as it is further developed. In load-lifting applications, the most important work would be to improve controllability and minimize charging-related energy losses. As this thesis shows, the current position control is not as smooth as for example a well-tuned proportional valve-controlled system would be. Nevertheless, the final position was reached within approximately ± 2 mm tolerance. The controllability could be improved by modifying the control algorithm and re-dimensioning the DHMPA unit for the load-lifting test rig. The DHMPA unit studied in this thesis was originally dimensioned for the test rig presented in 2.3.13 and therefore it is not optimally dimensioned for this application. If the controllability could be improved, the energy efficiency of the DHMPA could also be increased as less energy is needed for correcting the position error.

For improving the energy-efficiency, four main subjects for development can be stated based on the results of this thesis:

1) Correct dimensioning of the system components
2) Careful optimization of the controller
3) Implementation of tankless pump unit
4) Minimizing thermal losses in the HP accumulator

As mentioned, the correct dimensioning would probably increase the energy-efficiency of the DHMPA unit as well. This would include not only the adjustment of on/off valve

capacities, accumulator volume or dimensions of the converters, but also the flow rate and pressure range of the pump unit. It was shown that the selection of the operating pressure range can have a notable effect on the efficiency of the DHMPA. In addition, the locations of the converter pistons could be measured more accurately with for example laser or ultrasonic sensors instead of the three inductive sensors. This could ensure that all the converter pistons are operated at proper range as the locations are exactly known instead of the evaluating piston positions based on volume estimations. Consequently, this requires changes in the control algorithm as well.

As the system control consists of five controller and three cost function parameters, the system tuning is very challenging. The controller includes setting of pressure range, position tolerance limits, two P terms and one I term gain while the cost function considers the weight of switching cost, volume cost and crossflow cost. Each of these parameters have an effect on the final system behaviour and efficiency. In addition, the selection of these is not only matter of an absolute value, but also their relationship with each other. Therefore, a careful study of the tuning parameters is needed in order to improve the system behaviour and efficiency.

In the test conducted in this thesis, part of input energy was lost in LP line PRV. The amount of this energy was 6.2% of the input energy. However, this loss could be minimized by utilizing a tankless pump unit. The tankless implementation for hydraulic hybrid actuator was presented in [49] and discussed in Section 2.3.13.

One source of energy losses was the HP accumulator, as the gas temperature rose during charging. This led to decreased efficiency as thermal energy was conducted out of the system through accumulator walls. This effect could be dampened by isolating the accumulator so that the thermal conductivity is limited, or by utilizing a separate gas storage unit for the HP accumulator that could contain thermal storage element. If the separate gas chamber would be the same as the nominal volume of the HP accumulator, it would increase the amount of utilizable hydraulic fluid significantly in the HP accumulator. This would also lead to longer pauses between the pump cycles. In addition, the charging flow rate could be decreased closer to the average input flow rate. This could lower the peak temperatures caused by the charging, and thus, decrease the thermal conduction rate. Therefore, by minimizing the thermal losses in the accumulator, the total efficiency could be improved.

6 Conclusion

This thesis has experimentally defined and determined three characteristic efficiencies of the Digital Hydraulic Multi-Pressure Actuator for use in load-lifting applications: traditional, total, and regeneration efficiencies. The traditional efficiency was defined in order to compare energy consumption between the DHMPA and traditional systems, though it does not reflect the correct efficiency of the system, as the effect of energy regeneration from the load-mass is not considered in the calculations. The total efficiency, nevertheless, was defined in order to determine the true efficiency of the system. It considers the effect of the regeneration by adding the amount of regenerated energy into the input energy of the system. Finally, the regeneration efficiency was determined in order to evaluate performance, and the effect of the energy regeneration on the total system efficiency.

These characteristic efficiencies of the DHMPA were obtained in a vertical load-lifting and lowering experiment with a 1180 kg load-mass. The experiment consisted of 500 pre-defined duty cycles, each of which provided a new reference position for the DHMPA. The load-mass was moved periodically up and down in 40 mm steps. The cumulative energy balance of the DHMPA was determined by measuring input/output pressures, flow rates and load-mass position during the test. This balance was then utilized in order to determine the three characteristic efficiencies. The efficiency of the pump unit was excluded in the analysis. In addition, the temperature of the hydraulic fluid and the HP accumulator gas were measured, thus providing valuable information of the thermal losses in the system. The measurement data was obtained with a separate data acquisition system, and the data was analysed in MATLAB. The results were validated by calibration of the sensors and comparing the values with those of the DHMPA.

The DHMPA was found, on average, to respond well to the position step signal. However, some unexpected errors and oscillations occasionally occurred. This could be due to two factors. First, the DHMPA unit was not optimally dimensioned for the vertical load-lifting test rig used in this study. Second, the control system might not be optimally tuned, as it consists of several parameters that affect the system. Moreover, the possibility of a hardware fault, such as halting on/off valve, could not be excluded. Nevertheless, these problems could have been avoided by dimensioning the unit specifically for the test rig and carefully tuning the system. However, several combinations of different tuning parameters were tested, and none showed a flawless response. Nevertheless, the system efficiency could probably be improved by carefully studying and optimising the tuning parameters.

The traditional efficiency, that was defined as the ratio between the charged input energy and the cumulative lifted load-mass potential energy, was found to be over 128%. Obviously, this finding does not reflect the correct total efficiency of the system, as it exceeds 100%. The reason for this is that the calculation of the traditional efficiency does not consider the amount of extra energy input obtained by the energy regeneration. Nevertheless, including this regenerated energy into the total input energy revealed the total efficiency of the DHMPA unit to be over 63%. This efficiency was defined as the ratio of the output potential energy to the sum of charged and regenerated input energy. The achieved total efficiency is remarkably higher than efficiency levels generally reported for current hydraulic systems. Finally, the energy regeneration efficiency was

determined as the ratio between recoverable and regenerated energy, indicating that up to 80% of the recoverable potential energy can be restored to the DHMPA for later use.

This thesis extends previous work developing the DHMPA unit. However, this was the first time the DHMPA unit was evaluated in a purely load-lifting test rig, while previous research has concentrated only on a boom mock-up test rig and excavator swing-motion. As this thesis was the first attempt to evaluate the energy efficiency of DHMPA under pure load-lifting conditions, the evaluation of energy efficiency was limited to determining energy balance ratios instead of comparing the energy consumption to a corresponding reference data. Nevertheless, this thesis shows promising results for the DHMPA unit in load-lifting applications, as the efficiencies determined were remarkably better than those generally found in traditional hydraulics. Furthermore, the sources of energy losses were detected and pointed for further investigation.

This thesis provides the first experimental results for the DHMPA unit applied in a pure load-lifting test rig. Although efficiencies determined for the DHMPA appear to be superior to those of traditional hydraulic systems, several areas still remain to be developed before applying the DHMPA into real-life load-lifting applications. Future work should focus on improving the control and tuning of the system, as well as the dimensioning of the DHMPA for the test rig. In addition, the efficiency could be improved by implementing a tankless pump unit and minimizing thermal losses in the HP accumulator. Additionally, the control algorithm should be evaluated for further improvements and better control strategies for load-lifting applications. Furthermore, for conducting more comprehensive research, reference data would be needed for the same test rig and duty cycle using different technologies, as this would allow more precise comparison of the performance and energy consumption of the DHMPA to other desired solutions.

References

[1] K. Stelson, “Saving the world's energy with fluid power” in *Proceedings of the 8th JFPS International Symposium on Fluid Power*, Okinawa, 2011.

[2] H. Kauranne, J. Kajaste and M. Vilenius, Hydraulitekniikka, 2nd edition ed., Helsinki: Sanoma Pro Oy, 2013. In Finnish. ISBN 978-952-63-0707-7.

[3] Z. Dong, D. Ma, Q. Liu and X. Yue, “Motion control of valve-controlled hydraulic actuators with input saturation and modelling uncertainties,” *Advances in Mechanical Engineering,* vol. 10, no. 11, pp. 1-8, 2018. doi: https://doi.org/10.1177/1687814018812273.

[4] M. Heikkilä, “Energy Efficient Boom Actuation Using a Digital Hydraulic Power Management System,” Tampere University of Technology, Tampere, 2016. Doctoral Dissertation. vol. 1388. ISBN: 978-952-15-3758-5.

[5] K.-E. Rydberg, “Energy Efficient Hydraulics – System solutions for loss minimization,” in *National Conference on Fluid Power*, Linköping, 2015.

[6] N. Manring, Hydraulic Control Systems, Hoboken, New Jersey: John Wiley & Sons, Inc., 2005. ISBN: 0-471-69311-1.

[7] X. Liang and T. Virvalo, “What's wrong with energy utilization in hydraulic cranes,” *The Fifth International Conference on Fluid Power Transmission and Control,* 2001.

[8] M. Huova, A. Aalto, M. Linjama and K. Huhtala, “Study of Energy Losses in Digital Hydraulic Multi-Pressure Actuator,” in *Proceedings of 15th Scandinavian International Conference on Fluid Power*, Linköping, 2017. pp. 214-223. ISBN: 978-91-7685-369-6. doi:10.3384/ecp17144214.

[9] L. Siivonen, M. Linjama, M. Huova and M. Vilenius, “Pressure Based Fault Detection and Diagnosis of a Digital Valve System,” in *Power Transmission and Motion Control (PTMC 2007)*, 2007. pp. 67-79. ISBN: 978-0-86197-140-4.

[10] M. Linjama and H. Kalevi, “Digital pump-motor with independent outlets,” in *The 11th Scandinavian International Conference on Fluid Power*, Linköping, 2009.

[11] M. Karvonen, “Energy Efficient Digital Hydraulic Power Management of a Multi Actuator System,” Tampere University of Technology, Tampere, 2016. Doctoral Dissertation. vol. 1384. ISBN: 978-952-15-3737-0.

[12] Q. Zhongyi, Q. Long and Z. Jinman, “Review of energy efficient direct pump controlled cylinder electro-hydraulic technology,” *Renewable and Sustainable Energy Reviews,* vol. 35, pp. 336-346, 2014. ISSN 1364-0321. doi: https://doi.org/10.1016/j.rser.2014.04.036.

[13] D. Lovrec, M. Kastrevc and S. Ulaga, “Electro-hydraulic load sensing with a speed-controlled hydraulic supply system on forming-machines,” *The International Journal of Advanced Manufacturing Technology,* vol. 41, no. 1, pp. 1066-1075, 2009. doi:https://doi.org/10.1007/s00170-008-1553-y.

[14] G. Smith and E. Stapleton, “Load sensing hydraulic system”. United States Patent US4977928A, 1990.

[15] M. Huova, “Energy Efficient Digital Hydraulic Valve Control,” Tampere University of Technology, Tampere, 2015. Doctoral Dissertation. vol 1298. ISBN: 978-952-15-3553-6.

[16] C. Du, A. Plummer and N. Johnston, “Performance analysis of an energy-efficient variable supply pressure electro-hydraulic motion control system,” *Control*

Engineering Practice, vol. 48, no. 1, pp. 10-21, 2016. doi: https://doi.org/10.1016/j.conengprac.2015.12.013.

[17] R. Scheidl, H. Kogler and B. Winkler, "Hydraulic switching control - objectives, concepts, challenges and potential applications," *Magazine of Hydraulics, Pneumatics, Tribology, Ecology, Sensorics, Mechatronics,* pp. 7-17, 1 2013.

[18] R. Scheidl, B. Manhartsgruber, H. Kogler and B. Winkler, "The Hydraulic Buck Converter - Concept and Experimental Results," in *6th International Fluid Power Conference IFK*, Dresden, 2008.

[19] M. Linjama and A. Laamanen, "Is it time for digital hydraulics?," in *The Eighth Scandinavian International Conference on Fluid Power*, Tampere, 2003. pp. 347-366. ISBN: 952-15-0972.

[20] M. Huova and M. Linjama, "Energy efficient digital hydraulic valve control utilizing pressurized tank line," in *Proceedings of the 8th International Fluid Power Conference*, Dresden, 2012. pp. 111-122. doi:https://doi.org/10.4271/2013-01-2347.

[21] M. Linjama and M. Vilenius, "Improved digital hydraulic tracking control of water hydraulic cylinder drive," *International Journal of Fluid Power,* vol. 6, no. 1, pp. 29-39, 2005. doi:https://doi.org/10.1080/14399776.2005.10781209.

[22] L. Siivonen, M. Linjama, M. Huova and M. Vilenius, "Fault detection and diagnosis of digital hydraulic valve system," in *The Tenth Scandinavian International Conference on Fluid Power*, Tampere, 2007. pp. 211-226. ISBN: 978-952-15-1758-7.

[23] M. Linjama, H.-P. Vihtanen, A. Sipola and M. Vilenius, "Secondary controlled multi-chamber hydraulic cylinder," in *The 11th Scandinavian International Conference on Fluid Power*, Linköping, 2009.

[24] M. Huova, A. Laamanen and M. Linjama, "Energy Efficiency of Three-Chamber Cylinder with Digital Valve System," *International Journal of Fluid Power,* vol. 11, no. 3, pp. 15-22, 2010. doi:10.1080/14399776.2010.10781011.

[25] E. Bishop, "Digital hydraulic transformer - approaching theoretical perfection in hydraulic drive efficiency," 2009.

[26] E. Bishop, "Digital hydraulic transformer - for energy efficient hydraulic drives," Linz, 2009.

[27] J. Mattila and T. Virvalo, "Energy-efficient Motion Control of a Hydraulic Manipulator," in *International Conference on Robotics and Automation*, San Francisco, 2000. ISBN: 0-7803-5886-4. doi:10.1109/ROBOT.2000.846483.

[28] A. Hansen, H. Pedersen, T. Andersen and L. Wachmann, "Investigation of energy saving separate meter-in separate meter-out control," in *12th Scandinavian International Conference on Fluid Power*, Tampere, 2011.

[29] J. Aardema and D. Koehler, "System and method for controlling an independent metering valve". United States Patent US5960695A, 1999.

[30] K. Choi, J. Seo, Y. Nam and K. Kim, "Energy-saving in excavators with application of independent metering valve," *Journal of Mechanical Science and Technology,* vol. 29, no. 1, pp. 387-395, 2015. doi:https://doi.org/10.1007/s12206-014-1245-5.

[31] M. Linjama, "Digital fluid power - state of the art," in *The Twelfth Scandinavian International Conference on Fluid Power*, Tampere, 2011. Vol. 12, pp. 331-354. ISBN: 978-952-15-2520-9.

[32] M. Linjama ja K. Huhtala, ”Digital Hydraulic Power Management System - Towards Lossless Hydraulics,” tekijä: *Proceedings of the Third Workshop on Digital Fluid Power*, Tampere, 2010. pp. 5-22.

[33] M. Heikkilä, J. Tammisto, M. Huova, K. Huhtala and M. Linjama, “Experimental evaluation of a digital hydraulic power management system,” in *Proceedings of the Third Workshop on Digital Fluid Power*, Tampere, 2010. pp. 129-142. http://urn.fi/URN:NBN:fi:tty-201604253879.

[34] J. Zimmerman, E. Busquets and M. Ivantysynova, “40% Fuel Savings by Displacement Control Leads to Lower Working Temperatures – A Simulation Study and Measurements,” in *Proceedings of the 52nd National Conference on Fluid Power*, Las Vegas, 2011. pp. 693-701.

[35] E. Busquets, J. Zimmerman, R. Hippalgaonkar, M. Bertolin and M. Ivantysynova, “A hydraulic hybrid excavator with Displacement-Controlled actuation and pump-switching technology,” Purdue University, [Online]. Available: https://www.gfpsweb.org/?q=content/hydraulic-hybrid-excavator-displacement-controlled-actuation-and-pump-switching-technology. [Accessed 19 March 2020].

[36] R. Hippalgaonkar and M. Ivantysynova, “A Series-Parallel Hydraulic Hybrid Mini-Excavator with Displacement Controlled Actuators,” in *13th Scandinavian International Conference on Fluid Power*, Linköping, 2013. pp. 31-42. ISBN: 978-91-7519-572-8. doi:10.3384/ecp1392a4.

[37] E. Busquets and M. Ivantysynova, “Toward Supervisory-Level Control for the Energy Consumption and Performance Optimization of Displacement-Controlled Hydraulic Hybrid Machines,” in *Proceedings of the 10th IFK International Conference on Fluid Power*, Lafayette, 2016. Vol. 3, pp. 163-174.

[38] E. Busquets and M. Ivantysynova, “A Multi-Actuator Displacement Controlled System with Pump Switching - A Study of the Architecture and Actuator-Level Control,” *Transactions of the Japanese Fluid Power System Society,* vol. 8, no. 2, pp. 66-75, 2015. doi:https://doi.org/10.5739/jfpsij.8.66.

[39] T. Minav, C. Bonato, P. Sainio and M. Pietola, “Direct Driven Hydraulic Drive,” in *The 9th International Fluid Power Conference*, Aachen, Germany, 2014.

[40] T. Minav, P. Sainio and M. Pietola, “Direct-Driven Hydraulic Drive without conventional oil tank,” in *Proceedings of the ASME/BATH 2014 Symposium on Fluid Power & Motion Control*, Bath, 2014. doi: https://doi.org/10.1115/FPMC2014-7834.

[41] T. Minav, C. Bonato, P. Sainio and M. Pietola, “Efficiency of direct driven hydraulic drive for non-road mobile working machines,” in *International Conference on Electrical Machines*, Berlin, Germany, 2014. pp. 2431-2435. ISBN: 978-1-4799-4389-0. doi:10.1109/ICELMACH.2014.6960527.

[42] T. Minav, P. Sainio and M. Pietola, “Efficiency of direct driven hydraulic setup in arctic conditions,” in *Scandinavian International Conference on Fluid Power*, Tampere, 2015. ISBN: 978-952-15-3530-7.

[43] T. Minav, J. Heikkinen, T. Schimmel and M. Pietola, “Direct Driven Hydraulic Drive: Effect of Oil on Efficiency in Sub-Zero Conditions,” *Energies,* vol. 12, no. 2, p. 219, 2019. doi:https://doi.org/10.3390/en12020219.

[44] J. Juhala, H. Kauranne, J. Kajaste and M. Pietola, “Improving energy efficiency of work machine with Digital Hydraulics and pressure accumulator,” in *The 11th Scandinavian International Conference on Fluid Power*, Linköping, 2009. ISBN: 978-91-7393-588-3.

[45] H. Hänninen, “Reducing Energy Consumption of Reach Truck Utilizing Hydraulic Energy Recovery Systems,” Aalto University, Helsinki, 2016. Doctoral Dissertation. ISBN: 978-952-60-6991-3

[46] M. Huova, A. Aalto, M. Linjama, K. Huhtala, T. Lantela and M. Pietola, “Digital hydraulic multi-pressure actuator – the concept, simulation study and first experimental results,” *International Journal of Fluid Power,* vol. 18, no. 3, pp. 141-152, 2017. doi:10.1080/14399776.2017.1302775.

[47] M. Linjama, M. Huova, M. Pietola, J. Juhala and K. Huhtala, “Hydraulic Hybrid Actuator: Theoretical Aspects and Solution Alternatives,” in *Proceedings of the Fourteenth Scandinavian International Conference on Fluid Power*, Tampere, 2015. ISBN: 978-952-15-3658-8.

[48] M. Huova, M. Linjama, P. Kahra and J. Elonen, “New implementation of digital hydraulic multi-pressure actuator,” in *The 10th Workshop on Digital Fluid Power*, Linz, 2019.

[49] M. Paloniitty, M. Linjama and M. Huova, “Compact and efficient implementation of a pressurized tank line,” 2018. http://urn.fi/URN:NBN:fi:tty-201811262768.

[50] M. Linjama and M. Huova, “Model-based force and position tracking control of a multipressure hydraulic cylinder,” *Proceedings of the Institution of Mechanical Engineers, Part I: Journal of Systems and Control Engineering,* vol. 232, no. 3, pp. 324-335, 2018. doi:https://doi.org/10.1177/0959651817754035.

[51] H. Ahmed, O. Gottberg, H. Kauranne, J. Kajaste, O. Calonius, M. Huova, M. Linjama, J. Elonen, P. Kahra and M. Pietola, “Multi-Pressure actuator in enhancing the energy balance of micro-excavator,” in *16th Scandinavian International Conference on Fluid Power*, Tampere, 2019. ISBN: 978-952-03-1125-4.

[52] H. Ahmed, “Energy efficiency analysis of multi-pressure hydraulic system,” Tampere University, Tampere, 2019. Master’s Thesis. http://urn.fi/URN:NBN:fi:tty-201903201314.

[53] Epec Oy, “Technical Manual 5050 / MAN000539,” Epec Oy, Seinäjoki, 2013.